



12-2022

## Repeatability and Reproducibility Analyses for Structured Light Scanning

Leah Jacobs

*University Tennessee Knoxville, ljacobs6@vols.utk.edu*

Follow this and additional works at: [https://trace.tennessee.edu/utk\\_gradthes](https://trace.tennessee.edu/utk_gradthes)



Part of the [Manufacturing Commons](#)

---

### Recommended Citation

Jacobs, Leah, "Repeatability and Reproducibility Analyses for Structured Light Scanning. " Master's Thesis, University of Tennessee, 2022.

[https://trace.tennessee.edu/utk\\_gradthes/7055](https://trace.tennessee.edu/utk_gradthes/7055)

This Thesis is brought to you for free and open access by the Graduate School at TRACE: Tennessee Research and Creative Exchange. It has been accepted for inclusion in Masters Theses by an authorized administrator of TRACE: Tennessee Research and Creative Exchange. For more information, please contact [trace@utk.edu](mailto:trace@utk.edu).

To the Graduate Council:

I am submitting herewith a thesis written by Leah Jacobs entitled "Repeatability and Reproducibility Analyses for Structured Light Scanning." I have examined the final electronic copy of this thesis for form and content and recommend that it be accepted in partial fulfillment of the requirements for the degree of Master of Science, with a major in Mechanical Engineering.

Tony L Schmitz, Major Professor

We have read this thesis and recommend its acceptance:

Chad E Duty, Tony L. Schmitz, Scott Smith, Bradley H Jared

Accepted for the Council:

Dixie L. Thompson

Vice Provost and Dean of the Graduate School

(Original signatures are on file with official student records.)

# Repeatability and Reproducibility Analyses for Structured Light Scanning

A Thesis Presented for the  
Master of Science  
Degree  
The University of Tennessee, Knoxville

Leah June Jacobs  
December 2022

© by Leah June Jacobs, 2022  
All Rights Reserved.

*dedication...*

*This thesis work is dedicated to my parents, Margo and Philip Jacobs, who have always loved me unconditionally and taught me to always go after my dream of being a mechanical engineer.*

# Acknowledgments

I would like to thank the following people without whom this research would not be possible and without whom I would not have made it through my Master of Science degree: Dr. Tony Schmitz for having me as part of his research group and opening my eyes to the impact of advanced manufacturing, Dr. Joshua Penney for answering all my questions, Dr. Timothy No who taught me how to use the GOM Inspect software and the Artec scanner before we received the GOM scanners, Drs. Chad Duty, Scott Smith and Bradley Jared for being a part of my committee, and Dr. Wayne Davis for encouraging me to explore the research opportunities that opened doors for me at the University of Tennessee.

# Abstract

Structured light scanning is used to create a digital twin of a manufactured part. Features can be extracted from this digital twin to determine if the part meets the designer's intent and required tolerances. This thesis describes repeatability and reproducibility studies for a selected structured light scanning system and measurement artifact. The repeatability study used five repeated scans at 15 measurement positions. Repeatability was assessed by randomly selecting one of the five scans and creating the mesh for the 15 positions. This process was performed 50 times and the statistics for the feature dimension variations were calculated to isolate the scanning effects only. The same sequence was then performed for 10 of the 15 positions and five of the 15 positions to evaluate the repeatability sensitivity to number of measurement positions. Reproducibility was assessed by selecting 15 positions to create a mesh and repeating the 15-position measurement sequence 10 times using different positions for each mesh construction. The statistics for the feature dimension variations were then calculated. This incorporated the effects of both scanning and the position and orientation of the part relative to the scanner. This sequence was repeated for 10 positions and five positions to evaluate the corresponding sensitivity.

# Table of Contents

- 1 Introduction** **1**
  - 1.1 Background . . . . . 1
    - 1.1.1 Structured Light Scanning . . . . . 2
    - 1.1.2 Repeatability and Reproducibility . . . . . 3
  
- 2 GOM Inspect Software** **4**
  - 2.1 GOM Inspect Workspaces . . . . . 5
    - 2.1.1 Start . . . . . 5
    - 2.1.2 Setup . . . . . 5
    - 2.1.3 Digitize . . . . . 6
    - 2.1.4 Inspection . . . . . 6
    - 2.1.5 Report . . . . . 11
    - 2.1.6 Mesh Editing . . . . . 11
  - 2.2 Information on ATOS Q . . . . . 13
  
- 3 Repeatability and Reproducibility Methods** **15**
  - 3.1 Measurement Artifact . . . . . 15
  - 3.2 Repeatability and Reproducibility Assessment
    - Procedure . . . . . 16
  - 3.3 Repeatability . . . . . 30
  - 3.4 Reproducibility . . . . . 30
  - 3.5 Verification . . . . . 31



<b>4</b>	<b>Repeatability Data</b>	<b>45</b>
<b>5</b>	<b>Reproducibility Data</b>	<b>60</b>
<b>6</b>	<b>CMM Comparison</b>	<b>74</b>
<b>7</b>	<b>Discussion</b>	<b>76</b>
7.1	Results . . . . .	76
7.2	Difficulties Encountered During the Study . . . . .	77
<b>8</b>	<b>Conclusions</b>	<b>88</b>
	<b>Bibliography</b>	<b>93</b>
<b>A</b>	<b>Tips and Tricks</b>	<b>95</b>
A.1	GOM Inspect Software . . . . .	95
A.2	Other . . . . .	96
<b>B</b>	<b>Suggested or Useful GOM Tutorials</b>	<b>97</b>
B.1	Found on the GOM Training Website . . . . .	97
<b>C</b>	<b>Other Useful Information</b>	<b>98</b>
C.1	Term and Acronym Definitions . . . . .	98
C.2	The Website Links from the Bibliography . . . . .	98
<b>D</b>	<b>The text of the program to combine individual CSV files into a single Excel workbook as separate sheets</b>	<b>100</b>
<b>E</b>	<b>Report developed using the CMM</b>	<b>102</b>
<b>F</b>	<b>Structured Light Scanner to CMM Comparison Graphs</b>	<b>105</b>
	<b>Vita</b>	<b>136</b>

# List of Tables

3.1	Reproducibility Position Locations (values are angles of the rotary table that supported the part in units of deg) . . . . .	32
8.1	Summary of the Repeatability and Reproducibility of the Circle Diameters and Heights for the 15 Position Meshes . . . . .	89
8.2	Summary of the Repeatability and Reproducibility of the Circle Diameters and Heights for the 10 Position Meshes . . . . .	89
8.3	Summary of the Repeatability and Reproducibility of the Circle Diameters and Heights for the 5 Position Meshes . . . . .	91

# List of Figures

2.1	Image of the Start Workspace . . . . .	7
2.2	Image of the Setup Workspace . . . . .	7
2.3	Image of the Digitize Workspace . . . . .	8
2.4	Image of the Measurement Template Selection Window . . . . .	8
2.5	Image of the Cut Out Points Tool . . . . .	9
2.6	Image of the Selected Points that are not Part of the Scanning Object . . . . .	9
2.7	Image of the New Measurement Series Window . . . . .	9
2.8	Image of the Transform Measurement Series Window . . . . .	10
2.9	Image of the Polygonize Tool Window . . . . .	10
2.10	Image of the Inspection Workspace . . . . .	10
2.11	Image of the Report Workspace . . . . .	12
2.12	Image of the Mesh Editing Workspace . . . . .	12
2.13	Tool to Close Holes in Polygonized Mesh . . . . .	14
2.14	Image of the GOM ATOS Q Scanner [16] . . . . .	14
3.1	Image of the Part Used During the Study . . . . .	17
3.2	Image of the Part Including the Locations of Circles and Heights . . . . .	17
3.3	Creation of Planes 1, 2 and 3 . . . . .	19
3.4	Creation of the Local Coordinate System . . . . .	19
3.5	Setting the Local Coordinate System as the Global Coordinate System . . . . .	20
3.6	Construction of Cylinders Based on Holes . . . . .	20
3.7	Creation of the Center Points from Cylinders and Plane 1 . . . . .	21
3.8	Creation of the Circles Based on the Cylinders . . . . .	21

3.9	Creation of Distances Between Circle Centers . . . . .	23
3.10	Constructing Fitting Planes Along Ledges for Heights . . . . .	23
3.11	Construction of the Height Surface Points . . . . .	24
3.12	Construction of Height Distances Using Projected Point Distance . . . . .	24
3.13	Multisection Parallel Dialog Box . . . . .	25
3.14	Select All Points in Mesh . . . . .	25
3.15	Construction of Cross-sections . . . . .	26
3.16	Only Useful Information Kept . . . . .	26
3.17	Construction of Fitting Circles on each Cross-section . . . . .	26
3.18	Points Used to Create Circle were Counted by GOM . . . . .	28
3.19	Points Used to Create Circles were Averaged . . . . .	28
3.20	Image of the Circles on a Cross-section . . . . .	28
3.21	Export CSV File for each Mesh . . . . .	29
3.22	Use Macro Excel Program to Compile CSV Files . . . . .	29
3.23	All CSV Files in a Single Excel Workbook . . . . .	33
3.24	Data for Each Element Compiled into a Single Column of Separate Excel Workbook . . . . .	34
3.25	Histogram Formed in the Worksheet . . . . .	35
3.26	Adjustments Made to Increase Readability . . . . .	35
3.27	Circle 1 Histogram for 50 Randomly Selected Scan Sets at Same 15 Positions	36
3.28	Graph Showing the Range of the Measured Diameters Plotted Against the Mean Diameter for 15, 10, and 5 Positions . . . . .	36
3.29	Variation in X Location Range for 10 Circles with 15 Scanning Positions . .	37
3.30	Variation in Y Location Range for 10 Circles with 15 Scanning Positions . .	38
3.31	Graph showing the range of the height measurements plotted against the mean height for 15, 10, and 5 positions . . . . .	38
3.32	Graph Plotting Mean Diameter for 15, 10, and 5 Positions with Error Bars Showing Standard Deviation for Circle 1 . . . . .	39
3.33	Graph Plotting Mean Diameter for 15, 10, and 5 Positions with Error Bars Showing Standard Deviation for Circle 10 . . . . .	39

3.34	Graph Showing the Temperature Variation that Occurred While Scanning the Part Using 15 Positions for Reproducibility . . . . .	40
3.35	Graph Showing the Temperature Variation that Occurred While Scanning the Part Using 10 Positions for Reproducibility . . . . .	40
3.36	Graph Showing the Temperature Variation that Occurred While Scanning the Part Using 5 Positions for Reproducibility . . . . .	41
3.37	Image of the CMM used to perform the Measurements . . . . .	41
3.38	Image of the Coordinate System Created in Calypso . . . . .	42
3.39	Creation of Clearance Planes Based on CAD . . . . .	42
3.40	Create Plane on Height Ledge . . . . .	43
3.41	Creation of Height Measurement Using Cartesian Distances . . . . .	43
3.42	Creation of Circles 2-10 on the Cylinders . . . . .	43
3.43	Creation of Distances Between Circle Centers . . . . .	44
3.44	Run the Program to get Actual Measurements . . . . .	44
4.1	Circle 10 Histogram for 50 Randomly Selected Scan Sets at Same 15 Positions	46
4.2	Location of the 15 Positions Around the Artifact for Repeatability . . . . .	46
4.3	Location of the 10 Positions Around the Artifact for Repeatability . . . . .	47
4.4	Location of the 5 Positions Around the Artifact for Repeatability . . . . .	47
4.5	Variation in Diameter Range for 10 Circles with 15 Scanning Positions . . . . .	48
4.6	Variation in Diameter Standard Deviation for 10 Circles with 15 Scanning Positions . . . . .	48
4.7	Variation in X Location Range for 10 Circles with 15 Scanning Positions . . . . .	49
4.8	Variation in Y Location Range for 10 Circles with 15 Scanning Positions . . . . .	50
4.9	Variation in X Location Standard Deviation for 10 Circles with 15 Scanning Positions . . . . .	51
4.10	Variation in Y Location Standard Deviation for 10 Circles with 15 Scanning Positions . . . . .	52
4.11	Variation in Height Range for 15 Scanning Positions . . . . .	52
4.12	Variation in Height Standard Deviation for 15 Scanning Positions . . . . .	54

4.13	Variation in Diameter Range for 10 Circles with 5, 10, and 15 Scanning Positions	54
4.14	Variation in Diameter Standard Deviation for 10 Circles with 5, 10, and 15 Scanning Positions . . . . .	55
4.15	Variation in Height Range for 5, 10, and 15 Scanning Positions . . . . .	55
4.16	Variation in Height Standard Deviation for 5, 10, and 15 Scanning Positions	56
4.17	Range of Distances Between Circle Centers Using 15 Positions in Micrometers	56
4.18	Range of Distances Between Circle Centers Using 10 Positions in Micrometers	57
4.19	Range of Distances Between Circle Centers Using 5 Positions in Micrometers	57
4.20	Standard Deviation of Distances Between Circle Centers Using 15 Positions in Micrometers . . . . .	58
4.21	Standard Deviation of Distances Between Circle Centers Using 10 Positions in Micrometers . . . . .	58
4.22	Standard Deviation of Distances Between Circle Centers Using 5 Positions in Micrometers . . . . .	59
5.1	Location of the 15 Positions Around the Artifact for Reproducibility . . . . .	61
5.2	Location of the 10 Positions Around the Artifact for Reproducibility . . . . .	61
5.3	Location of the 5 Positions Around the Artifact for Reproducibility . . . . .	62
5.4	Diameter Range for 10 Circles with 15 Scanning Positions . . . . .	62
5.5	Diameter Standard Deviation for 10 Circles with 15 Scanning Positions . . . . .	63
5.6	X Location Range for 10 Circles with 15 Scanning Positions . . . . .	63
5.7	Y Location Range for 10 Circles with 15 Scanning Positions . . . . .	64
5.8	X Location Standard Deviation for 10 Circles with 15 Scanning Positions . . . . .	65
5.9	Y Location Standard Deviation for 10 Circles with 15 Scanning Positions . . . . .	66
5.10	Height Range for 15 Scanning Positions . . . . .	66
5.11	Height Standard Deviation for 15 Scanning Positions . . . . .	67
5.12	Diameter Range for 10 Circles with 5, 10, and 15 Scanning Positions . . . . .	67
5.13	Diameter Standard Deviation for 10 Circles with 5, 10, and 15 Scanning Positions . . . . .	68
5.14	Height Range for 5, 10, and 15 Scanning Positions . . . . .	68

5.15	Height Standard Deviation for 5, 10, and 15 Scanning Positions . . . . .	70
5.16	Range of Distances Between Circle Centers Using 15 Positions . . . . .	70
5.17	Range of Distances Between Circle Centers Using 10 Positions . . . . .	71
5.18	Range of Distances Between Circle Centers Using 5 Positions . . . . .	71
5.19	Standard Deviation of Distances Between Circle Centers Using 15 Positions .	72
5.20	Standard Deviation of Distances Between Circle Centers Using 10 Positions .	72
5.21	Standard Deviation of Distances Between Circle Centers Using 5 Positions .	73
6.1	Comparing Structured Light Scanning and CMM Measurements for Height 1	75
7.1	Comparing the Repeatability and Reproducibility Range Versus Mean Diam- eter Summary Graphs . . . . .	78
7.2	Comparing the Repeatability and Reproducibility Standard Deviation Versus Mean Diameter Summary Graphs . . . . .	79
7.3	Directly Comparing the Repeatability and Reproducibility of Range Versus Mean Diameter for 5, 10 and 15 Positions . . . . .	80
7.4	Directly Comparing the Repeatability and Reproducibility of Standard Deviation Versus Mean Diameter for 5, 10 and 15 Positions . . . . .	81
7.5	Comparing the Repeatability and Reproducibility Range Versus Mean Height Summary Graphs . . . . .	82
7.6	Comparing the Repeatability and Reproducibility Standard Deviation Versus Mean Height Summary Graphs . . . . .	83
7.7	Directly Comparing the Repeatability and Reproducibility of Range Versus Mean Height for 5, 10 and 15 Positions . . . . .	84
7.8	Directly Comparing the Repeatability and Reproducibility of Standard Deviation Over Mean Height for 5, 10 and 15 Positions . . . . .	85
8.1	Summary of the Reproducibility Standard Deviations Based on Circle Diam- eter and Number of Positions in Micrometers . . . . .	91
8.2	Summary of the Reproducibility Standard Deviations Based on Step Height and Number of Positions in Micrometers . . . . .	92

E.1	First page of measurements from the report made using the CMM . . . . .	102
E.2	Second page of measurements from the report made using the CMM . . . . .	103
E.3	Last page of measurements from the report made using the CMM . . . . .	104
F.1	Comparing Structured Light Scanning and CMM Measurements for Height 1	105
F.2	Comparing Structured Light Scanning and CMM Measurements for Height 2	106
F.3	Comparing Structured Light Scanning and CMM Measurements for Height 3	107
F.4	Comparing Structured Light Scanning and CMM Measurements for Height 4	108
F.5	Comparing Structured Light Scanning and CMM Measurements for Circle 2	109
F.6	Comparing Structured Light Scanning and CMM Measurements for Circle 3	110
F.7	Comparing Structured Light Scanning and CMM Measurements for Circle 4	111
F.8	Comparing Structured Light Scanning and CMM Measurements for Circle 5	112
F.9	Comparing Structured Light Scanning and CMM Measurements for Circle 6	113
F.10	Comparing Structured Light Scanning and CMM Measurements for Circle 7	114
F.11	Comparing Structured Light Scanning and CMM Measurements for Circle 8	115
F.12	Comparing Structured Light Scanning and CMM Measurements for Circle 9	116
F.13	Comparing Structured Light Scanning and CMM Measurements for Circle 10	117
F.14	Comparing Structured Light Scanning and CMM Measurements for X Location of Circle 2 . . . . .	118
F.15	Comparing Structured Light Scanning and CMM Measurements for X Location of Circle 3 . . . . .	119
F.16	Comparing Structured Light Scanning and CMM Measurements for X Location of Circle 4 . . . . .	120
F.17	Comparing Structured Light Scanning and CMM Measurements for X Location of Circle 5 . . . . .	121
F.18	Comparing Structured Light Scanning and CMM Measurements for X Location of Circle 6 . . . . .	122
F.19	Comparing Structured Light Scanning and CMM Measurements for X Location of Circle 7 . . . . .	123



F.20 Comparing Structured Light Scanning and CMM Measurements for X	
Location of Circle 8 . . . . .	124
F.21 Comparing Structured Light Scanning and CMM Measurements for X	
Location of Circle 9 . . . . .	125
F.22 Comparing Structured Light Scanning and CMM Measurements for X	
Location of Circle 10 . . . . .	126
F.23 Comparing Structured Light Scanning and CMM Measurements for Y	
Location of Circle 2 . . . . .	127
F.24 Comparing Structured Light Scanning and CMM Measurements for Y	
Location of Circle 3 . . . . .	128
F.25 Comparing Structured Light Scanning and CMM Measurements for Y	
Location of Circle 4 . . . . .	129
F.26 Comparing Structured Light Scanning and CMM Measurements for Y	
Location of Circle 5 . . . . .	130
F.27 Comparing Structured Light Scanning and CMM Measurements for Y	
Location of Circle 6 . . . . .	131
F.28 Comparing Structured Light Scanning and CMM Measurements for Y	
Location of Circle 7 . . . . .	132
F.29 Comparing Structured Light Scanning and CMM Measurements for Y	
Location of Circle 8 . . . . .	133
F.30 Comparing Structured Light Scanning and CMM Measurements for Y	
Location of Circle 9 . . . . .	134
F.31 Comparing Structured Light Scanning and CMM Measurements for Y	
Location of Circle 10 . . . . .	135

# Chapter 1

## Introduction

Structured light scanning is used to create a three-dimensional rendering of a physical object and is performed using a structured light scanner. The scanner contains a projector which projects a structured light pattern onto the test object and one or more cameras which capture the distorted pattern created by the object's surface. The images captured by the cameras are analyzed to identify the object's shape. Using the calibrated spatial relationship between the projector and cameras, a point cloud is generated showing the exterior surface of the object by stitching multiple images from different positions around the object. The point cloud is polygonized to generate a mesh for use as a 3-D rendering of the object. This mesh can then be exported as an STL file for analysis, used as a stock model to define machining paths, and/or used to determine locations for material repair by additive processes.

### 1.1 Background

This thesis assesses the repeatability and reproducibility of structured light scanning for a commercially available system using an artifact. Therefore, background information on structured light scanning and repeatability/reproducibility is provided.

### 1.1.1 Structured Light Scanning

A structured light scanner is composed of a projector, which shines the selected structured pattern onto the test object, and one or more cameras which capture(s) the reflected, distorted pattern (caused by the object shape). The object's shape is identified by analyzing the distortion after the system is calibrated and the spatial relationship between the projector and camera(s) is known. Structured light scanning has become a well-established process for manufacturing environment measurements.

Evaluation of structured light scanning performance has been performed by several research groups. These studies have included evaluating the precision of a custom setup in comparison to a commercial scanner [2], the measurement performance [5], the precision of several types of optical scanners in comparison to a coordinate measuring machine (CMM) [11] and each other [4] [7], the overall uncertainty [9], and the repeatability and reproducibility for different resolutions [15] using structured light scanners.

Custom structured light systems can be built using commercial off-the-shelf hardware and differ significantly in accuracy and precision. Experimental structured light systems are composed of (typically) two industrial cameras and a high resolution projector. It has been shown that the camera used in the custom systems greatly affects the precision and accuracy [2]. The scanner performance can be determined by comparing a scan of a 3-D ball lattice to the data from a CMM. This establishes the error in size, form, and position when the scan data and CMM data are compared. The uncertainty was determined to be in the micrometer range for one setup [5]. Other artifacts can also be used to determine accuracy and precision of a scanner including different size gauge blocks [1]; cylinders, spheres, and prismatic volumes [10]; multiple different sized precision spheres in a single plane [12]; and even a freeform geometry [11]. The calibrated artifacts can be used to determine the measurement uncertainty of structured light systems [9]. McCarthy et al. demonstrated that structured light scanners are typically less accurate than CMMs [11]. Though the accuracy varied depending on the scanner used, the structured light scanner was generally the fastest and most accurate of the systems tested [4] [7]. In this thesis, a CMM is subsequently used to measure the artifact for comparison to the structured light

scanner results. Differences in resolution change the measurement uncertainty; therefore, the resolution is typically kept constant for repeatability and reproducibility studies [15]. For this study the GOM inspect software and ATOS Q defaults are used to provide data for the measurement repeatability and reproducibility analyses.

### **1.1.2 Repeatability and Reproducibility**

Repeatability is one aspect of a measurement system's ability to provide trustworthy data and is assessed using the variation observed when a single operator uses the same instrument to measure a single object several times. Repeatability is defined as the closeness of the agreement between the results of successive measurements of the same measurand carried out under the same conditions of measurement [14]. The dispersion in these measurements depends on the combination of the instrument and part.

Reproducibility is another measure of the instrument's capability to supply trusted data and is a measure of variation when the measurement conditions are modified by, for example, different users or different measurement conditions while measuring a single object with a single instrument. Reproducibility is defined as the closeness of the agreement between the results of measurements of the same measurand carried out under changed conditions of measurement [14]. Reproducibility can be increased by lowering the number of people using the measurement system or by improving the instruction details on how to perform the measurement [8].

Variability of a measurement includes contributions from calibration, stability, and linearity. Calibration includes comparison of a measurement against a feature with low uncertainty (such as a gage block). Stability represents the change in the measurement over time due to external factors, such as temperature in the instrument environment. Linearity describes the measurement variation from a linear input/output relationship over the instrument's full range [3].

# Chapter 2

## GOM Inspect Software

The GOM Inspect Professional suite of software has a user-friendly interface that provides guidance on steps to take not only during the scanning process, but also for post-processing and analysis. The various applications are sorted into workspaces which, when used together, can be used to perform scans and obtain data. The first step required to obtain a usable scan is to connect the scanner (in this case an ATOS Q) to the computer and the power source before turning the scanner on. The scanner must then warm up for several minutes to reach a steady-state temperature and improve the scan accuracy. At this point, calibration may need to be performed to enable an accurate scan.

The next steps in the scanning process are completed using the digitize workspace. First, the user must select the scan template (the basic scanning template works well) as a basis for the measurement. Then, the user positions the scanning object so that as many reference points as possible are visible to the scanner (these reference points are GOM-specific targets that are attached by self-adhesive to the part surface) and performs the first scan. If the scanner is not fully warmed up, the GOM Inspect software will issue a warning. Next, the user changes the position of the object as viewed by the scanner and scans again until the entire object has been scanned. Afterwards, post-processing begins with polygonizing the point cloud into a mesh. The post-processing steps occur in the mesh editing workspace using the automatic hole filling tool to fill any holes smaller than 10  $\mu\text{m}$ . At this point, the user can export the scan as an STL file or the scan can be analyzed in the inspection

workspace, which is discussed in section 2.1 in more detail along with all the other applicable workspaces.

GOM also has a free version of the GOM Inspect suite available with most of the same workspaces available as the Professional version.

## 2.1 GOM Inspect Workspaces

The GOM Inspect software has multiple workspaces with applications that work together to create a project which can be used to scan, analyze, and produce a report on an object. These workspaces include: Start, Setup, Digitize, Inspection, Report, and Mesh Editing, which are described in the following sections.

### 2.1.1 Start

The Start workspace (Fig. 2.1) is where new projects can be created and old projects can be opened. This workspace can also be used to open a project template or a recently opened project. A project template contains a pre-selected set of report pages for use in the project. Sample Data and Get Started provide access to meshes and projects from GOM to help with learning the software.

### 2.1.2 Setup

The Setup workspace (Fig. 2.2) is used to set up the scanner; adjust the camera focus, projector focus, and camera aperture; and calibrate a scanner or touch probe. A common activity is calibrating the scanner. Calibration is initiated by selecting the “calibrate sensor” button at the top of the workspace. In the dialog box that appears, care must be taken to ensure the settings are appropriate, and that the calibration object matches the sensor lenses that are in use before choosing “OK”. Next, the user follows the onscreen instructions to position the scanner and calibration panel to calibrate the scanner. At the end of the calibration process, a dialog box appears to indicate if the calibration was successful. A successful calibration is represented by two green circles with checkmarks. The user expands

the dialog box and saves the calibration results as a text file before selecting “OK” to complete the calibration.

### **2.1.3 Digitize**

The Digitize workspace (Fig. 2.3) is used to scan an object in order to create a 3-D mesh. It starts with the template selection tool (Fig. 2.4) that contains a basis for how to collect images and combine the images into a point cloud. The user completes the first scan of the object by using one of the three triggering methods. These include: 1) pressing the scan button in the program on the toolbar, 2) pressing the space bar, or 3) pressing the forward button on the presentation remote (as long as the batteries are charged). The user then continues taking scans until the visible part of the object has been completely scanned. This generally requires rotating the object to new views while ensuring at least three reference points are visible in each scan. Larger objects generally require more scans. At this point, the user removes surface that supports the object from the scan using the “cut out points” tool (Fig. 2.5). If there are any other points that are not part of the object being scanned, the user selects them using the selection tool and presses control and delete on the keyboard (Fig. 2.6). At this point, the user can create another measurement series using the “new measurement series” tool (Fig. 2.7) to add any part of the object that was missed in the first set of scans. After removing the background points as previously described, the two measurement series are combined using the “transform measurement series” tool (Fig. 2.8) and common reference points. The user must always remove the background points before transforming the measurement series. Once scanning is complete, the “polygonise” tool (Fig. 2.9) ) is applied to create a mesh from the point cloud. From here, post-processing occurs in the Inspection and Mesh editing workspaces.

### **2.1.4 Inspection**

The Inspection workspace (Fig. 2.10) is where a meshed part can be analyzed. This workspace can be used to create surface comparison, inspection sections, pointwise inspections, deviation labels, geometric dimensioning and tolerancing (GDT) measurements,

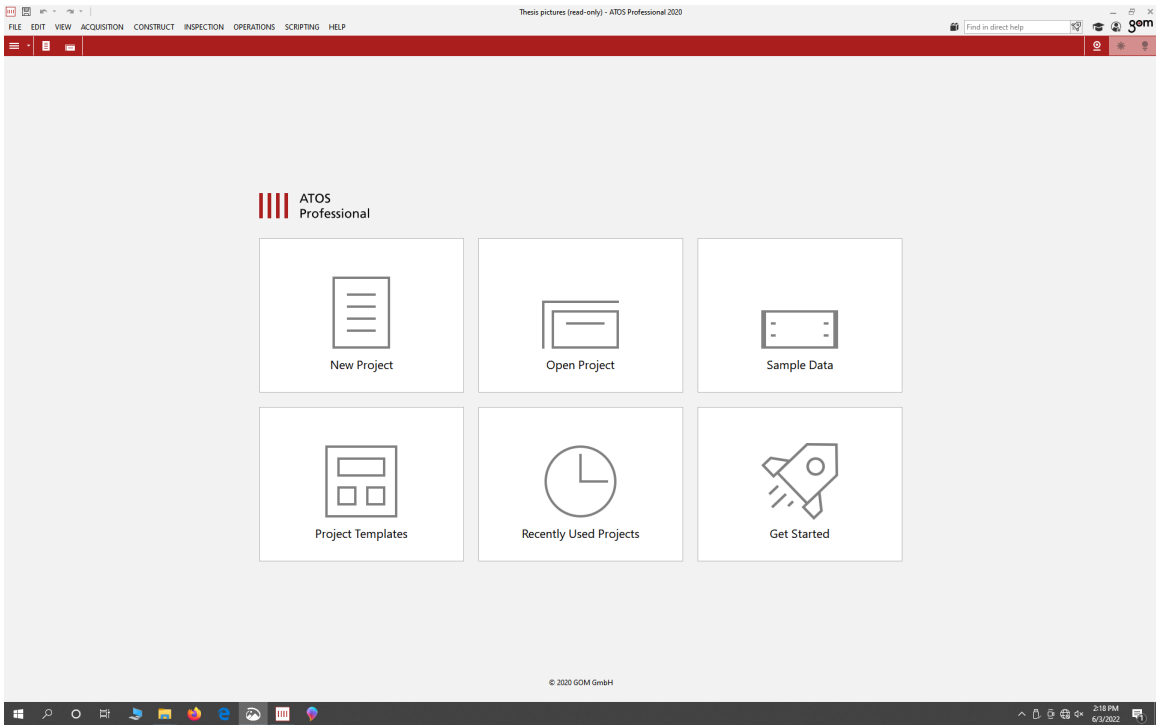


**Figure 2.1:** Image of the Start Workspace

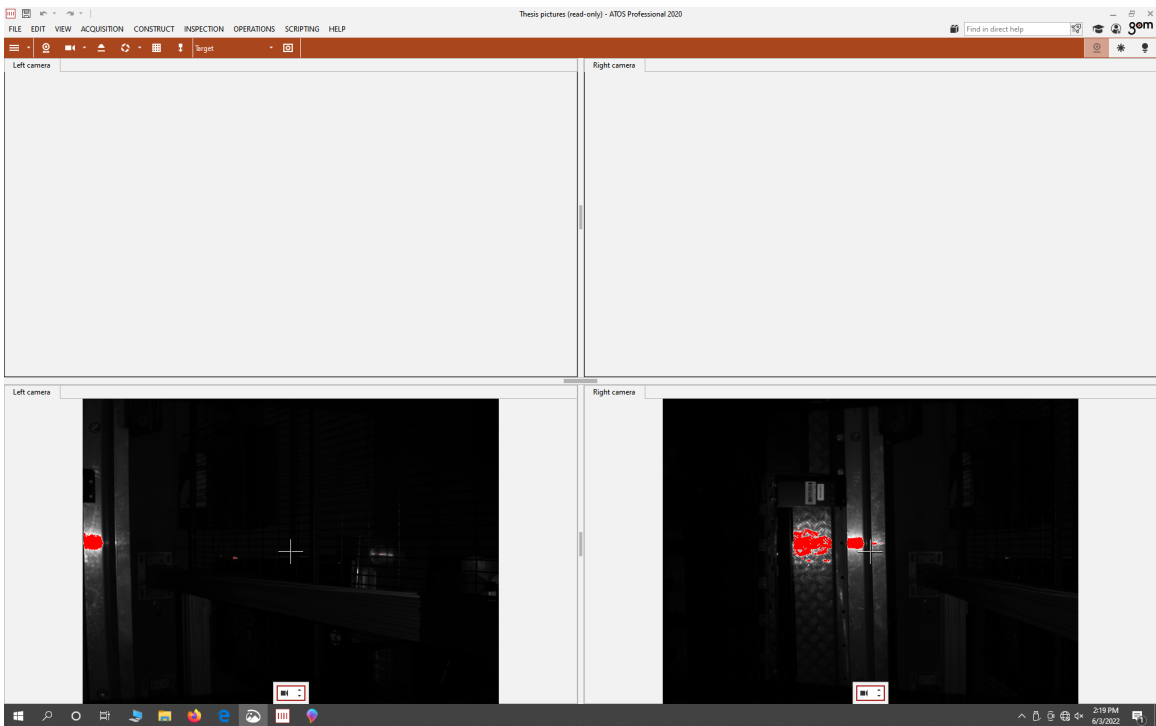


**Figure 2.2:** Image of the Setup Workspace



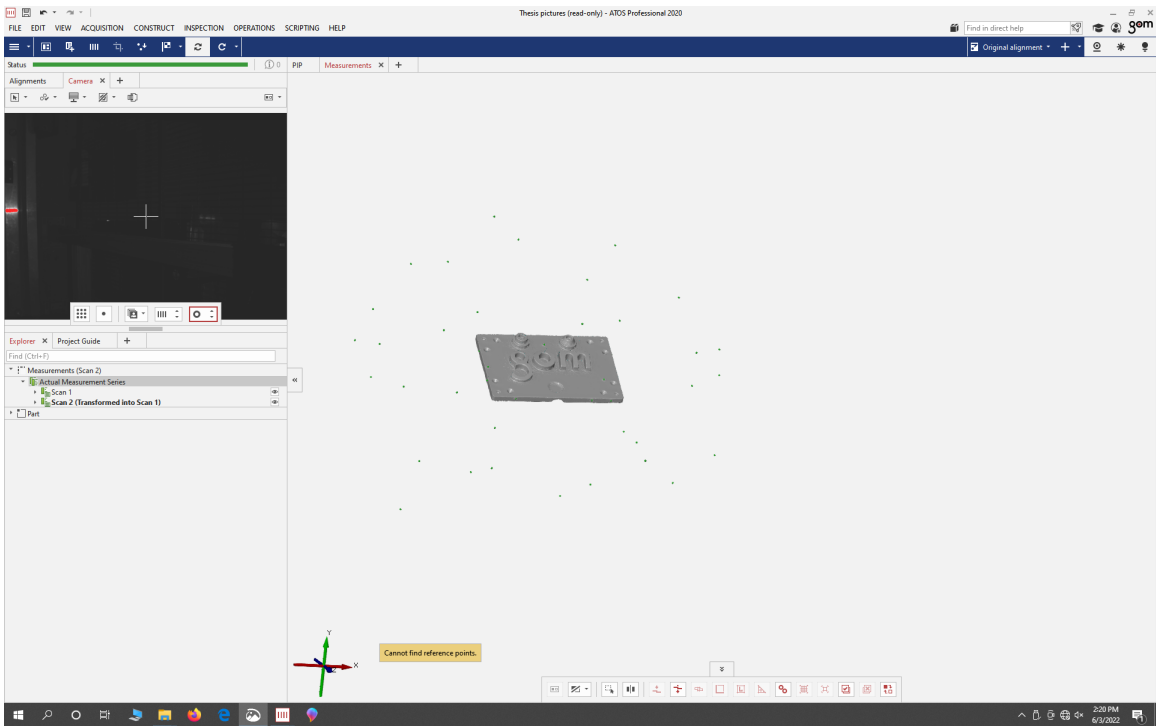


Figure 2.3: Image of the Digitize Workspace

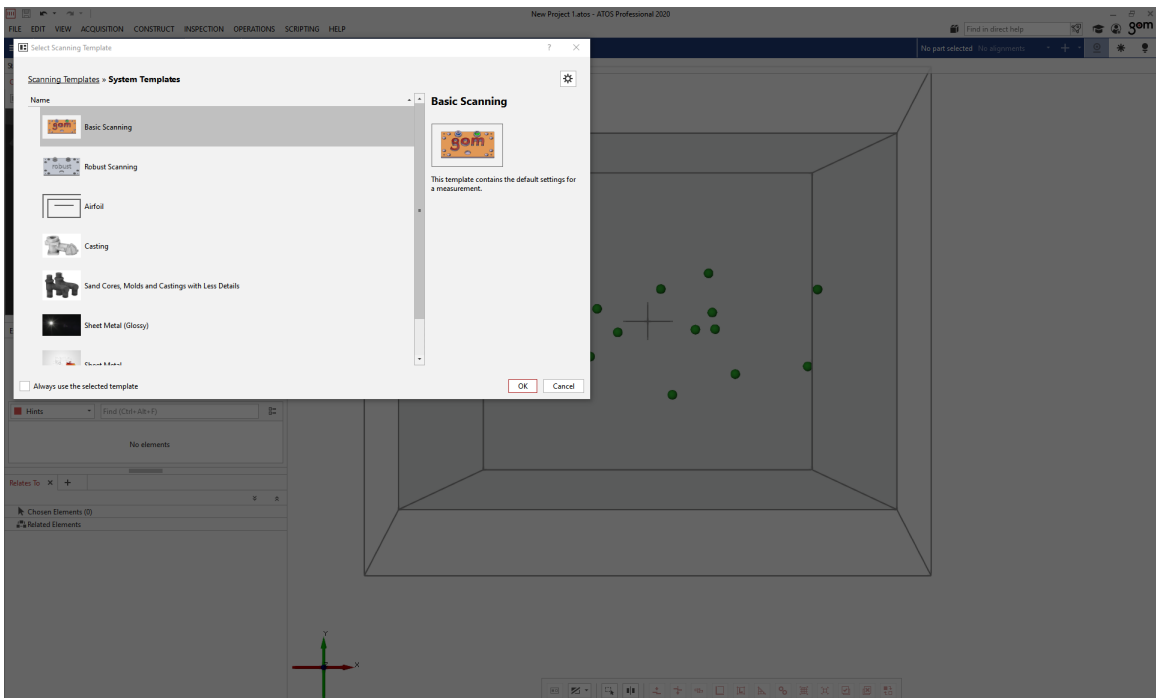
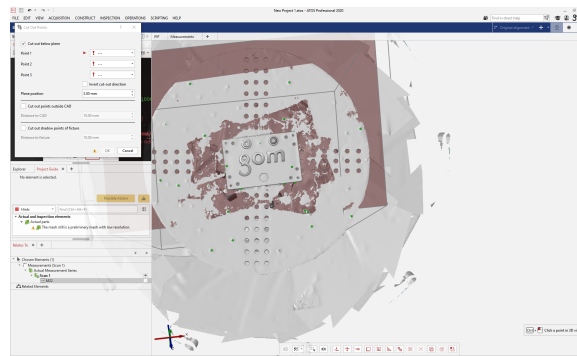
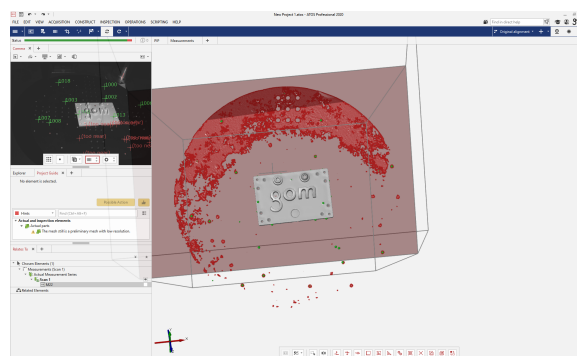


Figure 2.4: Image of the Measurement Template Selection Window



**Figure 2.5:** Image of the Cut Out Points Tool



**Figure 2.6:** Image of the Selected Points that are not Part of the Scanning Object

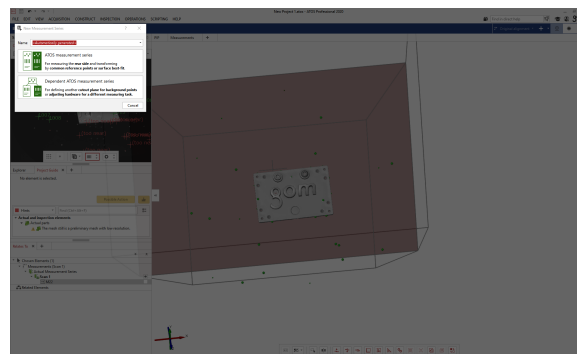


**Figure 2.7:** Image of the New Measurement Series Window

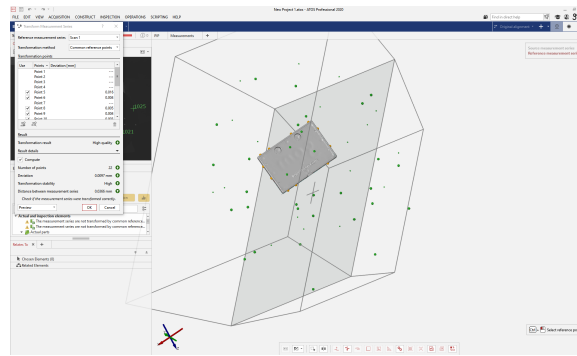


Figure 2.8: Image of the Transform Measurement Series Window

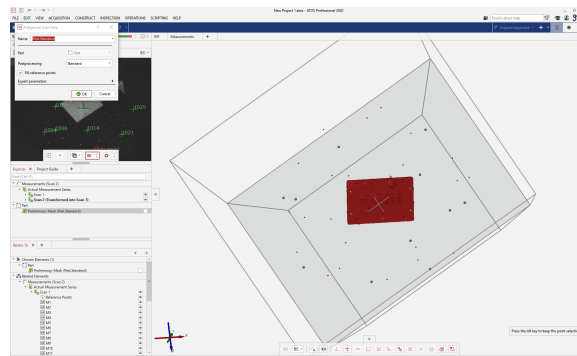


Figure 2.9: Image of the Polygonize Tool Window

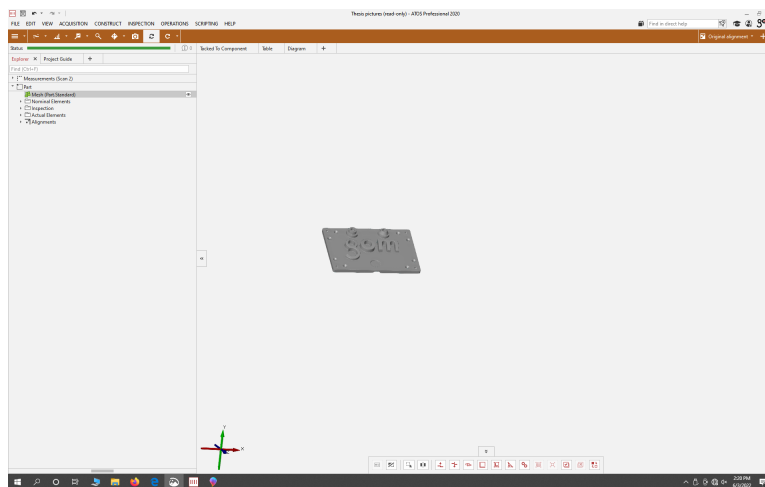


Figure 2.10: Image of the Inspection Workspace

and reporting pages either with an alignment between a mesh and CAD or on a mesh by itself. Surface comparison shows the distortion of the mesh surface when compared to the part computer-aided design (CAD). Inspection sections and pointwise inspections work similarly to surface comparisons, but along a specified curved or at a point, respectively. Deviation labels allow quick and easy verification of the distortion and numbers that can be placed on any point on the part. GDT allows the user to find the dimensions and determine if the tolerances are met when used in conjunction with the I-Inspect tool. The GDT tool also allows for these dimensions to be presented as part of a table. The “Create report page” tool allows images of the inspection to be compiled into a document that can be exported as a PDF. This will be addressed further in the Report section.

### **2.1.5 Report**

The Report workspace (Fig. 2.11) manages the style, order, and design of the report pages. In this workspace, the user can create pages of different sizes and types that are combined to generate reports and presentations that can be re-ordered and changed accordingly. The “Keywords” tool allows the user to standardize title pages with text boxes that can be completed with the desired information. Additionally, report pages can be used to override the inspection workspaces. The report page made in the report workspace can be exported as a PDF for convenient sharing and printing.

### **2.1.6 Mesh Editing**

The Mesh editing workspace (Fig. 2.12) is used to manipulate the polygonized mesh of a part, e.g., by applying the “Close holes” tool either automatically or interactively (Fig. 2.13). The automatic mode (Fig. 2.13a) works by highlighting the entire mesh using the “Select all” tool and entering the parameters before pressing “OK”. This allows the program to find all the holes smaller than the specified size and fill them in (e.g., 10  $\mu\text{m}$ ). The interactive mode (Fig. 2.13b) works by clicking on the mesh near the location of the hole that needs closing. Other tools in this workspace include the: smooth mesh, thin mesh, create mesh bridge, repair mesh, and refine mesh tools. The “Thin mesh” tool lowers the detail of the

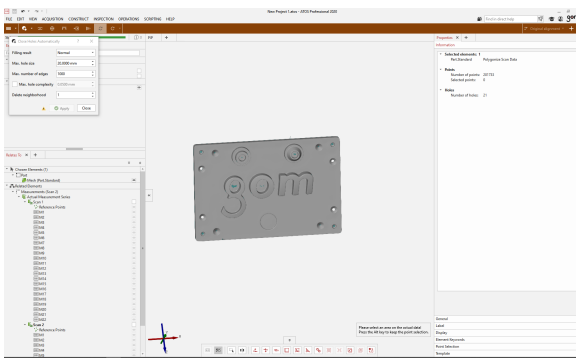


mesh in the section that is selected. The “Create mesh bridge” tool creates a mesh bridge between two selected points as long as the points are on the edge of the mesh, and the “Refine mesh” tool increases the mesh density and detail.

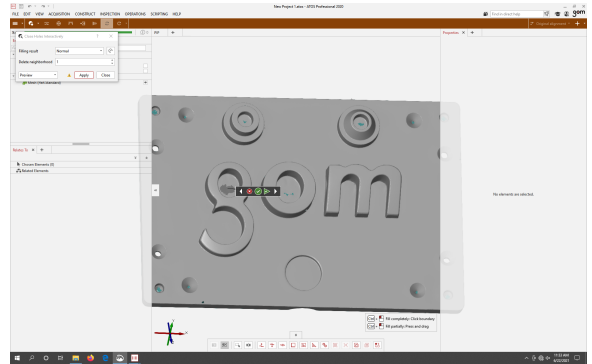
## 2.2 Information on ATOS Q

The ATOS Q structured light scanner (Fig. 2.14) used in this study collects eight million points per scan and uses LEDs as a light source. The scanner can be set up with multiple measurement areas from 100 mm x 70 mm to 500 mm x 370 mm. The measuring area applied in the measurements presented here is 350 mm x 260 mm. The distance between points ranges from 0.04 mm to 0.15 mm and the working distance of the scanner is 490 mm. The scanner weighs approximately 4 kg and has a volume of approximately 340 mm x 240 mm x 83 mm. The ATOS Q scanner connects with the computer that runs GOM Inspect using a 10 m long fiber optic cable. The computer has a Windows 10 operating system. The measuring areas are labeled as measurement volumes. There are five measurement volumes that are named using the width of the measuring area (in mm).

The five measuring volumes are: 100, 170, 270, 350 and 500. The 350 measuring volume is the one used during this project. In order to change the measuring volume of the ATOS Q, the original optics are unscrewed and stored, and the new optics are screwed into the scanner body. The scanner is then calibrated using the appropriate calibration panel. The ATOS Q has stereo cameras that are located at fixed positions relative to its projector. The camera positions produce three views: right, left, and combined. The ATOS Q is also capable of triple scan and filtering ambient light. Triple scan performs three scans, at two times and three times the original exposure time. The professional version of GOM Inspect is used to analyze the repeatability and reproducibility of the GOM ATOS Q structured light scanner for this study. For additional information, visit the GOM website [6].



(a) Automatically



(b) Interactively

**Figure 2.13:** Tool to Close Holes in Polygonized Mesh



**Figure 2.14:** Image of the GOM ATOS Q Scanner [16]

# Chapter 3

## Repeatability and Reproducibility

### Methods

Repeatability and reproducibility studies were completed using the GOM Inspect software and an ATOS Q scanner. The artifact used for the study contained 10 circular holes with different diameters and four steps with different heights (Fig. 3.1). This artifact was scanned using different strategies. For the repeatability study, 15 different positions were selected and five back-to-back scans were completed at each position. This information was then used to demonstrate repeatability by randomly selecting a single random scan from each position to produce a part model. Reproducibility was assessed by completing full scans at different positions. These procedures were also performed using a reduced number of positions (i.e., 10 and five) to see how the number of positions affects repeatability and reproducibility. Inspections were performed to measure the circle diameters, the four heights, the distance between circle centers, and the X and Y locations of the circle centers. The methods used during the study and results of the study are provided in the following sections.

### 3.1 Measurement Artifact

The first step in the study was to design a part containing several measurable features. The artifact used for the study was designed to be machined from 50.8 mm x 50.8 mm aluminum stock cut to a 101.6 mm length. The geometry included 10 holes of different diameters in



a two by five grid and four different step heights, two along each 101.6 mm length side as shown in 3.1. Once the part was designed with 10 holes ranging in diameter from 3 mm to 16 mm and four heights of 20, 25, 30, and 35 mm, the digital part was exported as an STL file. The locations of the circles and heights are displayed in Fig. 3.2. The STL file was then used to create computer numerically controlled (CNC) machining tool paths using Fusion 360. After selecting the cutting tools and defining the tool paths used to create each feature, the program was exported to a USB so it could be transferred to the five-axis Haas UMC-750 milling machine. Next, the cutting tools were loaded into the milling machine and the aluminum stock was placed on the machine table and located in the machine coordinate system. The program created in Fusion 360 was then executed on the milling machine to produce the artifact. Since the part was made from aluminum, it was too shiny to scan effectively, so the part was sandblasted to a satin finish.

## **3.2 Repeatability and Reproducibility Assessment**

### **Procedure**

The measurement artifact discussed in 3.1 was then scanned five times back-to-back in each of 15 positions to collect 75 scans. Then, a random scan from each position was selected to form a mesh composed of 15 measurement locations. The mesh was exported as an STL file and then imported into a multi-stage project. Using the Inspection workspace, cylinders were constructed in each of the holes. These cylinders were then intersected with a plane at the top of the part to create circles and center points for each of the holes. The diameter of the circles and X and Y locations were measured at this point. Using the center points of the circles and the two-point distance tool, the distances between the circle centers were measured, as well as the X and Y center coordinates.

The step heights were constructed using the projected point difference between planes at the top of the part and the bottom of the steps and the Z distance was measured. The multi-stage project enabled multiple meshes to be measured simultaneously allowing the data for the study to be contained in a single place for all of the elements. The elements included:

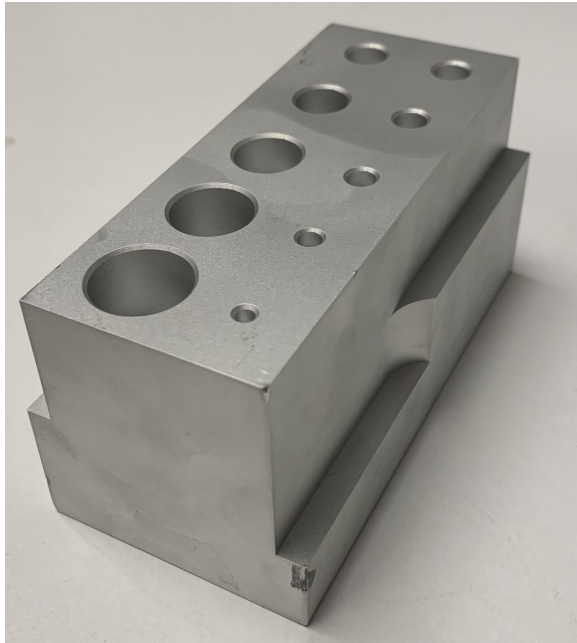


**Figure 3.1:** Image of the Part Used During the Study

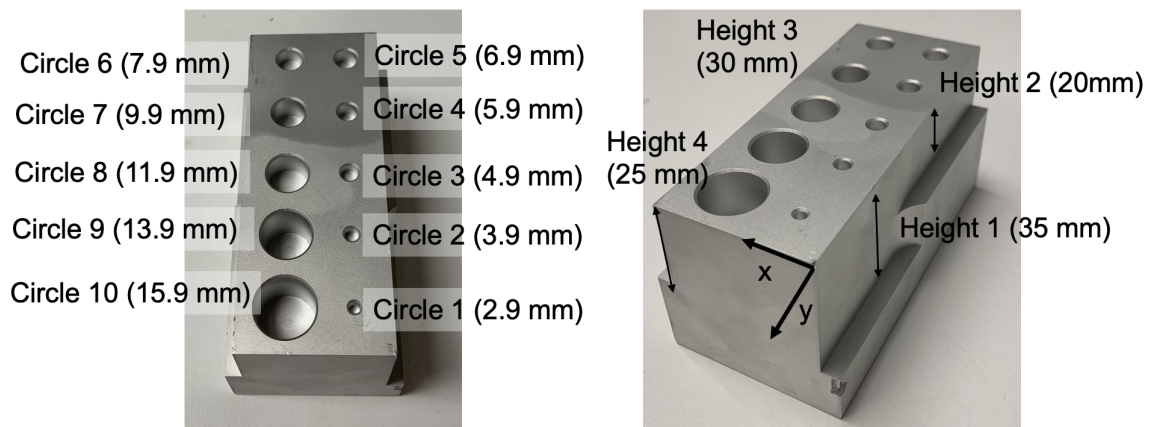
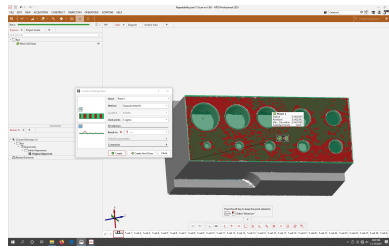


**Figure 3.2:** Image of the Part Including the Locations of Circles and Heights

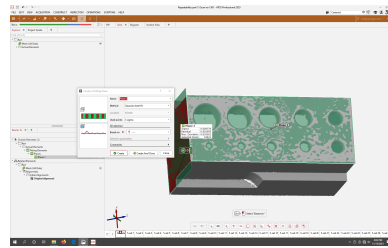
10 circles of different diameters, four different heights, 90 distances formed between circle centers, and 10 X and Y locations of circle centers.

The Inspection workspace was used to create the measured elements including circle diameters, heights, X and Y locations of the circle centers, and distances between the circle centers. Before these were defined, a local coordinate system was created to set the local coordinate system as a global coordinate system and line up all the meshes and their measurements. In order to create a local coordinate system, three geometric elements needed to be created first. For this study, three planes were used. These planes were constructed using the Construct fitting plane tool. The first plane (Plane 1) was constructed on top of the part by control clicking to select points on top of the part in the Construct fitting plane tool (Fig. 3.3a). Planes 2 and 3 were also created using this dialog box by clicking the short side of the part next to circles 1 and 10, the smallest and largest circle (Fig. 3.3b) and the long side with the five smallest circles respectively (Fig. 3.3c). The local coordinate system was defined using the Construct coordinate system by geometric elements tool. Inside the Construct coordinate system by geometric elements tool, the planes were selected in order to ensure that the positive Z axis was coming out the top of the part and the positive X axis was defined along the intersection of planes 1 and 2 (Fig. 3.4). Then, the local coordinate system was set as the global coordinate system using the by Coordinate system tool under the main alignment found in the operations menu (Fig. 3.5).

The next step in creating the elements started by constructing cylinders based on the holes in the part from smallest to largest going around counterclockwise (Fig. 3.6). Center points were then constructed in order using the Construct intersecting points tool with the cylinder as the line and Plane 1 as the intersecting element on top of the part for each cylinder (Fig. 3.7). The X and Y locations of these points were then determined using the Check tool in the I-Inspect tool referenced to the origin. The circles were then created using the Construct intersection circle cylinder/cone tool from the cylinders and points of creation elements (Fig. 3.8). The Check tool in the I-Inspect tool was used to find the diameters of the circles. The distances between circle centers were created using the Construct two point distance tool with the center point being referenced as point 1 and the centerpoint being measured to as point 2 (Fig. 3.9). The numerical XY distance was determined using the



(a) Plane 1



(b) Plane 2



(c) Plane 3

**Figure 3.3:** Creation of Planes 1, 2 and 3

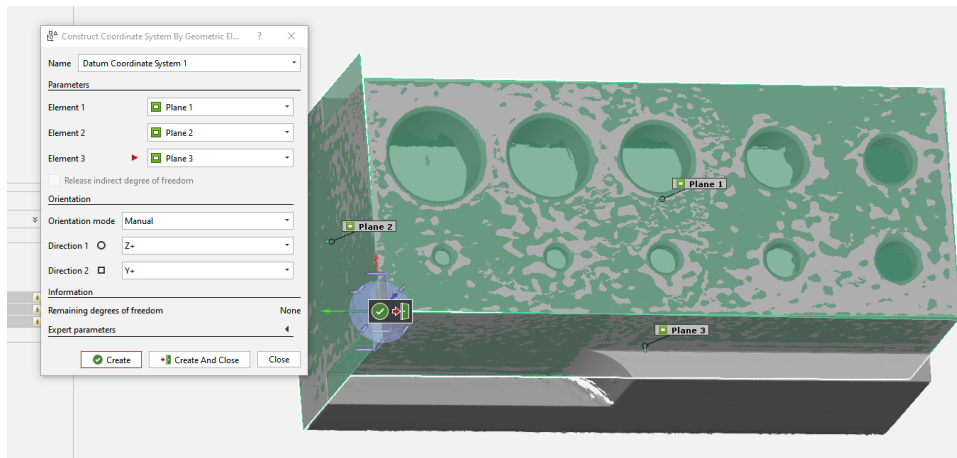


**Figure 3.4:** Creation of the Local Coordinate System

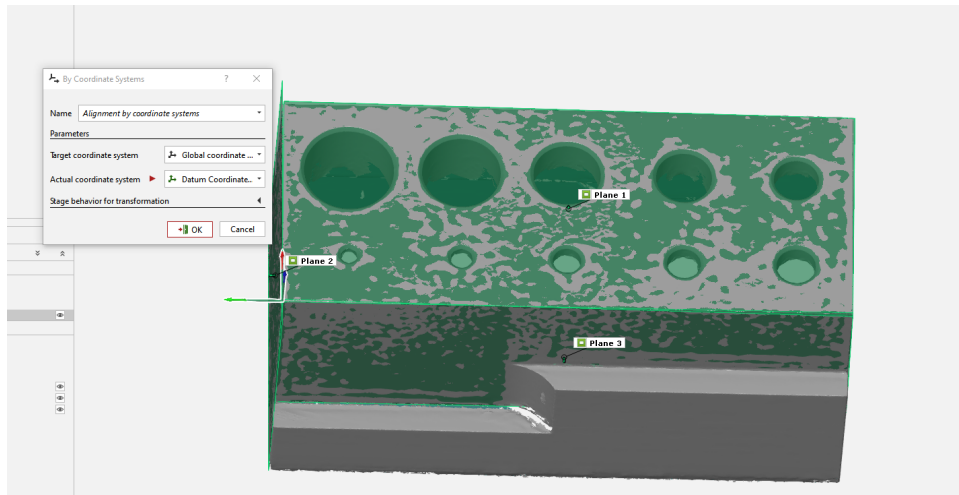


**Figure 3.5:** Setting the Local Coordinate System as the Global Coordinate System

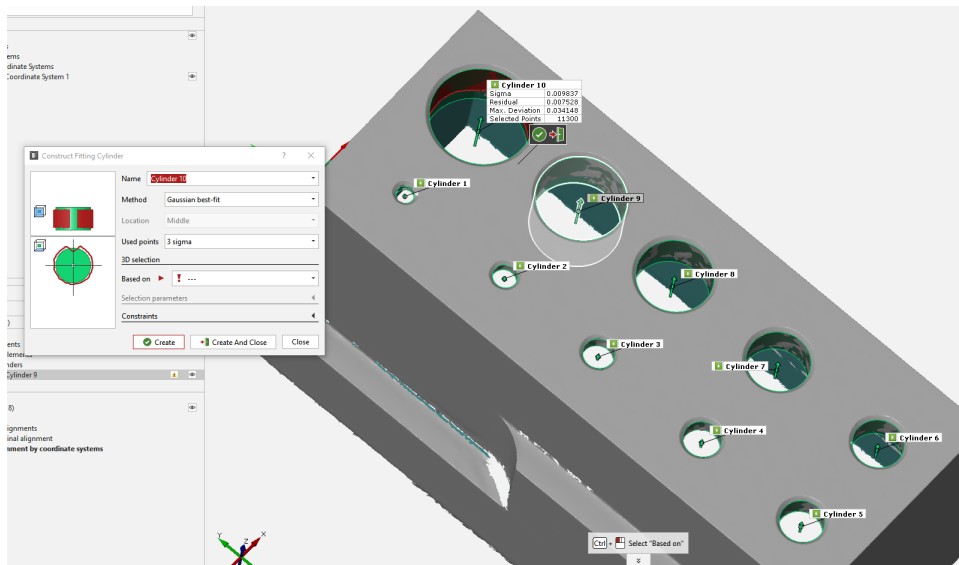


**Figure 3.6:** Construction of Cylinders Based on Holes

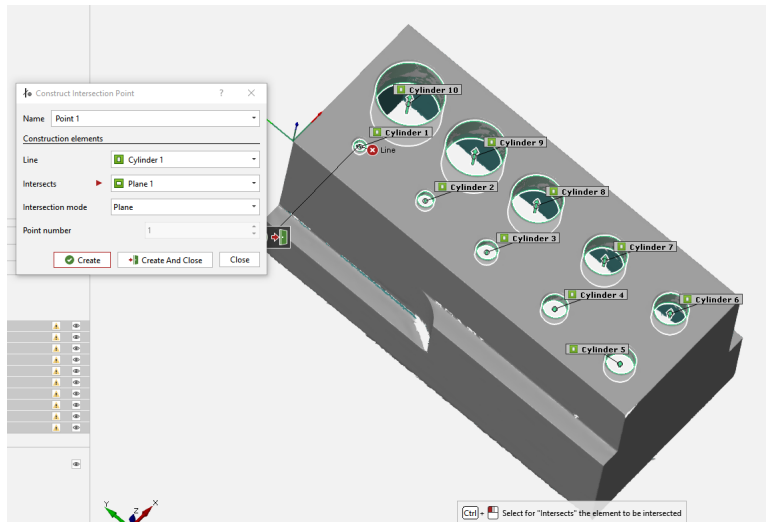


Figure 3.7: Creation of the Center Points from Cylinders and Plane 1

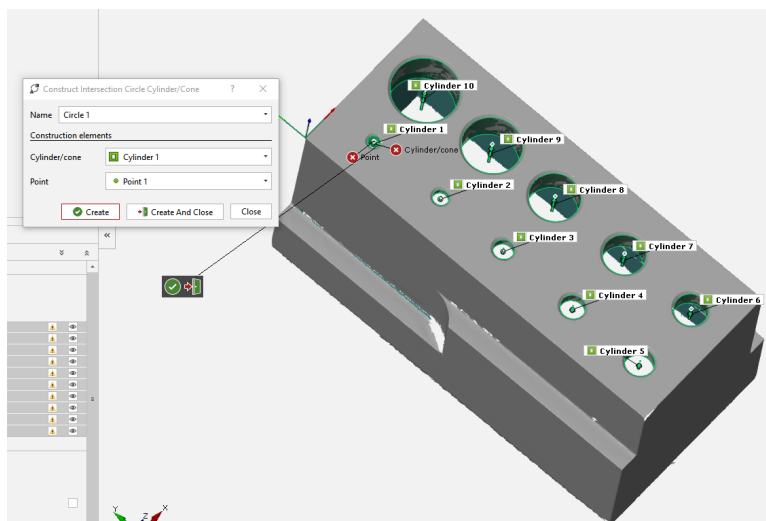
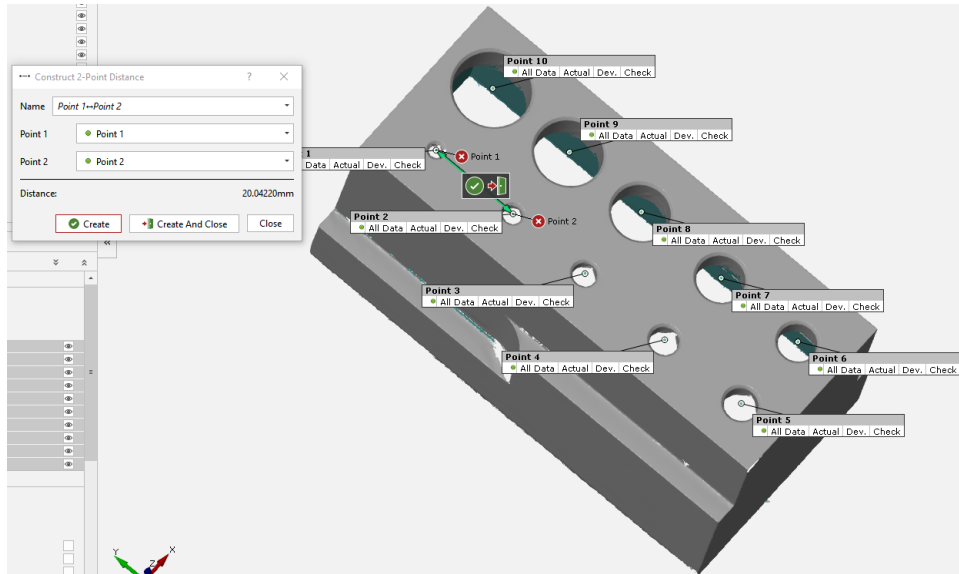


Figure 3.8: Creation of the Circles Based on the Cylinders

check tool under the I-Inspect toolbar. To create the heights, fitting planes needed to be constructed on each ledge using the Construct fitting plane tool with height 1 being the ledge closest to the origin continuing to height 4 by going counter-clockwise (Fig. 3.10). Surface points then needed to be created at the center of the height planes by using the Construct surface point tool and control clicking on the height planes for each individual point (Fig. 3.11). The height distances were created using the Construct projected point distance tool. Each surface point was projected onto Plane 1 on the top of the part (Fig. 3.12). Finally, the Z distance of the heights were determined using the Check tool in the I-Inspect toolbar. These elements were then used to determine the repeatability and reproducibility of the GOM ATOS Q structured light scanner for the selected artifact. Since the circle diameters were an important part of the study, extra steps were taken to determine how many points from a scan were used to construct the circles.

In order to show how the number of points used to create a circle affects the range in deviation of measurement, five cross sections (planes) at different Z heights for each hole were used to create circles for five diameters of each hole. First, cross sections had to be created to find the number of points used to create the circle. The first step to creating cross sections was to use Construct sections and select Multi section parallel to open the cross section element creation dialog box. To create the sections, first a reference plane was selected to which parallel cross sections could be created (Fig. 3.13). The next step was to select all the points in the mesh of the part using the Select entire mesh button (Fig. 3.14) and the distance between sections was entered as 0.1 mm. Smaller distances between sections take longer to run, but gives more options of cross sections to use to find the points. Too small of a distance would make the runtime impractical, but larger distances between the sections reduce the available data. Finally, the Create button is pressed and the cross-sections of the part are generated (Fig. 3.15). From here only cross sections containing useful information are kept to reduce the file size of the GOM project being used to create and contain these elements (Fig. 3.16). This ensures that the used cross-sections remain consistent even when the number of positions is reduced for the repeatability part of the study. In the end, only five cross-sections were used to find the number of points used to create the circles. The Construct fitting circles tool was used to create circles at the Z heights (Fig. 3.17). The



**Figure 3.9:** Creation of Distances Between Circle Centers

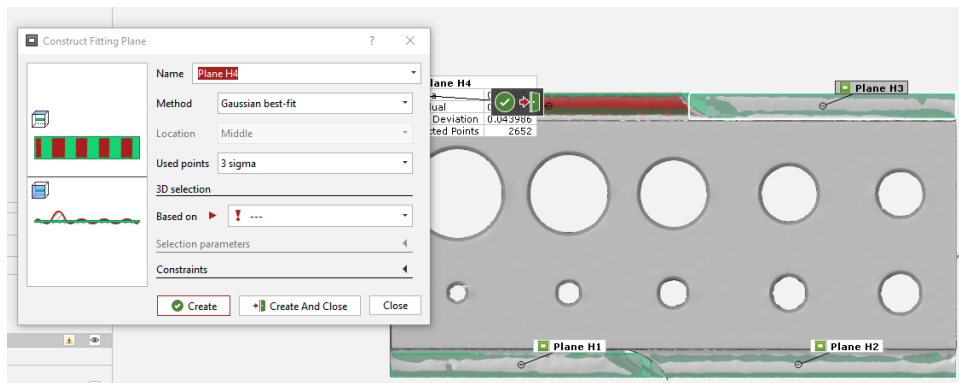


**Figure 3.10:** Constructing Fitting Planes Along Ledges for Heights



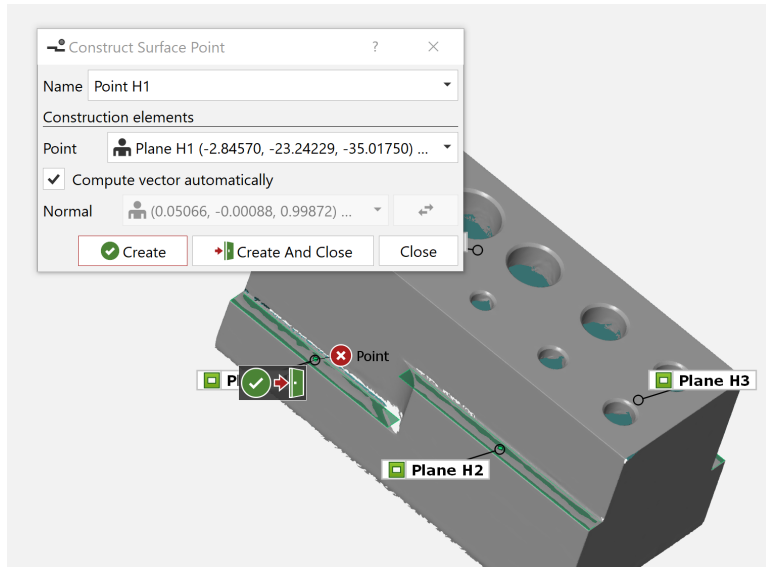


**Figure 3.11:** Construction of the Height Surface Points

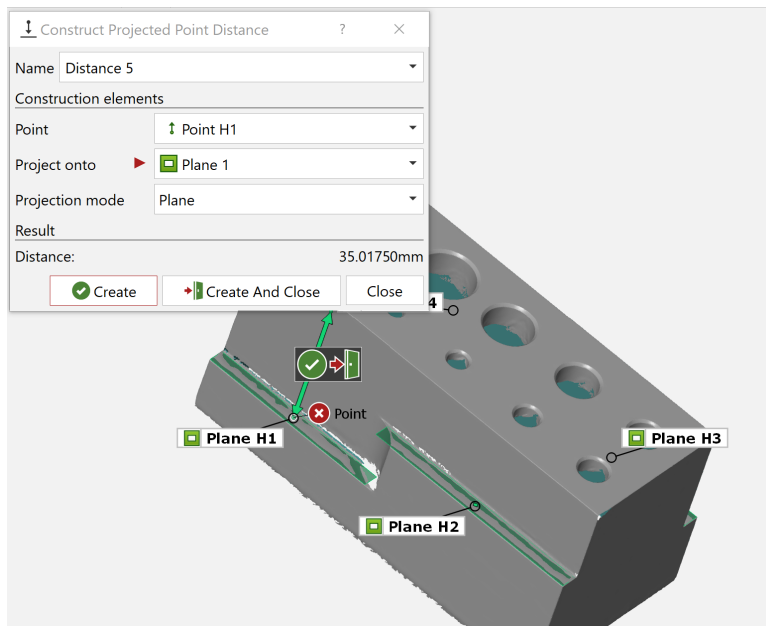


**Figure 3.12:** Construction of Height Distances Using Projected Point Distance

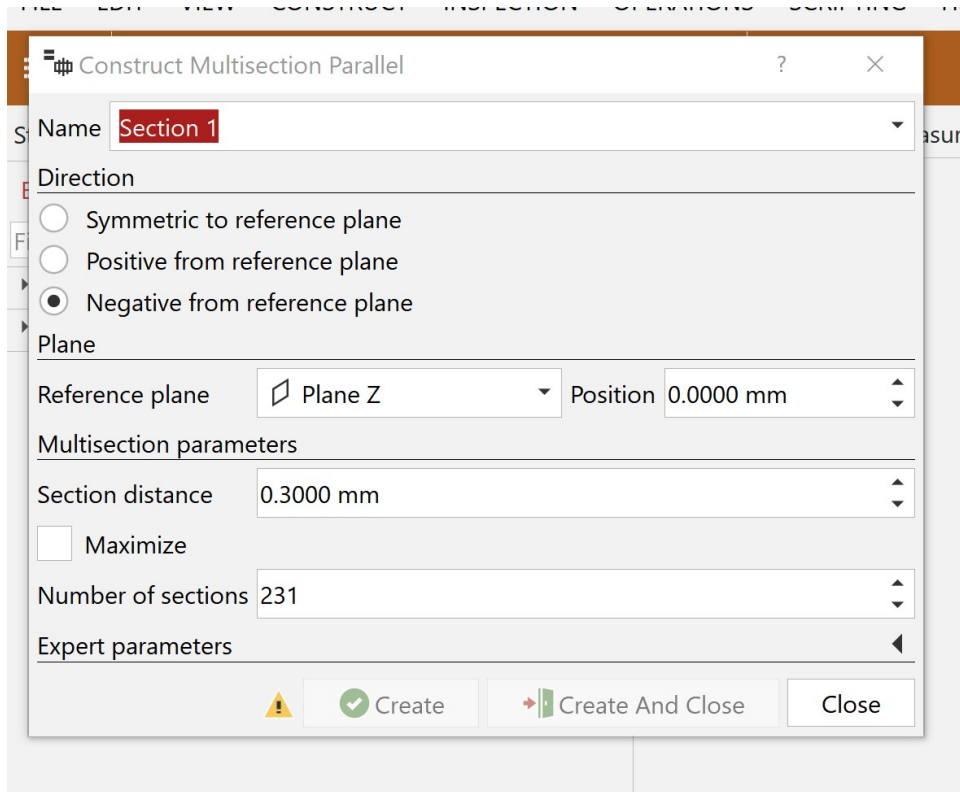


Figure 3.13: Multisection Parallel Dialog Box

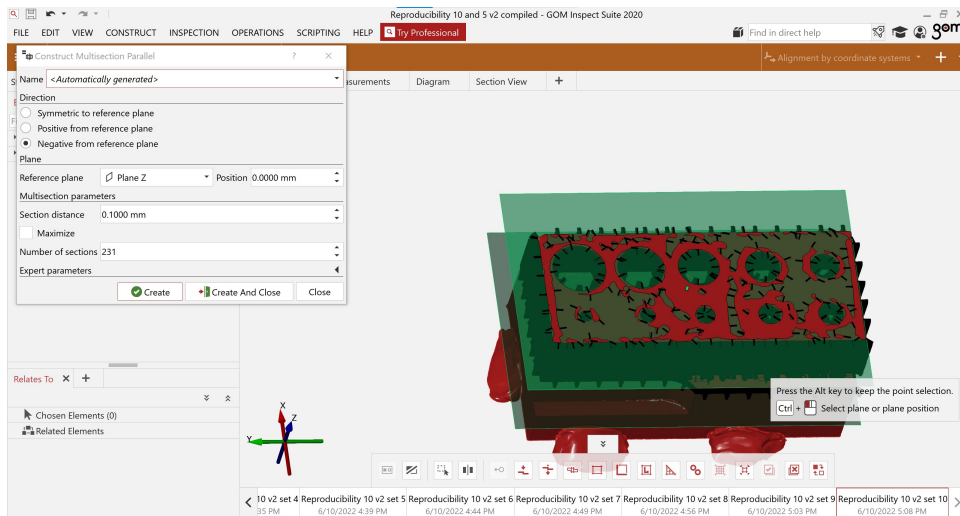


Figure 3.14: Select All Points in Mesh

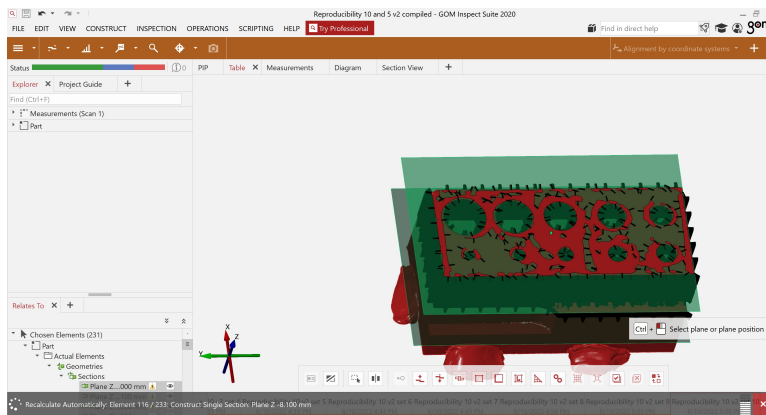


Figure 3.15: Construction of Cross-sections

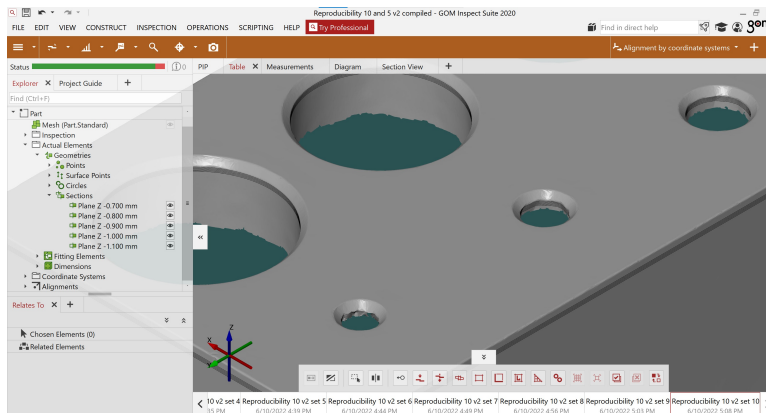


Figure 3.16: Only Useful Information Kept

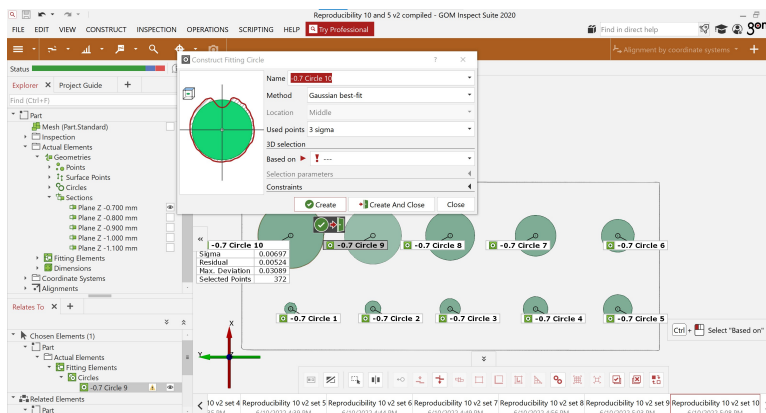


Figure 3.17: Construction of Fitting Circles on each Cross-section

points around each of these on each of the five cross-sections were counted by GOM Inspect (Fig. 3.18). These numbers were input into an Excel worksheet and averaged (Fig. 3.19). Then, all of the numbers were plotted as a bar graph. The results showed that circle 1 (smallest diameter) had fewer than 200 points. This was the least amount of points used to construct the circle fit and explains the higher deviation and larger range. The cross section images demonstrate how the lack of points make circle 1 appear less round because there were fewer points available from the scan (Fig. 3.20). The larger diameter circles, with more points used to create the circle fit, have lower deviations and smaller ranges. They also appear more circular in the cross-section images than circle 1, showing that the more points used to create circular elements, the higher the repeatability at the measurements.

Using the GDT tool in the inspection workspace, numerical measurements of the elements were produced. These measurements were then compiled by element in a table located under the Table tab in the inspection workspace. To create the histograms for each element several steps were completed. First, the actual dimensions of each element were exported from GOM Inspect as a CSV file for each set of 50 meshes (Fig. 3.21). The CSV files were then compiled into a single Excel workbook as individual sheet so that all the data for each position set was available in a single location using the macro excel program found on a Microsoft Excel Forum [13] (Figs. 3.22 and 3.23). The text of the program is provided in Appendix D. Next, the actual measurements of each element are collected into a single sheet in a separate Excel workbook. The actual measurements for each element from each mesh were combined into a single column of the Excel sheet (Fig. 3.24). Then, the data was selected and the histogram function was used to insert the graph into the sheet. Finally, the graph was formed in the worksheet (Fig. 3.25). After the graph was created, adjustments were made to increase readability (Fig. 3.26). For example, on the horizontal axis the bar width was adjusted to be 0.0005 mm. Using the compiled column of measurements, the mean, range, and standard deviation were determined for each element. These were used to create scatter plots comparing the range or standard deviation for heights, circle diameters, and X and Y center locations.

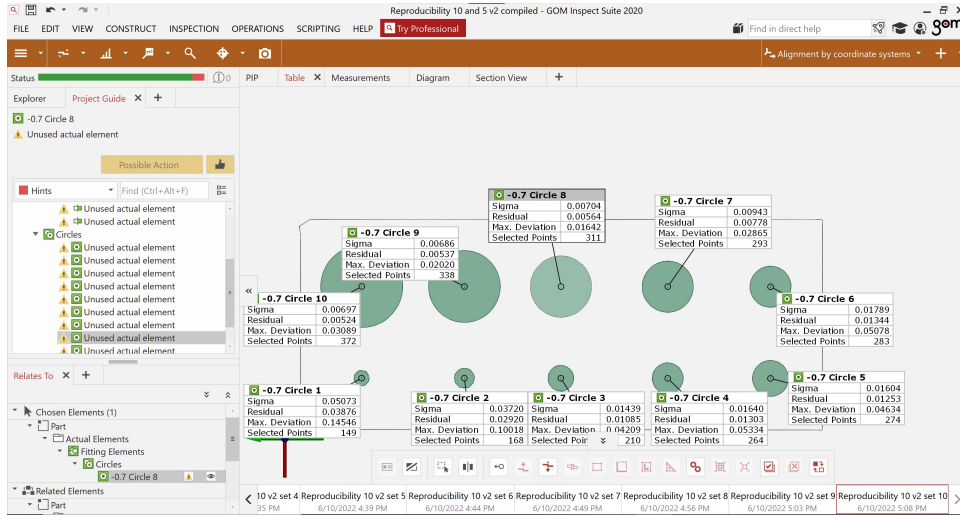


Figure 3.18: Points Used to Create Circle were Counted by GOM

	Average	Cross-section 1	Cross-section 2	Cross-section 3	Cross-section 4	Cross-section 5
Circle 1	163.2	178	160	158	160	160
Circle 2	241	238	238	239	242	248
Circle 3	322.8	304	327	335	325	323
Circle 4	362.2	338	364	374	361	374
Circle 5	373.8	355	373	386	382	373
Circle 6	448.4	424	441	455	460	462
Circle 7	476	430	460	491	504	495
Circle 8	529.8	497	528	540	550	534
Circle 9	576.6	518	572	590	591	612
Circle 10	663	614	658	690	680	673

Figure 3.19: Points Used to Create Circles were Averaged

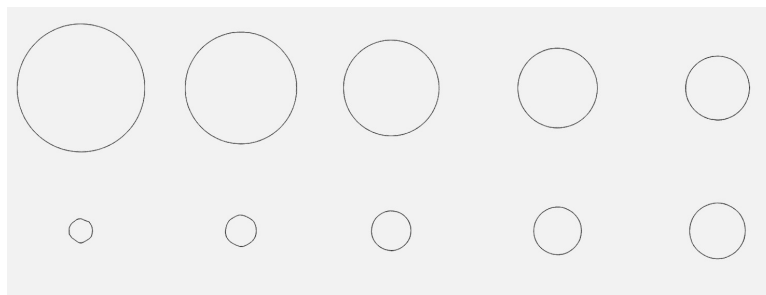


Figure 3.20: Image of the Circles on a Cross-section

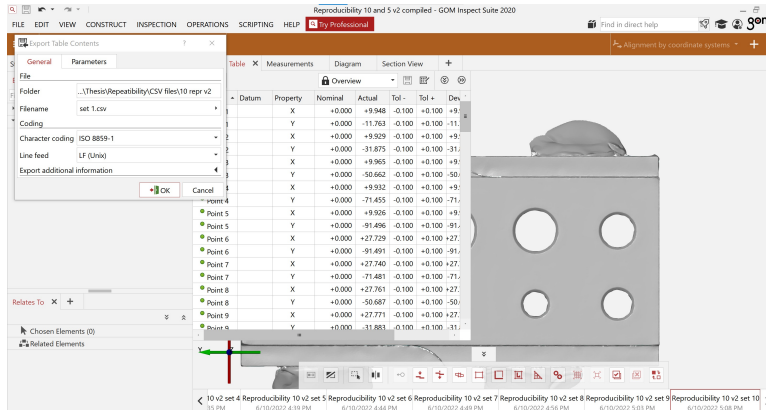


Figure 3.21: Export CSV File for each Mesh

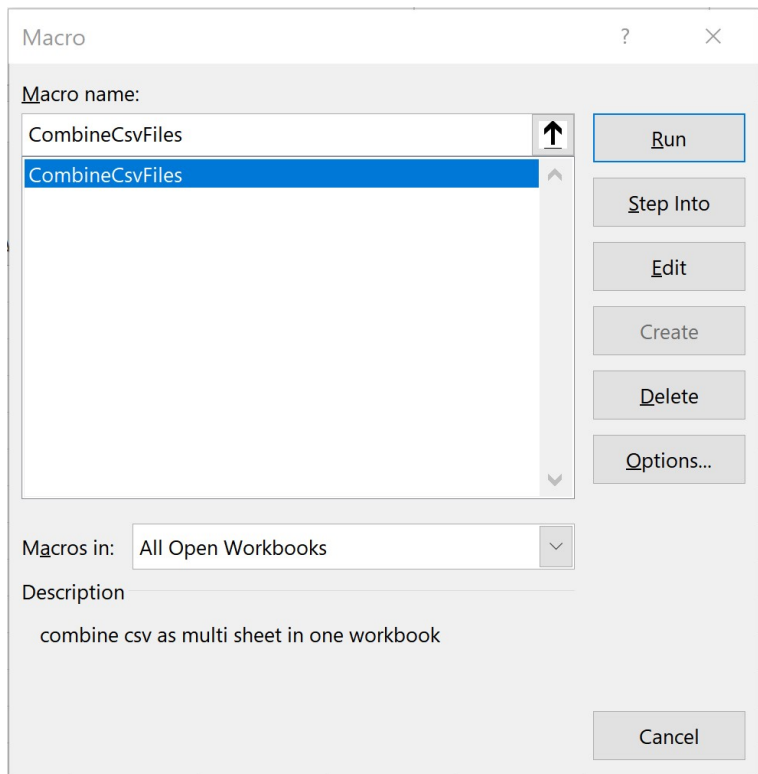


Figure 3.22: Use Macro Excel Program to Compile CSV Files

### 3.3 Repeatability

To assess repeatability, the measurements of the elements was completed for data sets created from 15 scan locations, where one of the five scans recorded at each location were randomly selected. The measurement of each element was plotted as a normalized histogram to show the distribution of the measurements. The following histogram (Fig. 3.27) shows the variance in measurements caused by using different combinations of scans taken from each of the fifteen positions. The circle diameters demonstrate that the smaller circles have a higher range than the larger circles. Example results are shown in Fig. 3.28 which plots the range of diameter variation versus the mean circle diameter. Fig. 3.28 also shows that decreasing the number of positions used to make the mesh increases the range. Example X location and Y location data for the centerpoint of each circle is displayed in Figures 3.29 and 3.30. Height results are shown in Fig. 3.31 which plots the range of the height measurements for each of the mean heights. The range is determined by subtracting the smallest measurement of an element from the largest measurement of the same element.

Repeatability was determined when reducing the number of positions used to form the measurements. Tests were performed with 15, 10, and 5 positions. The reduced position meshes were calculated using a subset of the positions used for the 15 position tests. The mean and standard deviation of the measurements were calculated for each number of positions. Scatterplots with error bars were used to describe scanner repeatability. Example results are shown in Figs. 3.32 and 3.33.

### 3.4 Reproducibility

In order to determine the reproducibility of the GOM ATOS Q when measuring the artifact, scans were completed at variable artifact locations/orientations. The number of locations was 15, 10, and 5. In each case, 10 repeats were performed using different locations. These scans were then used to repeat the measurements for circle diameter, height, distance between circle centers, and X and Y locations of circle centers. The individual sets of 10 meshes were analyzed to determine mean, standard deviation, and range of the measurements

for each element. Table 3.1 shows the angles of the rotary table that supported the part that were used for scanning during this portion of the study. During the scanning for the reproducibility, the temperature of the ambient air under the scanner was logged using a MadgeTech Temp101A data logger that took a reading every thirty seconds. Figures 3.34, 3.35 and 3.36 show that the temperature variation was approximately 1 deg in each case. The laboratory temperature was higher than standard metrology conditions (68 deg F/20 deg C), but the scanner was calibrated in the actual environment so this elevated temperature should not have a significant influence on the reproducibility results.

## 3.5 Verification

To verify the accuracy of the scanner data, a coordinate measuring machine (CMM) (Fig 3.37) was used to measure the circle diameters, step heights, distances between circles center, and the X and Y locations of the circle centers. This was completed using CALYPSO to program the ZEISS Duramax CMM using the part's CAD model. In order to program the CMM based on the CAD, the CAD has to be imported into CALYPSO as a STP file. Next, the coordinate system needed to be created by geometric elements including Planes 1, 2, and 3 to place the coordinate system at the same location that was used for the analysis of the scan data (Fig. 3.38). Once these were created, the clearance planes were set based on the CAD (Fig. 3.39). Next, planes were created on the height ledges (Fig. 3.40) so that the Cartesian distances between the height planes and Plane 1 along the top of the part could be determined (Fig. 3.41). Then, circles 2 through 10 were created using the Create circle on cylinder tool with the X, Y and diameter characteristics activated (Fig. 3.42). Circle 1 is not large enough to fit the sensor tip so any measurements that used Circle 1 were not taken. To create the distances between the circle centers, the Polar caliper distance tool was used (Fig. 3.43). The circle center distances were created using the circle as at the center and projected onto Plane 1. Finally the program was executed using manual alignment and a report was generated (Fig 3.44). This report is located in Appendix E and is compared to the mean values determined by structured light scanning.



**Table 3.1:** Reproducibility Position Locations (values are angles of the rotary table that supported the part in units of deg)

Set	15 Positions	10 Positions	5 Positions
Set 1	0, 24, 50, 70, 96, 120, 145, 170, 190, 215, 240, 265, 290, 315, 335	0, 35, 70, 110, 145, 180, 215, 250, 290, 325	45, 115, 190, 260, 335
Set 2	10, 35, 60, 80, 105, 130, 155, 180, 200, 225, 250, 275, 300, 320, 345	0, 45, 70, 110, 135 180, 225, 250, 290, 315	10, 80, 155, 225, 300
Set 3	0, 30, 45, 60, 90 120, 135, 150, 180, 210 225, 240, 285, 315, 330	20, 45, 90, 135, 155 200, 225, 270, 315, 335	0, 70, 140, 220, 290
Set 4	10, 40, 55, 70, 100 130, 145, 160, 190, 220 235, 250, 295, 325, 340	30, 60, 90, 120, 150 210, 240, 270, 300, 330	30, 120, 210, 240, 300
Set 5	5, 35, 50, 65, 95 125, 140, 155, 185, 215 230, 245, 290, 320, 335	10, 40, 70, 100, 130 190, 220, 250, 280, 310	50, 120, 190, 250, 330
Set 6	15, 45, 60, 75, 105 135, 150, 165, 195, 225 240, 255, 300, 330, 345	20, 50, 80, 110, 140 200, 230, 260, 290, 320	15, 70, 140, 220, 280
Set 7	20, 50, 65, 80, 110 140, 155, 170, 200, 230 245, 260, 305, 335, 350	20, 45, 70, 115, 135 180, 225, 270, 315, 335	20, 80, 170, 230, 315
Set 8	20, 35, 55, 85, 100 135, 155, 180, 230, 250 275, 290, 300, 315, 340	5, 50, 105, 135, 190 230, 280, 300, 325, 350	25, 70, 145, 245, 320
Set 9	25, 50, 75, 100, 120 145, 170, 195, 220, 240 265, 290, 315, 340, 355	25, 55, 90, 125, 160 240, 275, 300, 320, 355	35, 110, 190, 250, 310
Set 10	5, 20, 50, 65, 95 110, 140, 185, 200, 230 245, 275, 290, 320, 335	5, 50, 105, 140, 190 230, 255, 275, 290, 320	5, 75, 145, 225, 295

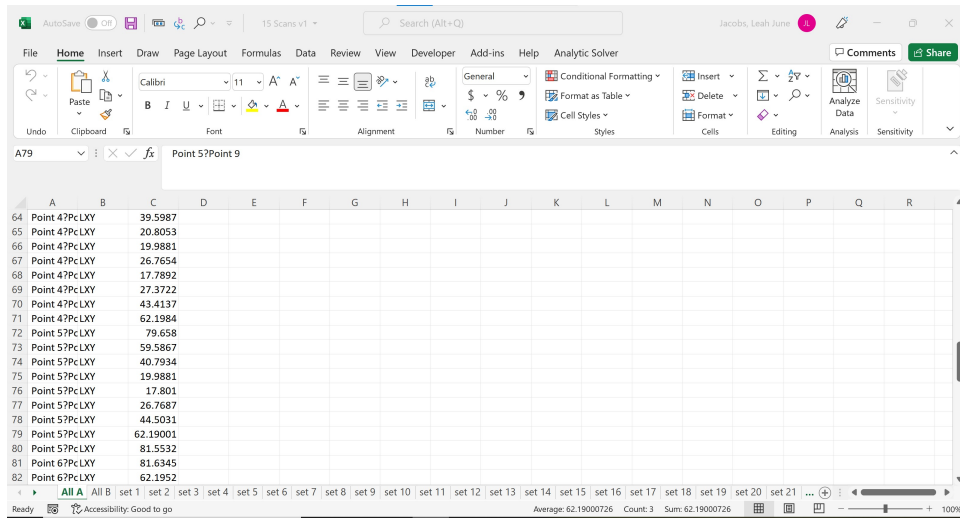


Figure 3.23: All CSV Files in a Single Excel Workbook

	A	B
6	9.9817	
7	9.9779	
8	9.9643	
9	9.9775	
10	9.9647	
11	9.9809	
12	9.959	
13	9.9681	
14	9.9625	
15	9.9648	
16	9.9695	
17	9.9738	
18	9.9741	
19	9.9681	
20	9.9703	
21	9.9437	
22	9.9801	
23	9.962	
24	9.9369	

◀ ▶ **Point 1 x** |  
 Ready Accessit

**Figure 3.24:** Data for Each Element Compiled into a Single Column of Separate Excel Workbook

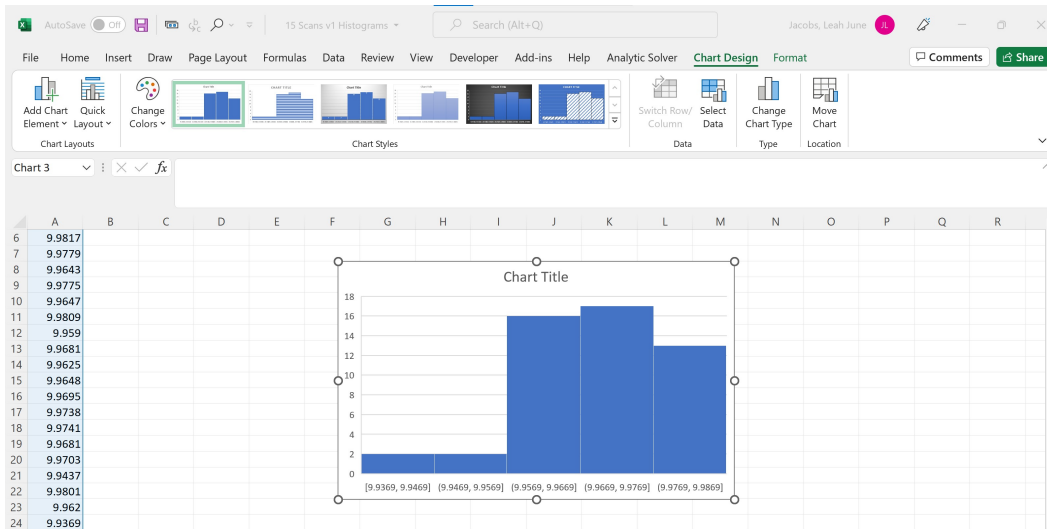


Figure 3.25: Histogram Formed in the Worksheet

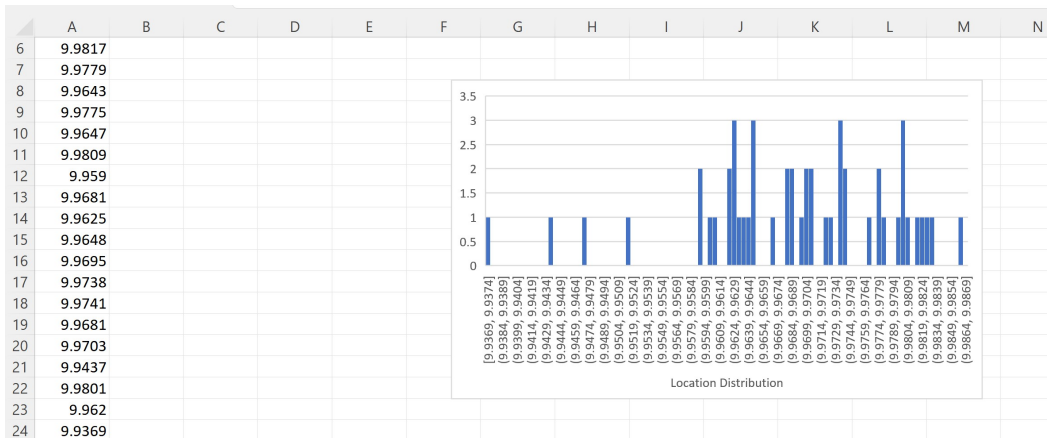
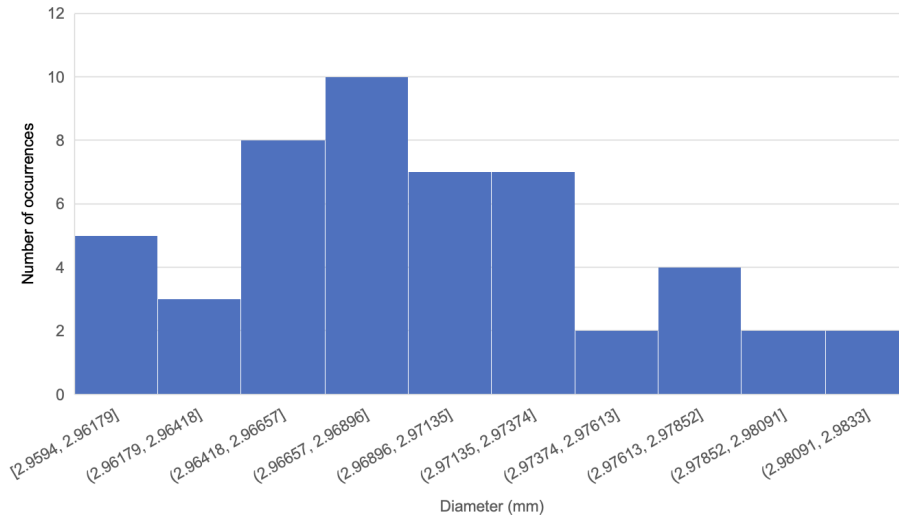
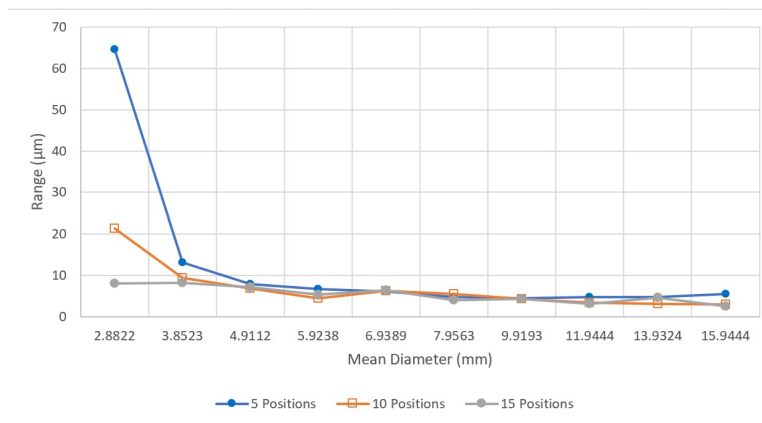


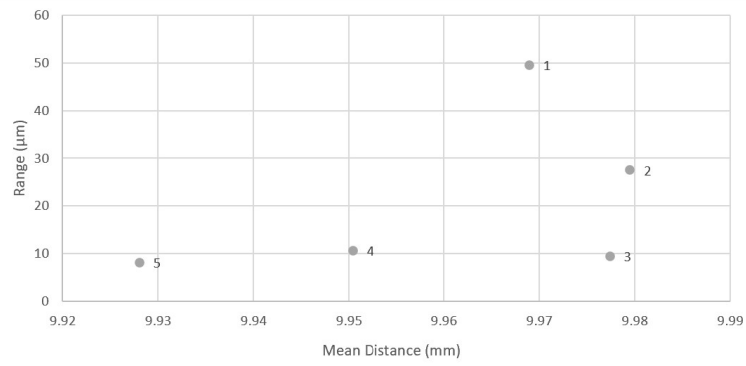
Figure 3.26: Adjustments Made to Increase Readability



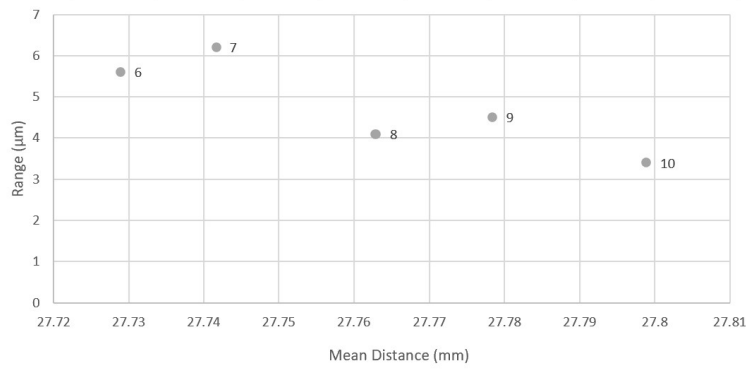
**Figure 3.27:** Circle 1 Histogram for 50 Randomly Selected Scan Sets at Same 15 Positions



**Figure 3.28:** Graph Showing the Range of the Measured Diameters Plotted Against the Mean Diameter for 15, 10, and 5 Positions

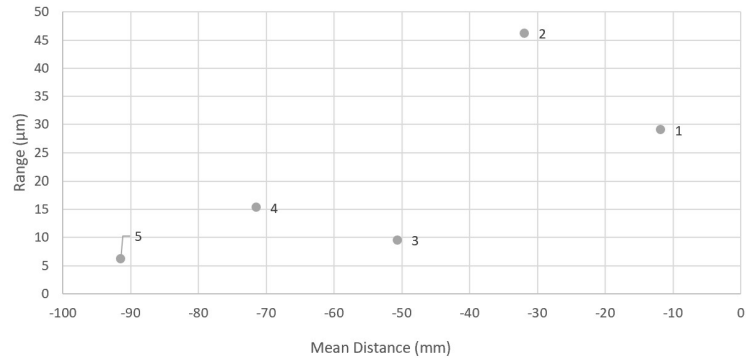


(a) 1-5 X Location

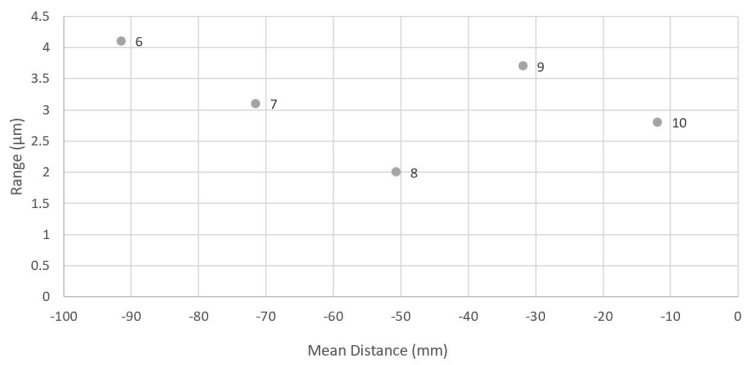


(b) 6-10 X Location

**Figure 3.29:** Variation in X Location Range for 10 Circles with 15 Scanning Positions



(a) 1-5 Y Location



(b) 6-10 Y Location

**Figure 3.30:** Variation in Y Location Range for 10 Circles with 15 Scanning Positions

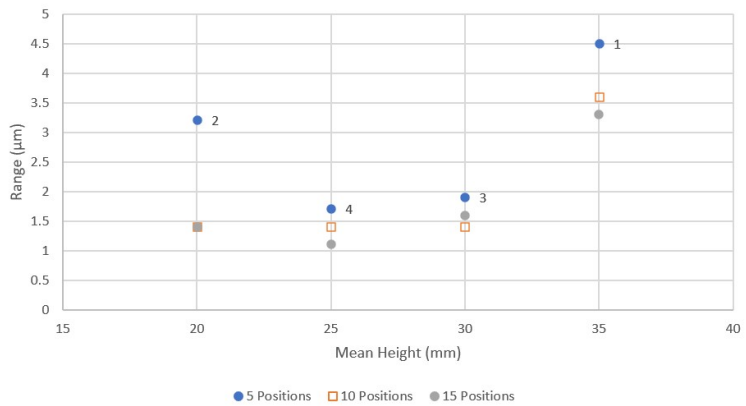


**Figure 3.31:** Graph showing the range of the height measurements plotted against the mean height for 15, 10, and 5 positions

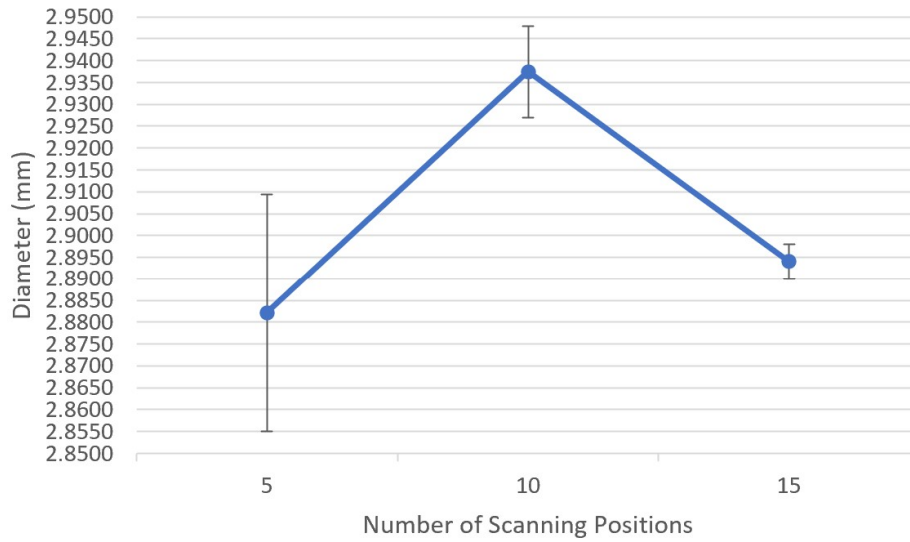


**Figure 3.32:** Graph Plotting Mean Diameter for 15, 10, and 5 Positions with Error Bars Showing Standard Deviation for Circle 1

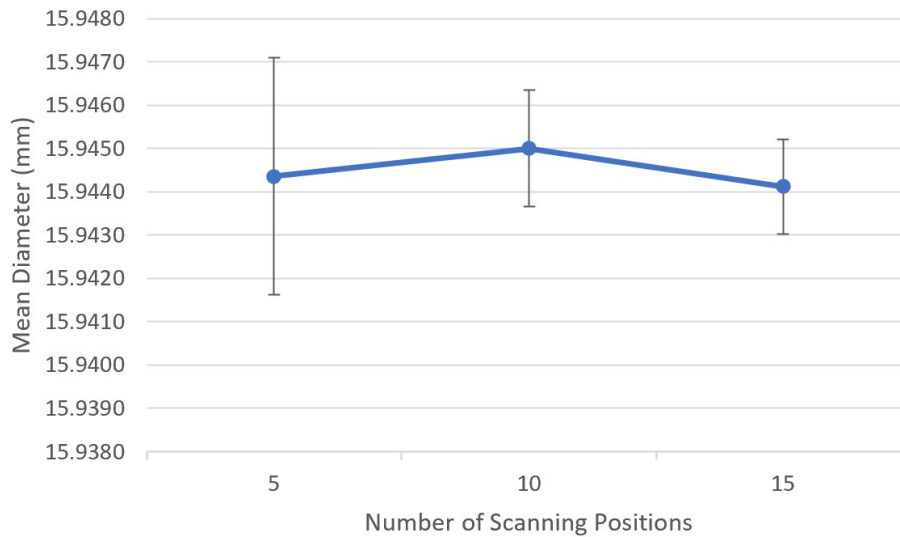


**Figure 3.33:** Graph Plotting Mean Diameter for 15, 10, and 5 Positions with Error Bars Showing Standard Deviation for Circle 10



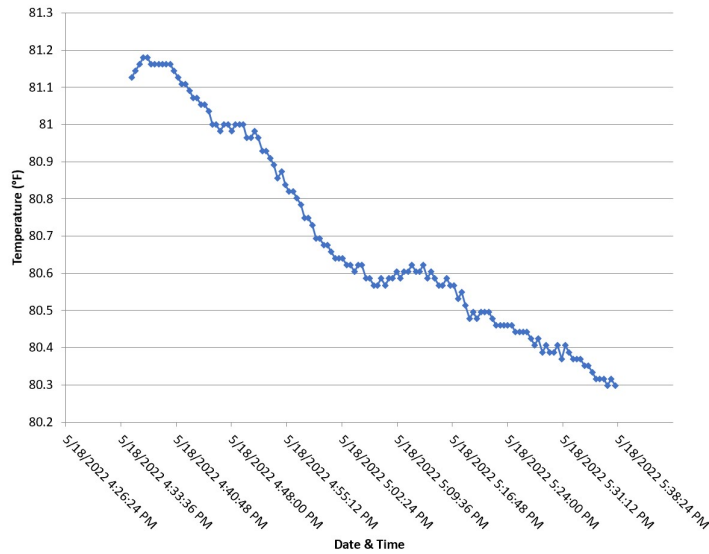


**Figure 3.34:** Graph Showing the Temperature Variation that Occurred While Scanning the Part Using 15 Positions for Reproducibility

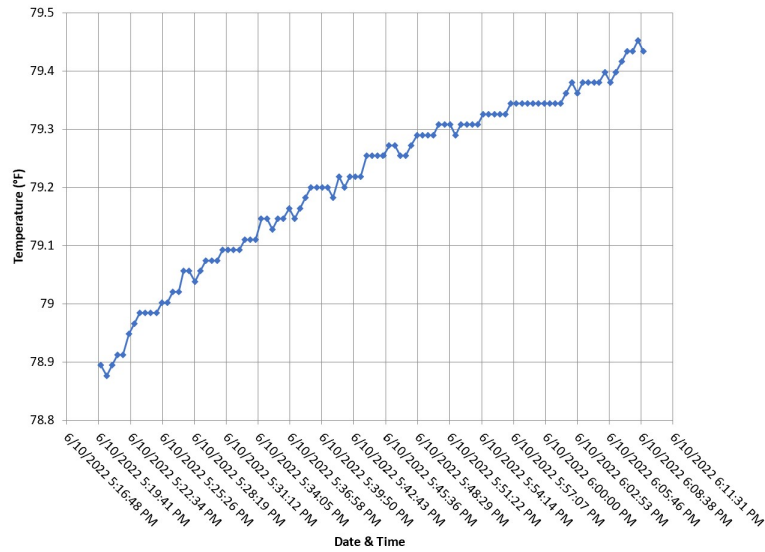


**Figure 3.35:** Graph Showing the Temperature Variation that Occurred While Scanning the Part Using 10 Positions for Reproducibility

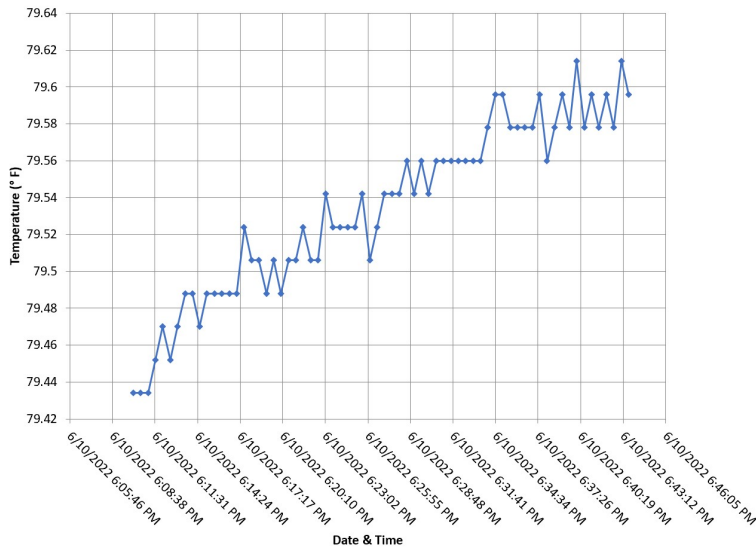


**Figure 3.36:** Graph Showing the Temperature Variation that Occurred While Scanning the Part Using 5 Positions for Reproducibility



**Figure 3.37:** Image of the CMM used to perform the Measurements

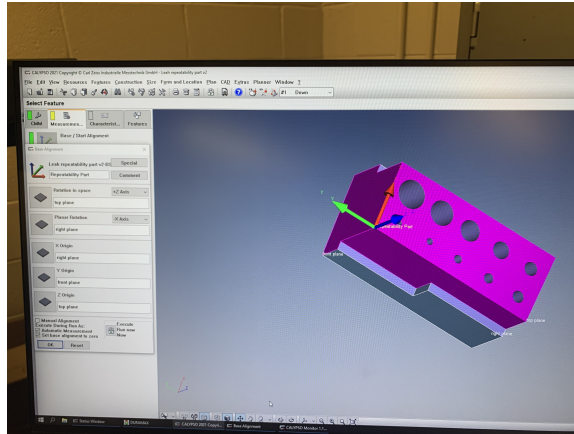


Figure 3.38: Image of the Coordinate System Created in Calypso

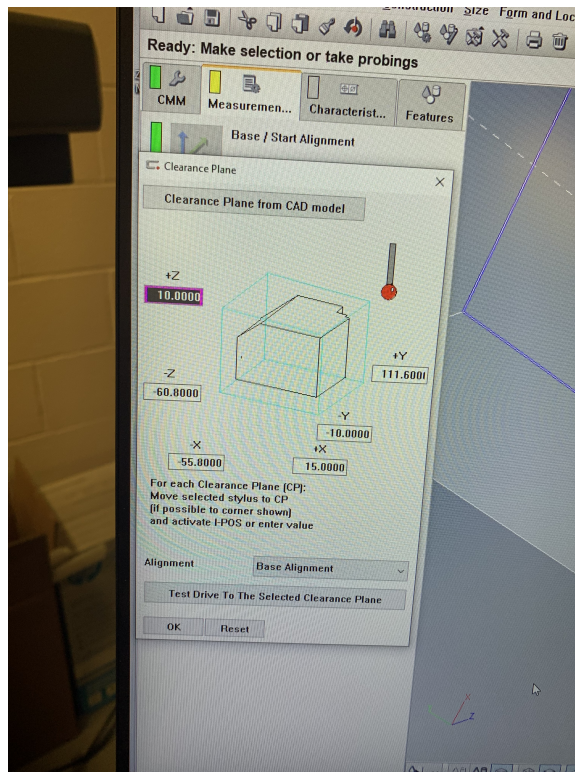


Figure 3.39: Creation of Clearance Planes Based on CAD

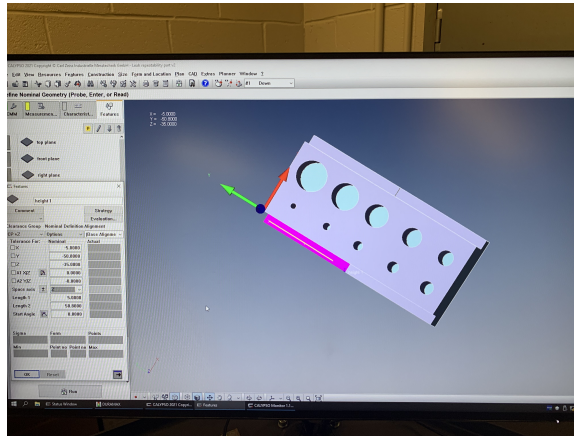


Figure 3.40: Create Plane on Height Ledge

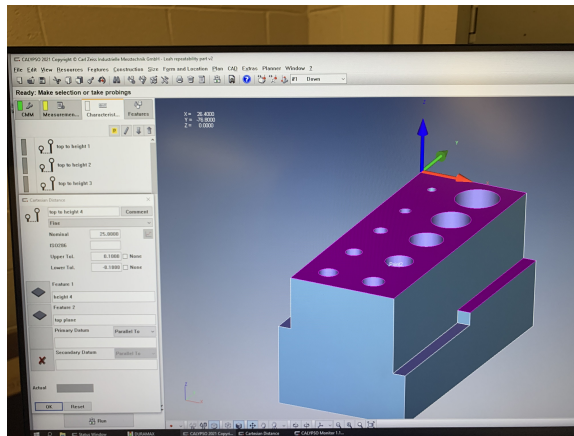


Figure 3.41: Creation of Height Measurement Using Cartesian Distances

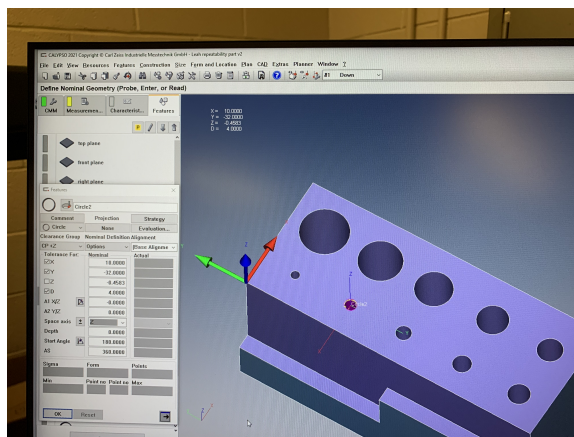


Figure 3.42: Creation of Circles 2-10 on the Cylinders

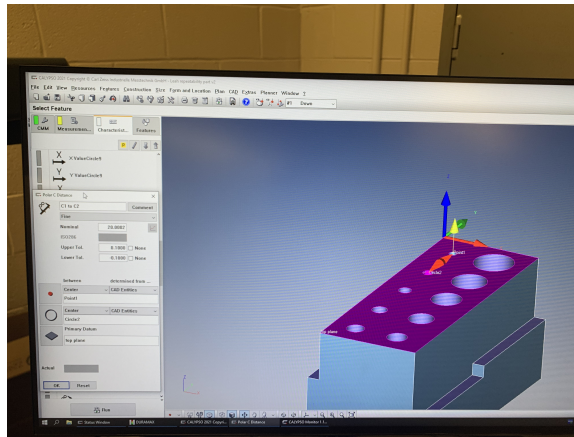


Figure 3.43: Creation of Distances Between Circle Centers

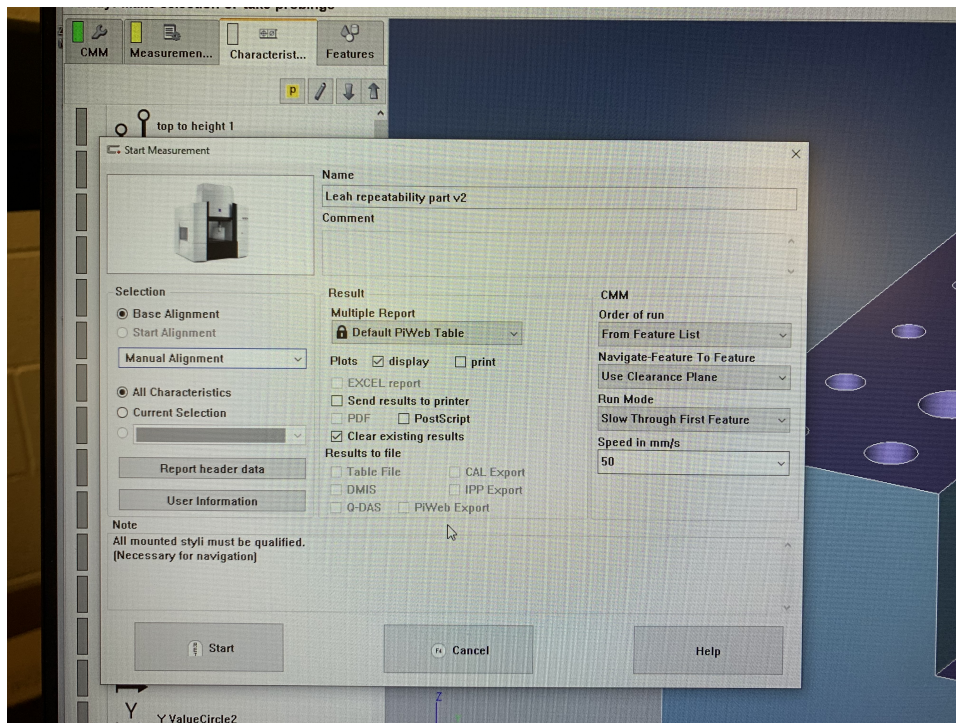


Figure 3.44: Run the Program to get Actual Measurements

# Chapter 4

## Repeatability Data

The measurements from the 50 individual meshes for each number of positions (15, 10, and 5) were used to determine the mean, standard deviation, and range for each feature. An example histogram is displayed in Fig. 3.27 for circle 1. The mean is 2.894 mm; the range is 8.1  $\mu\text{m}$ , and the standard deviation,  $\sigma$ , is 2.0  $\mu\text{m}$ . For comparison, Fig. 4.1 shows the results for circle 10. The mean is 15.944 mm, the range is 2.5  $\mu\text{m}$ , and  $\sigma$  is 0.5  $\mu\text{m}$ . The positions used to get the meshes are shown in Figs. 4.2, 4.3 and 4.4. These positions remained consistent for all 50 meshes used for the repeatability portion of the study.

To give an example of how the measurements from the 50 meshes are displayed, the 15 position graphs are used. First the plots showing the range and standard deviation plotted versus the mean diameter of the circles in Figs. 4.5 and 4.6. These plots show that the larger diameters have a smaller range and standard deviation in comparison to the circles with a smaller diameter. This behavior is also observed for the X and Y center locations of these circles.

The X and Y location plots using 15 positions are provided in Figs. 4.7, 4.8, 4.9 and 4.10. These plots indicate that even though the circles look to be in a line that there are subtle differences and also that the larger diameter circles have smaller standard deviation and range in the location of their centers. The heights are shown in Figs. 4.11 and 4.12 where no clear trend is observed in the data.

Summary plots for 15, 10, and 5 positions for all 10 circle diameters are provided in Figs. 4.13 and 4.14. These plots indicate that using a larger number of positions to create the

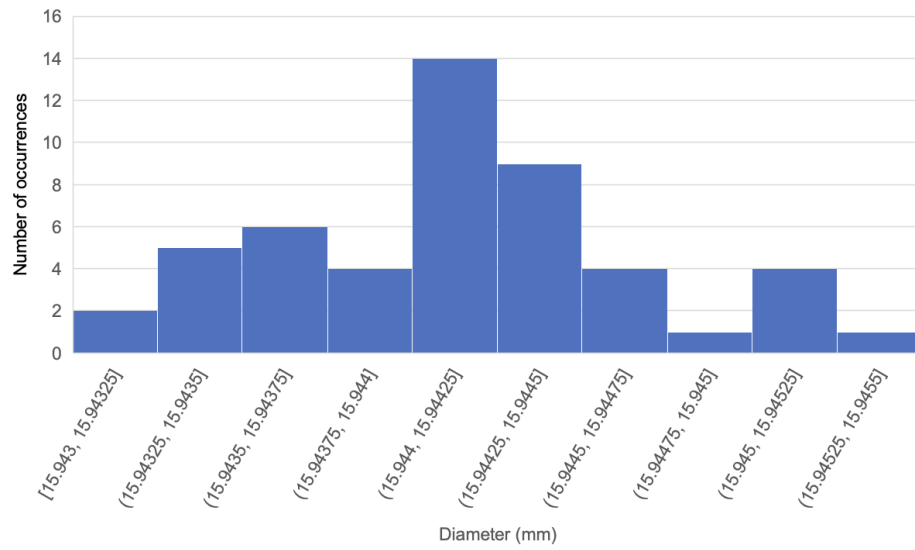


**Figure 4.1:** Circle 10 Histogram for 50 Randomly Selected Scan Sets at Same 15 Positions

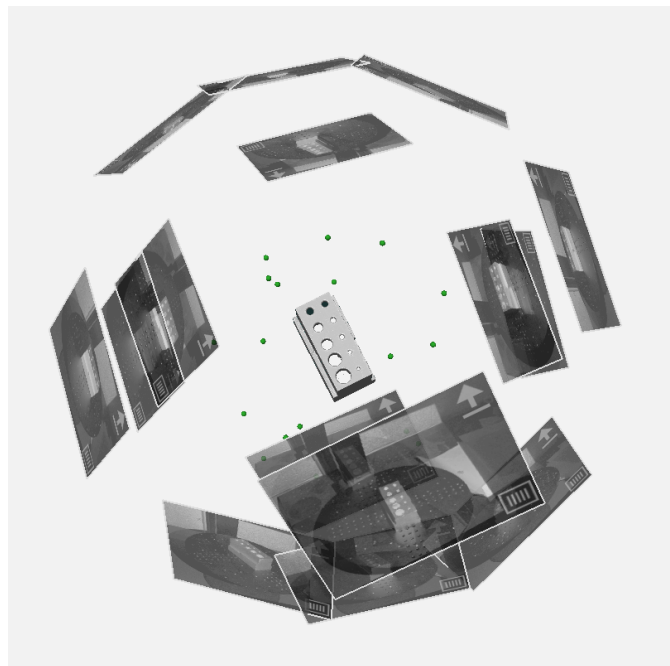


**Figure 4.2:** Location of the 15 Positions Around the Artifact for Repeatability

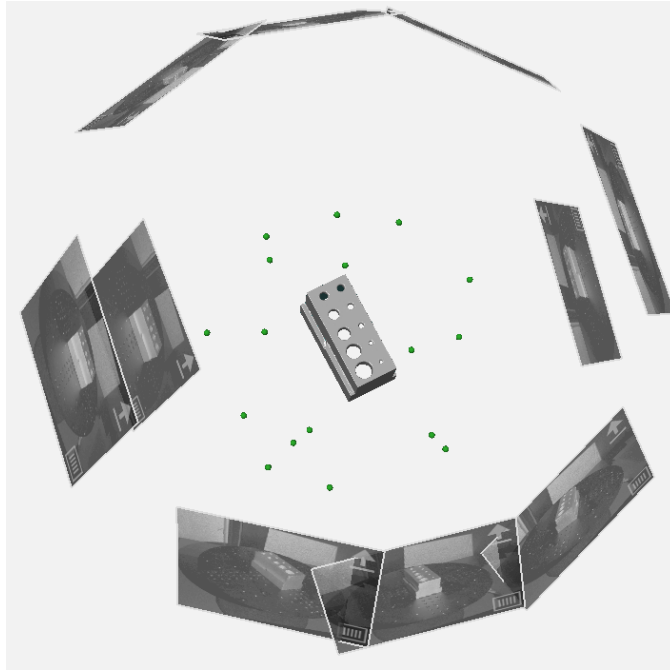


**Figure 4.3:** Location of the 10 Positions Around the Artifact for Repeatability

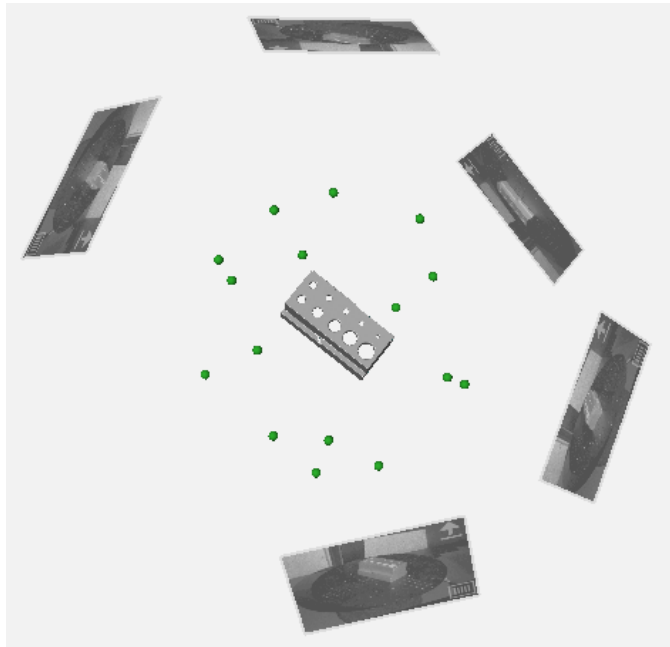


**Figure 4.4:** Location of the 5 Positions Around the Artifact for Repeatability



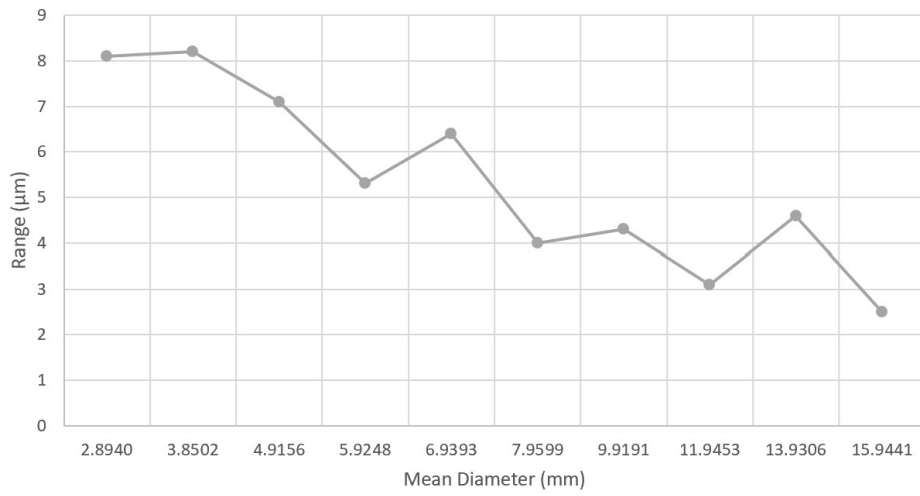


**Figure 4.5:** Variation in Diameter Range for 10 Circles with 15 Scanning Positions

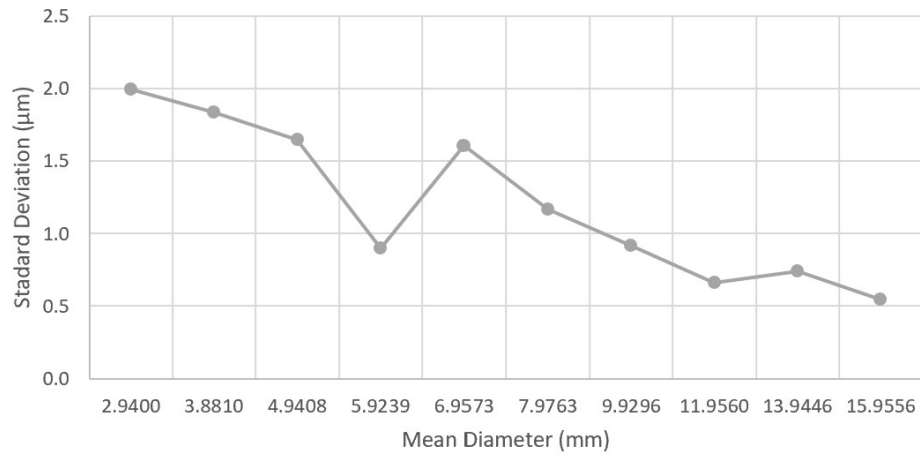
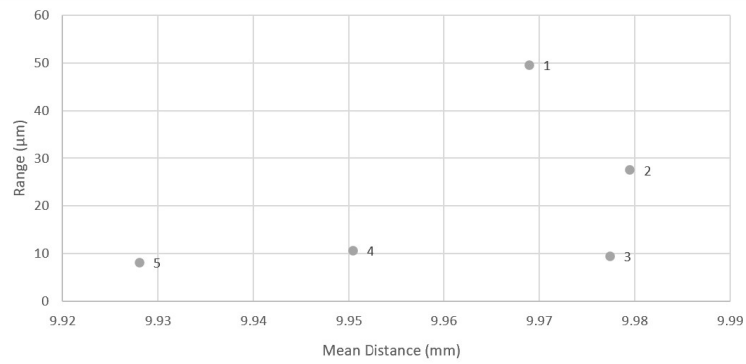
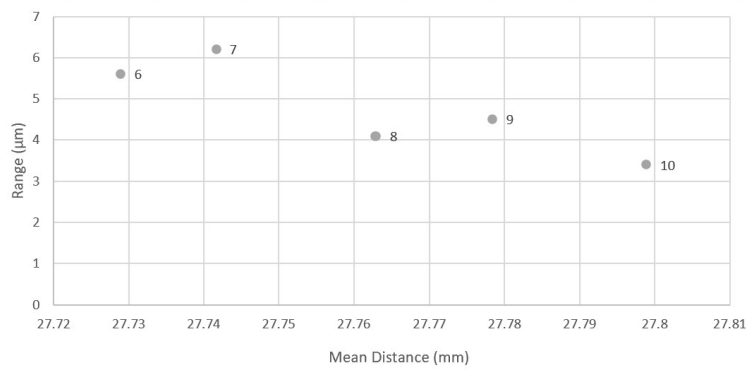


**Figure 4.6:** Variation in Diameter Standard Deviation for 10 Circles with 15 Scanning Positions

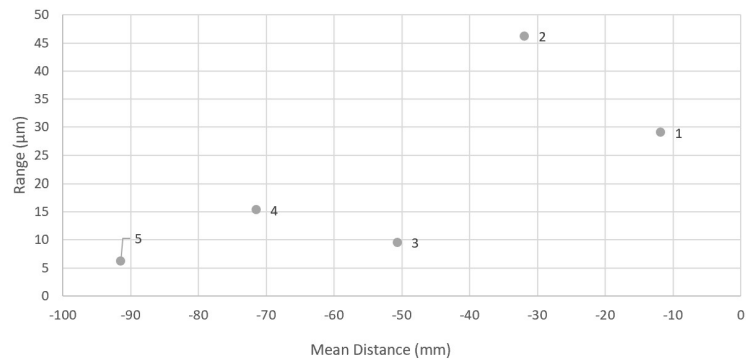


(a) 1-5 X Location

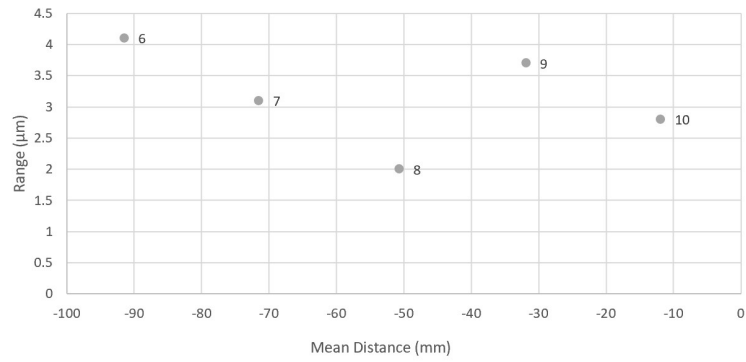


(b) 6-10 X Location

**Figure 4.7:** Variation in X Location Range for 10 Circles with 15 Scanning Positions

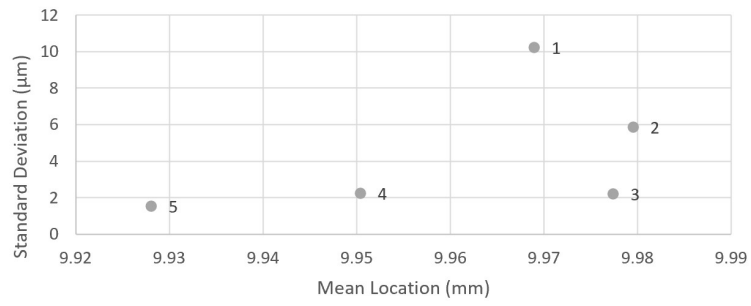


(a) 1-5 Y Location

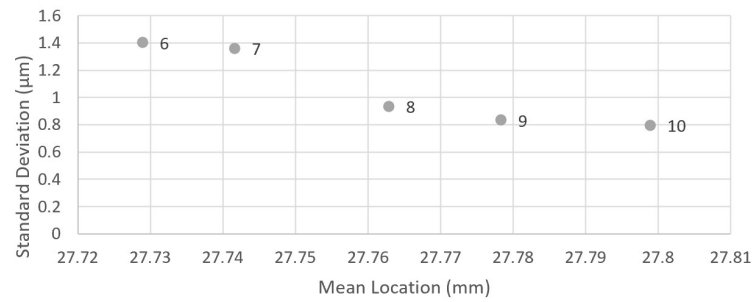


(b) 6-10 Y Location

**Figure 4.8:** Variation in Y Location Range for 10 Circles with 15 Scanning Positions



(a) 1-5 X Location



(b) 6-10 X Location

**Figure 4.9:** Variation in X Location Standard Deviation for 10 Circles with 15 Scanning Positions

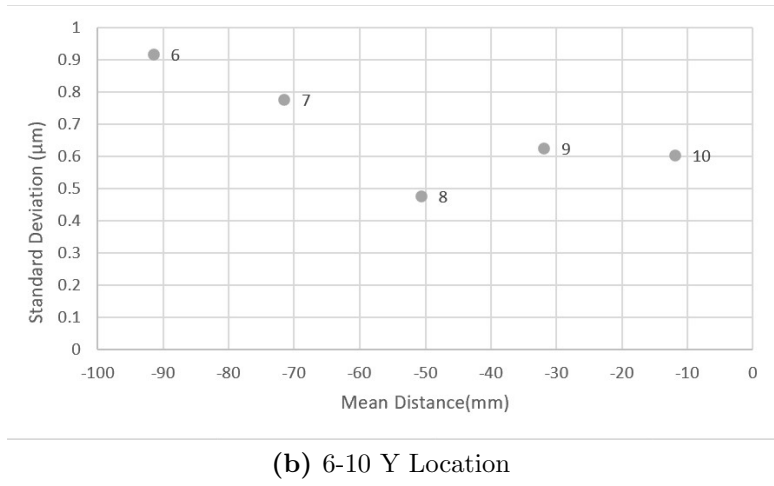
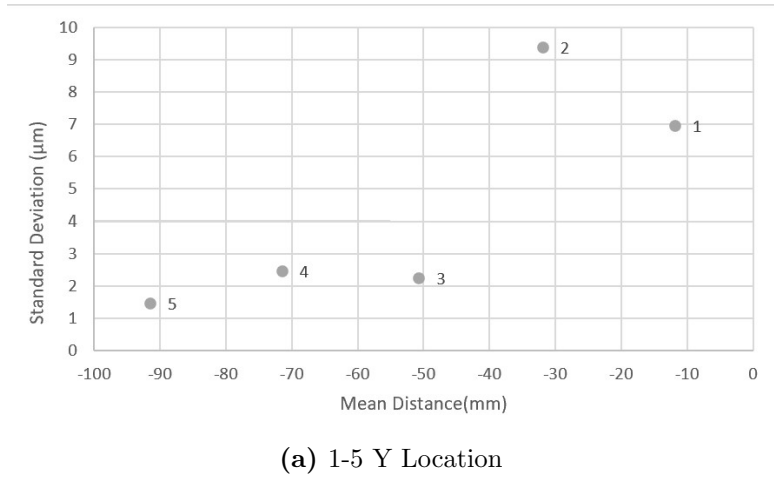


**Figure 4.10:** Variation in Y Location Standard Deviation for 10 Circles with 15 Scanning Positions

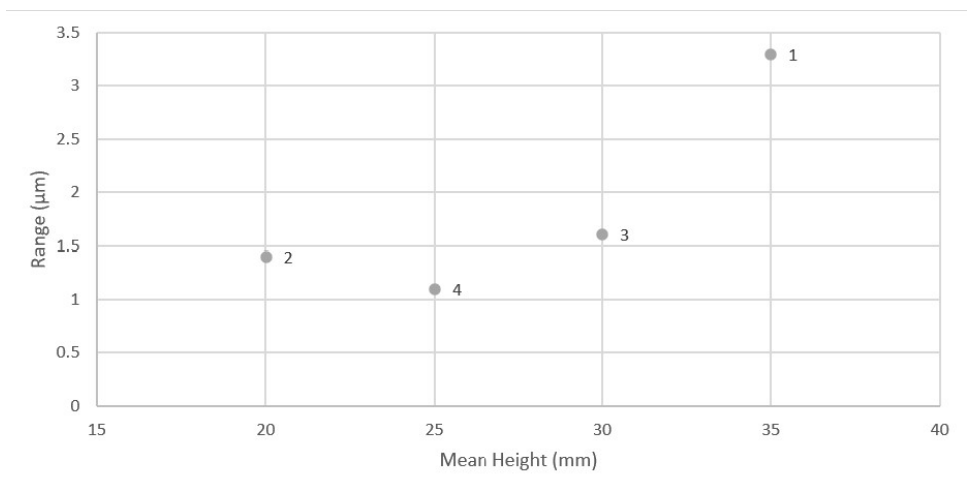


**Figure 4.11:** Variation in Height Range for 15 Scanning Positions

mesh increases repeatability. Higher repeatability is also obtained for larger circle diameters.

Summary plots for 15, 10, and 5 positions for all four heights are provided in Figs. 4.15 and 4.16. These plots indicate that using a larger number of positions to create the mesh increases repeatability.

Figures 4.17 through 4.22 show how the range and standard deviation of the distances between circle centers are affected by the number of scanning positions used to measure the part. These plots show that the 15 position meshes had a significantly smaller range and standard deviation when compared to the smaller number of positions.

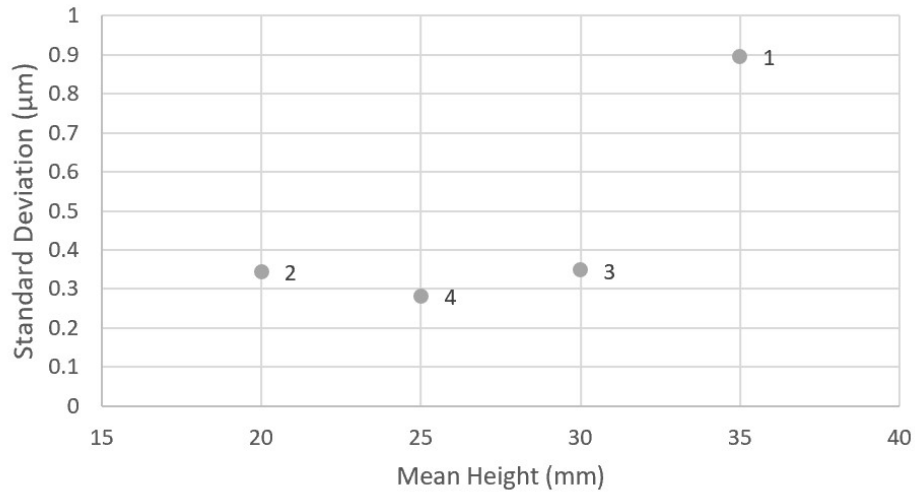


**Figure 4.12:** Variation in Height Standard Deviation for 15 Scanning Positions

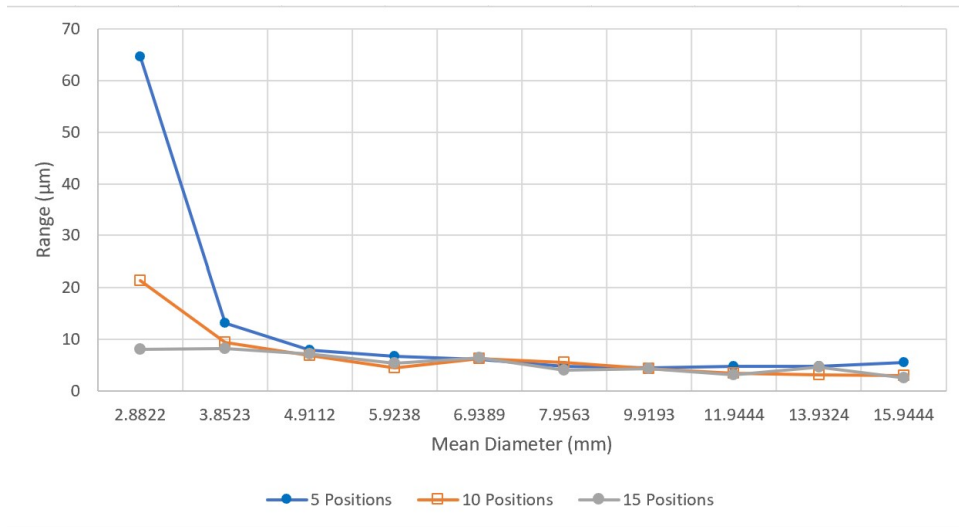


**Figure 4.13:** Variation in Diameter Range for 10 Circles with 5, 10, and 15 Scanning Positions

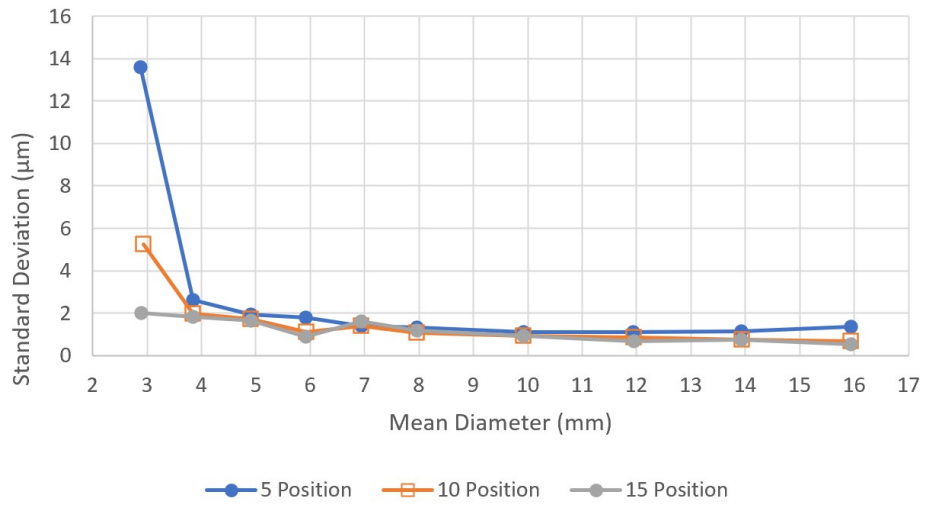


**Figure 4.14:** Variation in Diameter Standard Deviation for 10 Circles with 5, 10, and 15 Scanning Positions

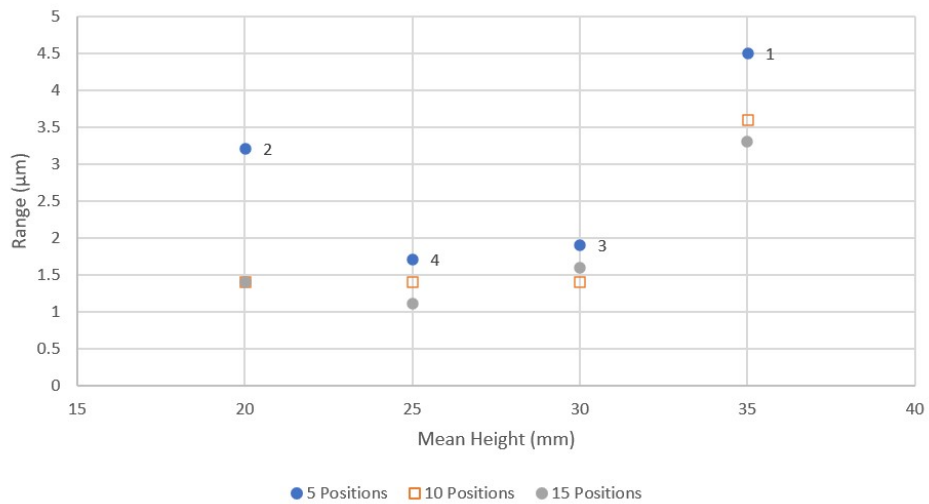


**Figure 4.15:** Variation in Height Range for 5, 10, and 15 Scanning Positions



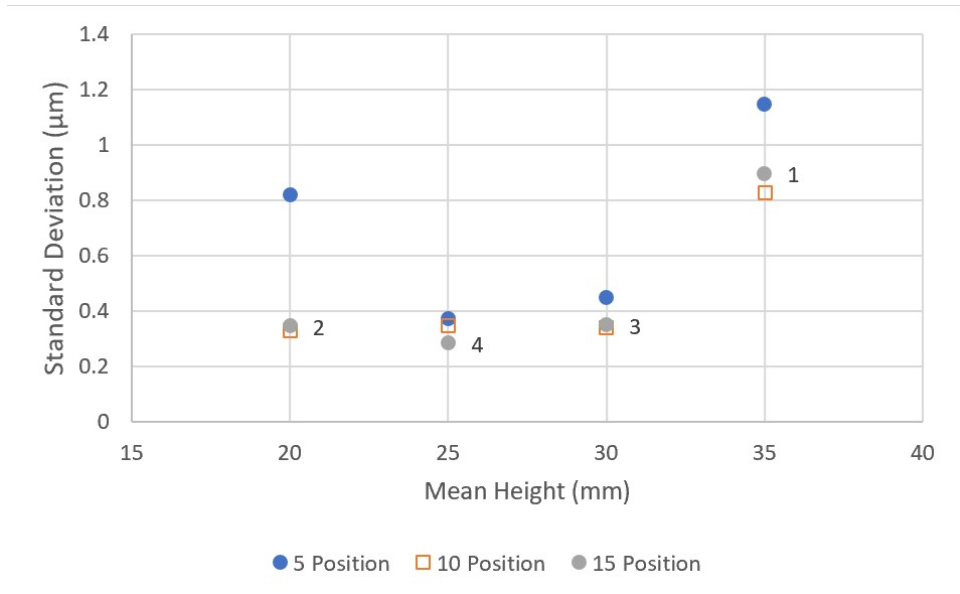


**Figure 4.16:** Variation in Height Standard Deviation for 5, 10, and 15 Scanning Positions

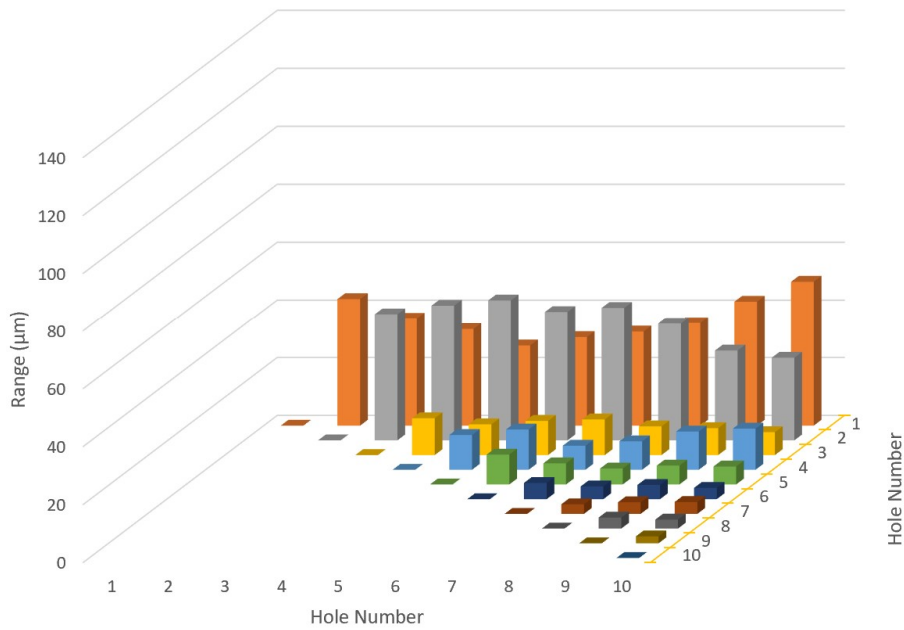


**Figure 4.17:** Range of Distances Between Circle Centers Using 15 Positions in Micrometers

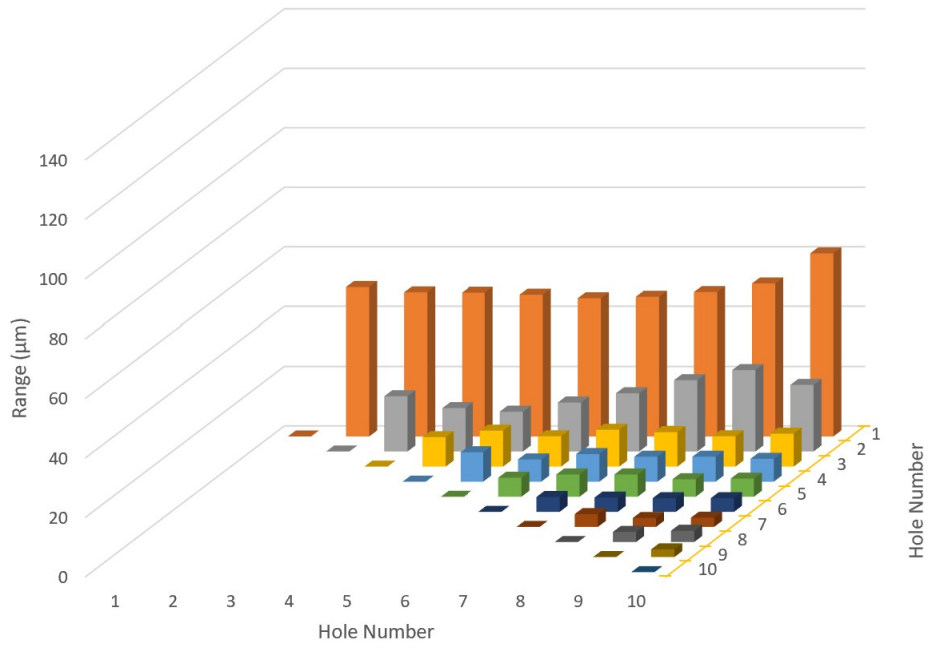


**Figure 4.18:** Range of Distances Between Circle Centers Using 10 Positions in Micrometers

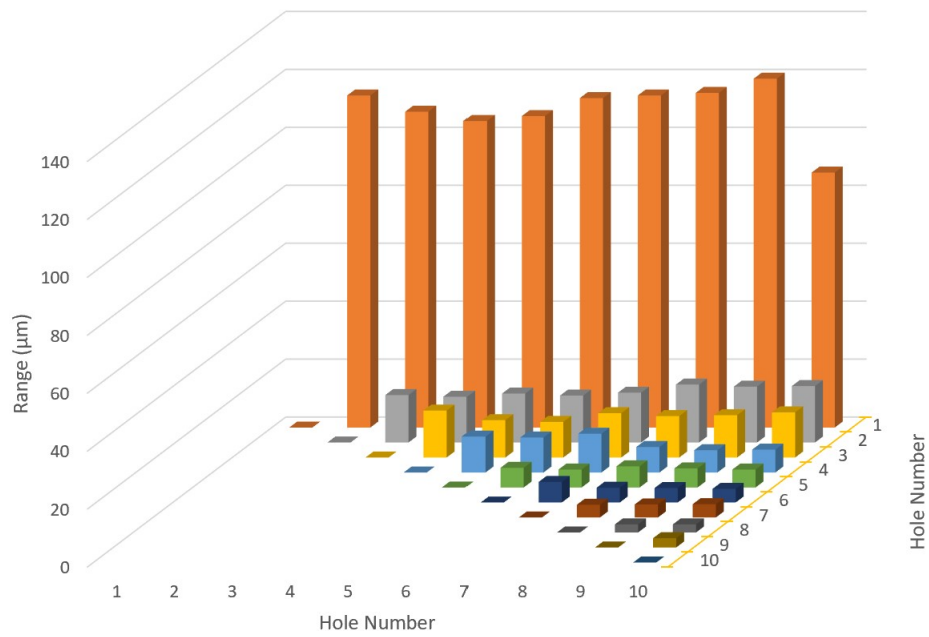


**Figure 4.19:** Range of Distances Between Circle Centers Using 5 Positions in Micrometers

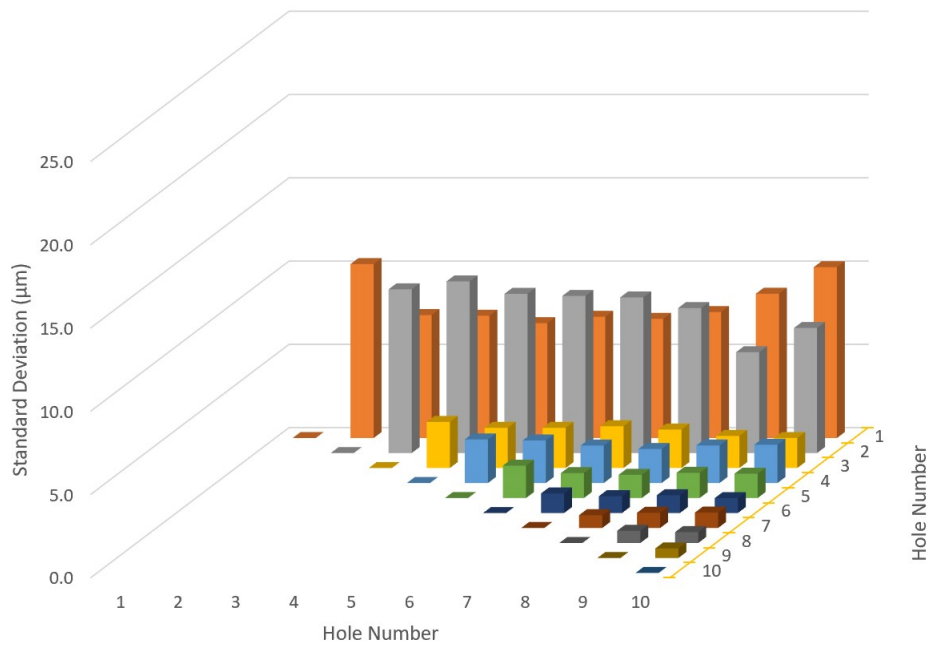


**Figure 4.20:** Standard Deviation of Distances Between Circle Centers Using 15 Positions in Micrometers

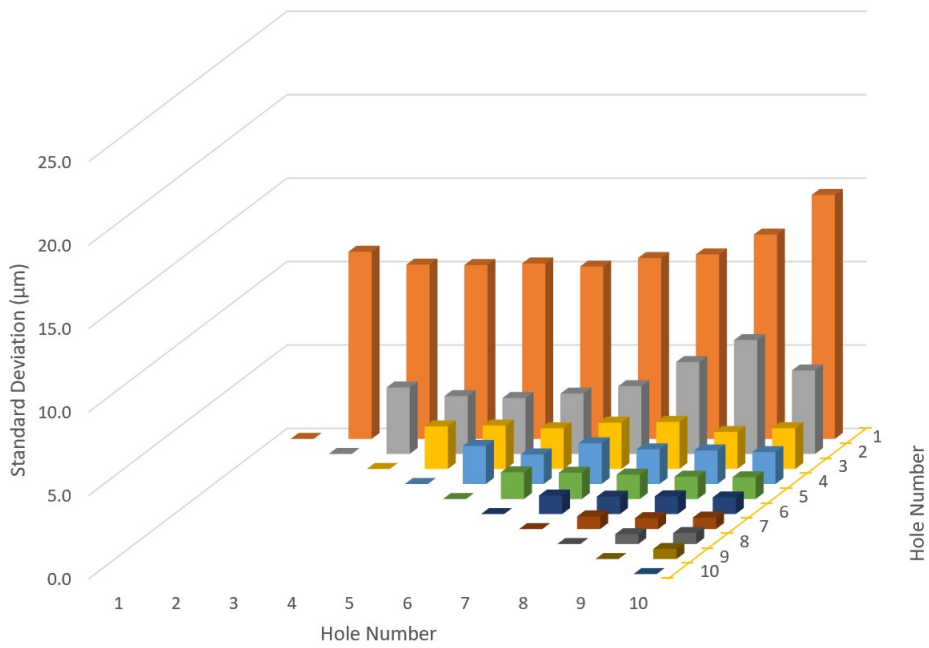


**Figure 4.21:** Standard Deviation of Distances Between Circle Centers Using 10 Positions in Micrometers

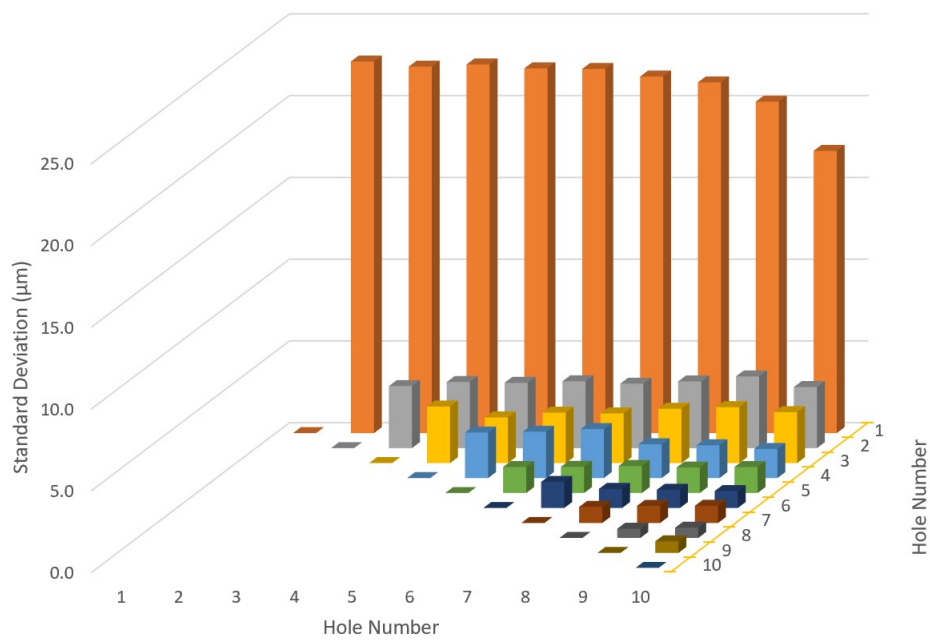


**Figure 4.22:** Standard Deviation of Distances Between Circle Centers Using 5 Positions in Micrometers

# Chapter 5

## Reproducibility Data

The measurements from the 10 meshes for each number of positions were used to determine the mean, standard deviation, and range for each feature. The positions used to get the meshes are shown in Figs. 5.1, 5.2 and 5.3. These positions were different for each of the 10 meshes used for the reproducibility portion of the study. To give an example of all the data and analysis, the 15 position results are used. The plots showing the range and standard deviation versus the mean diameter of the circles are displayed in Figs. 5.4 and 5.5. These plots show that the larger diameters have a smaller range and standard deviation in comparison to the circles with a smaller diameter.

This trend is also observed for the X and Y center locations of these circles. The X and Y location plots using 15 positions are provided in Figs. 5.6, 5.7, 5.8 and 5.9. These plots indicate that even though the circles look to be in a line that there are subtle differences and also that the larger diameter circles have smaller standard deviation and range in the location of their centers.

The height results are shown in Figs. 5.10 and 5.11. No clear trend is observed.

Summary plots for 15, 10, and 5 positions for all 10 circle diameters are provided in Figs. 5.12 and 5.13. These plots indicate that using a larger number of positions to create the mesh increases reproducibility. Higher reproducibility is also obtained for larger circle diameters. Summary plots for 15, 10, and 5 positions for all four heights are provided in Figs. 5.14 and 5.15. These plots indicate that using a larger number of positions to create the mesh increases reproducibility. Figures 5.16 through 5.21 show how the range and standard



**Figure 5.1:** Location of the 15 Positions Around the Artifact for Reproducibility

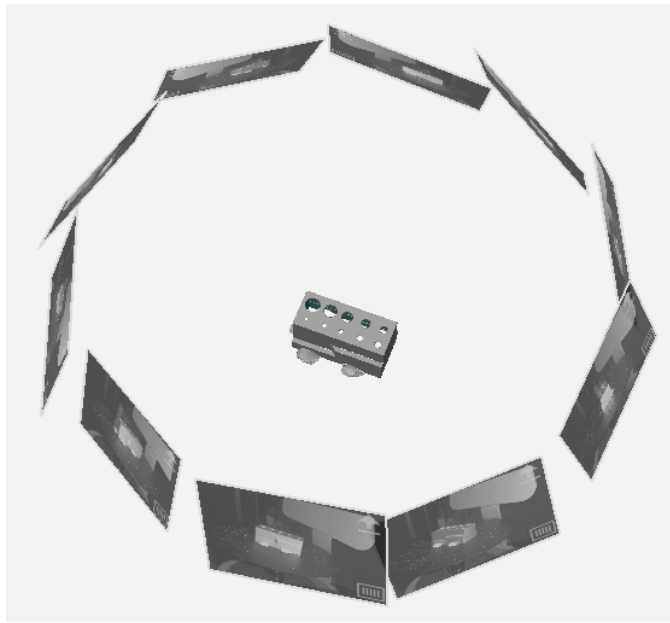


**Figure 5.2:** Location of the 10 Positions Around the Artifact for Reproducibility

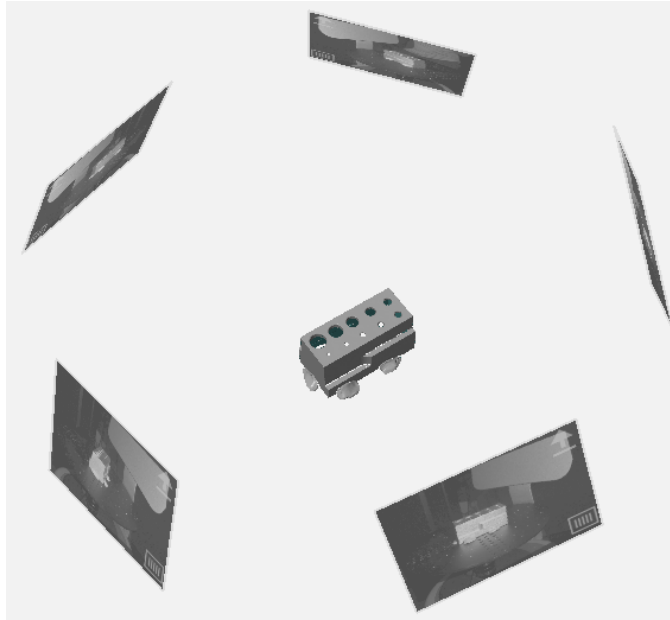


**Figure 5.3:** Location of the 5 Positions Around the Artifact for Reproducibility

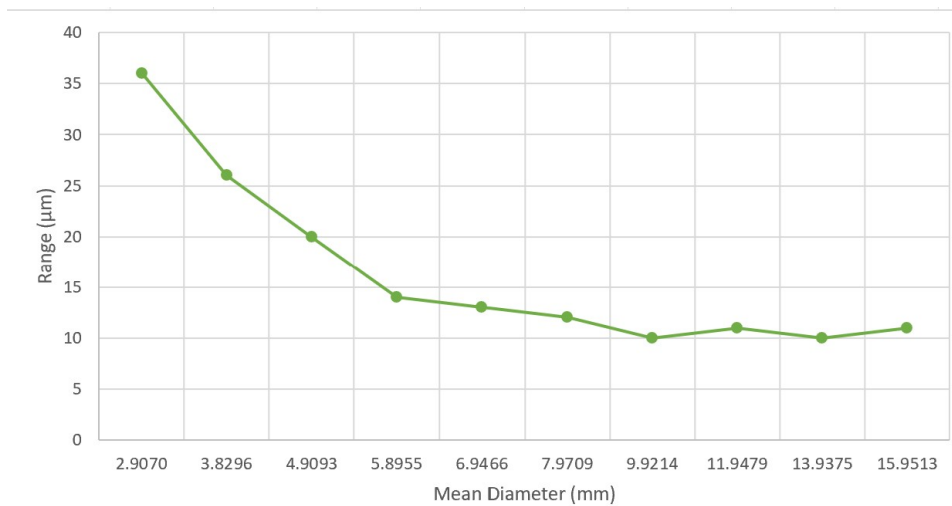


**Figure 5.4:** Diameter Range for 10 Circles with 15 Scanning Positions

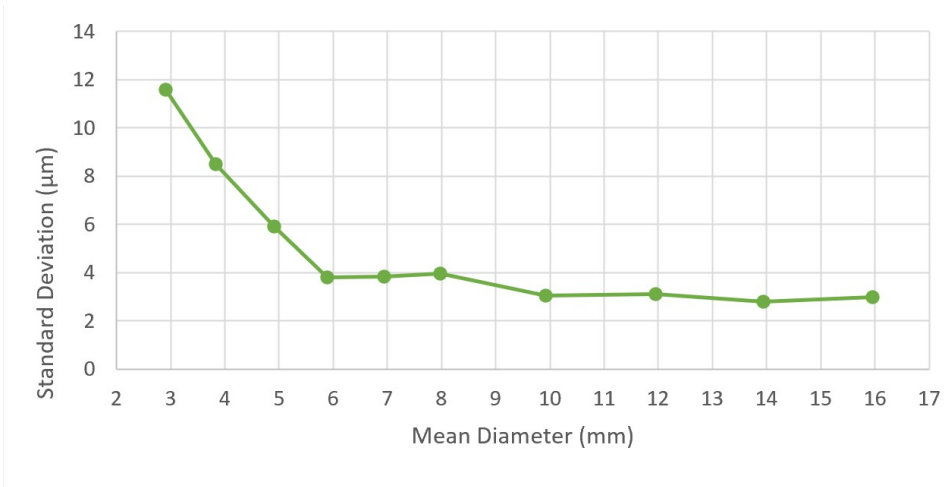
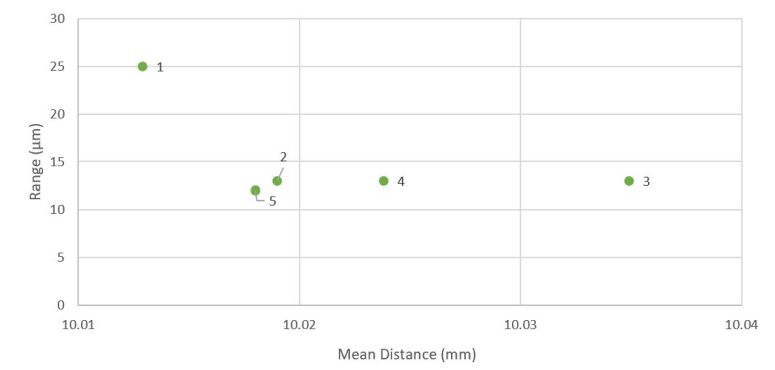
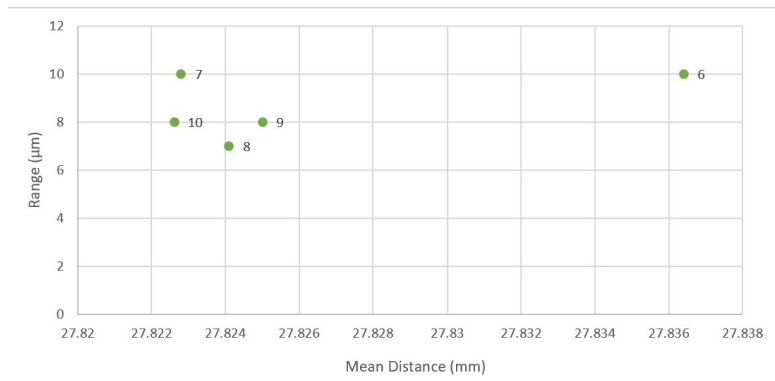


**Figure 5.5:** Diameter Standard Deviation for 10 Circles with 15 Scanning Positions



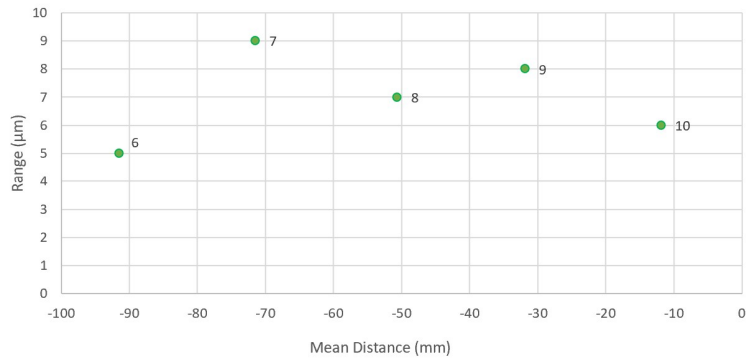
**(a)** 1-5 X Location



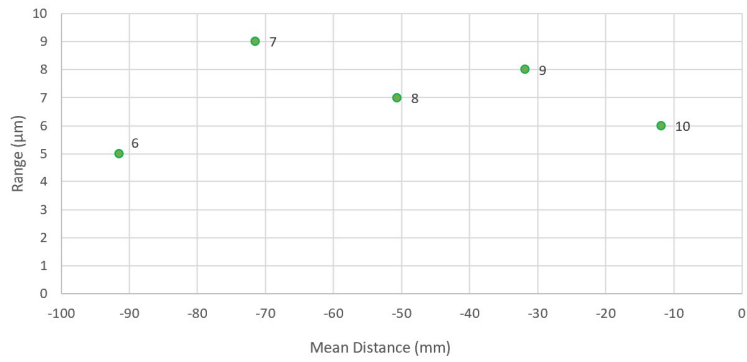
**(b)** 6-10 X Location

**Figure 5.6:** X Location Range for 10 Circles with 15 Scanning Positions



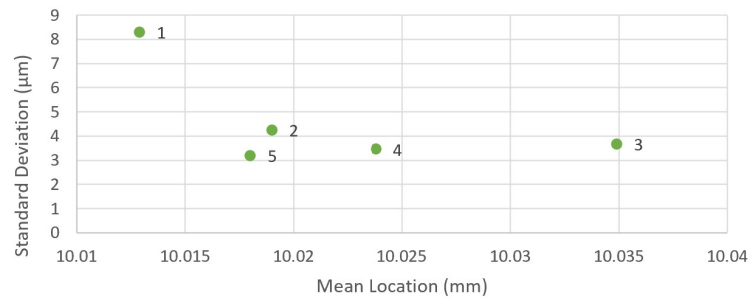


(a) 1-5 Y Location

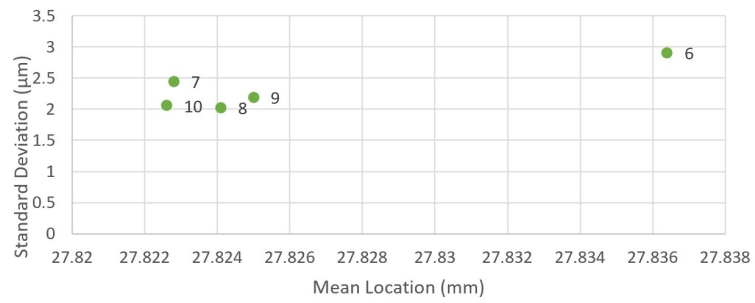


(b) 6-10 Y Location

**Figure 5.7:** Y Location Range for 10 Circles with 15 Scanning Positions

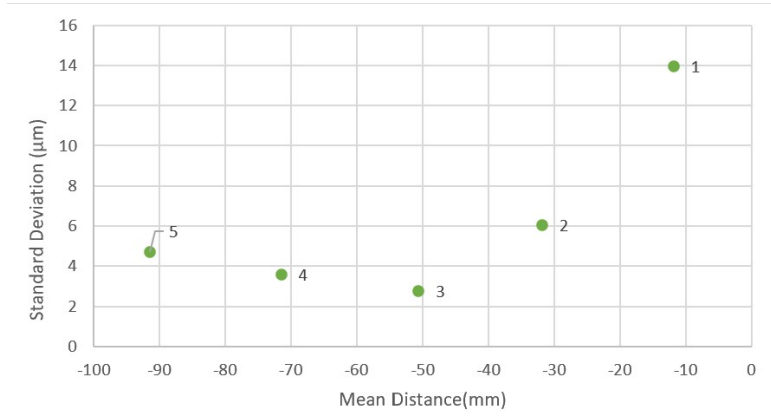


(a) 1-5 X Location

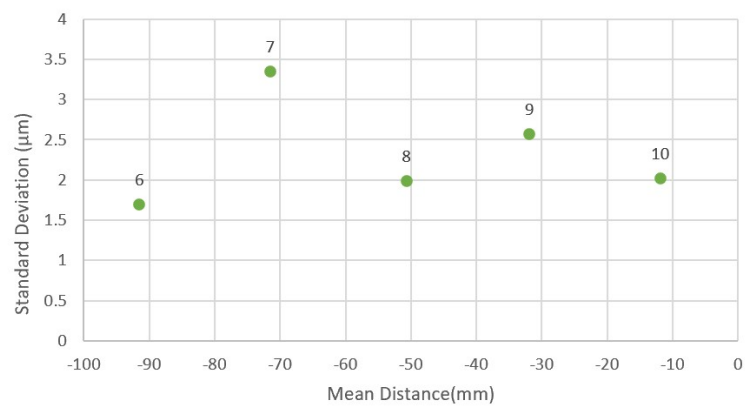


(b) 6-10 X Location

**Figure 5.8:** X Location Standard Deviation for 10 Circles with 15 Scanning Positions



(a) 1-5 Y Location



(b) 6-10 Y Location

**Figure 5.9:** Y Location Standard Deviation for 10 Circles with 15 Scanning Positions

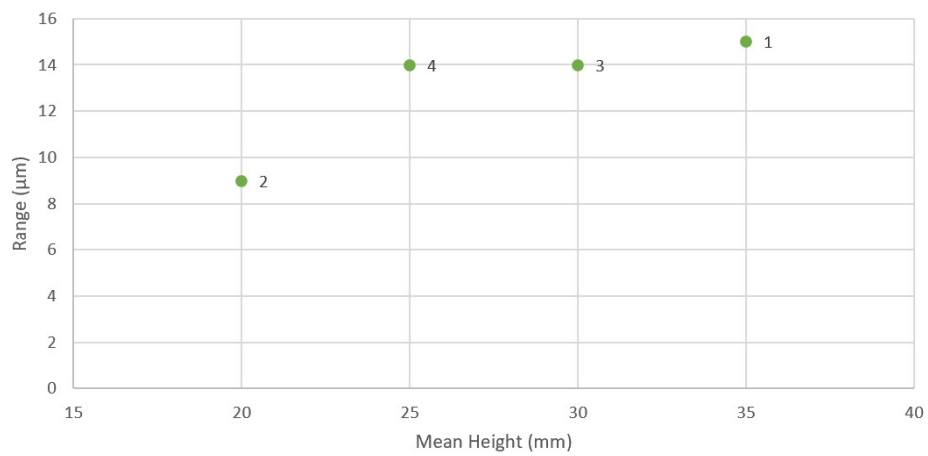


**Figure 5.10:** Height Range for 15 Scanning Positions

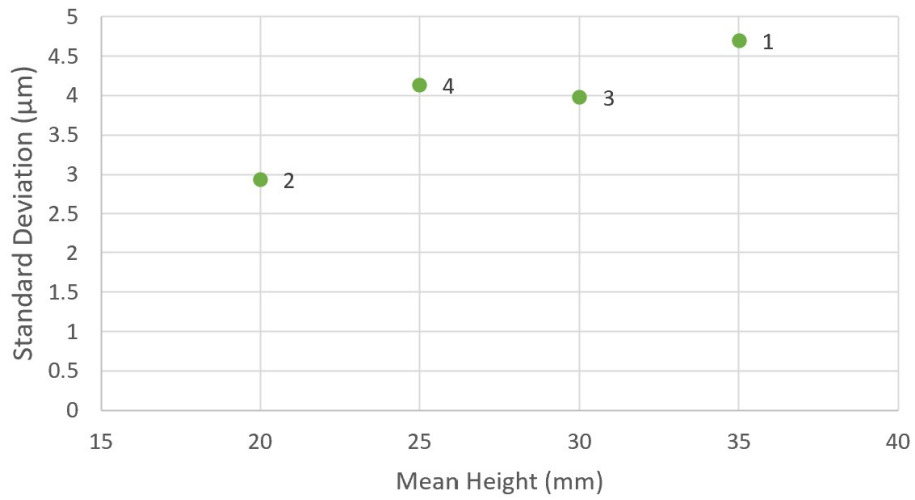


**Figure 5.11:** Height Standard Deviation for 15 Scanning Positions

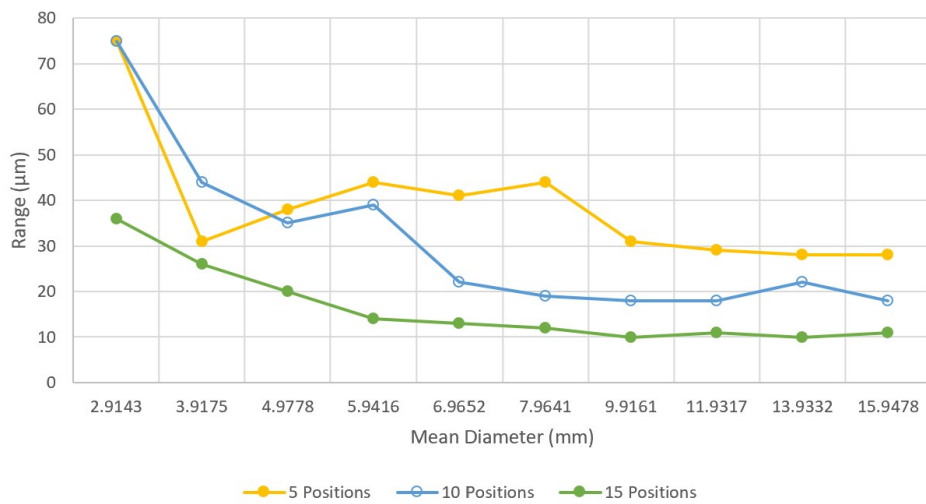


**Figure 5.12:** Diameter Range for 10 Circles with 5, 10, and 15 Scanning Positions

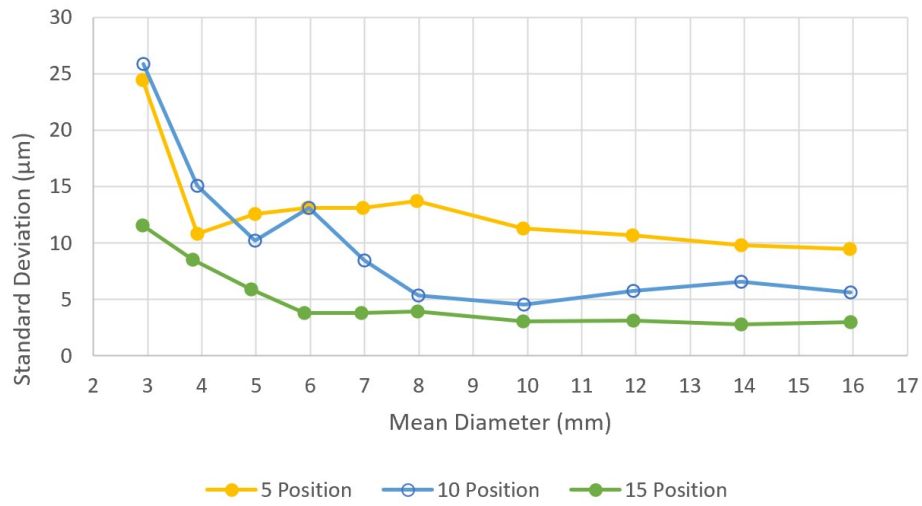


**Figure 5.13:** Diameter Standard Deviation for 10 Circles with 5, 10, and 15 Scanning Positions

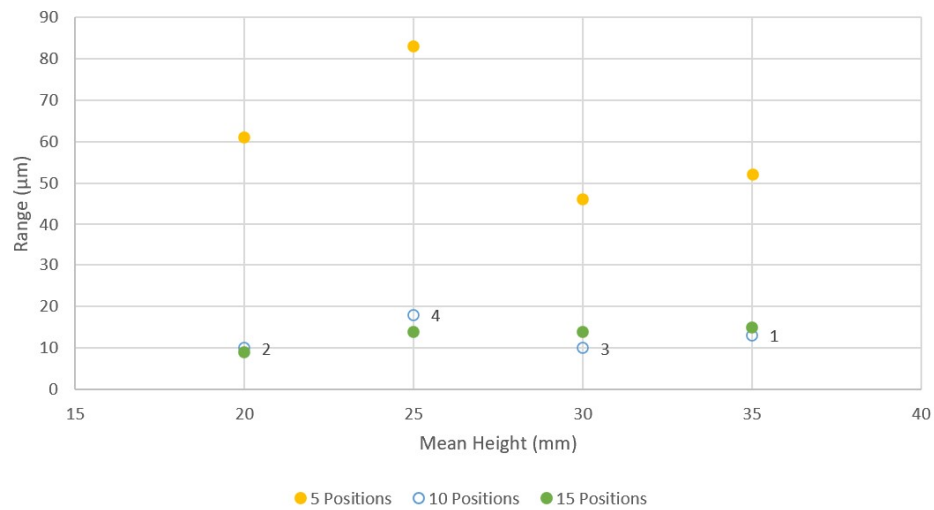


**Figure 5.14:** Height Range for 5, 10, and 15 Scanning Positions

deviation of the distances between circle centers are affected by the number of scanning positions used to measure the part. These plots show that the 15 position meshes had a smaller range and standard deviation when compared to the smaller number of positions.

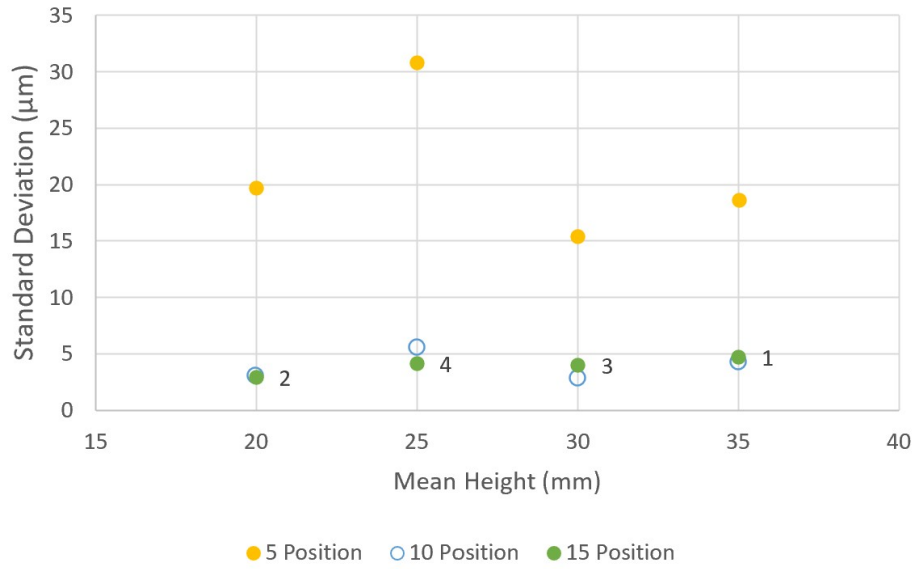


**Figure 5.15:** Height Standard Deviation for 5, 10, and 15 Scanning Positions

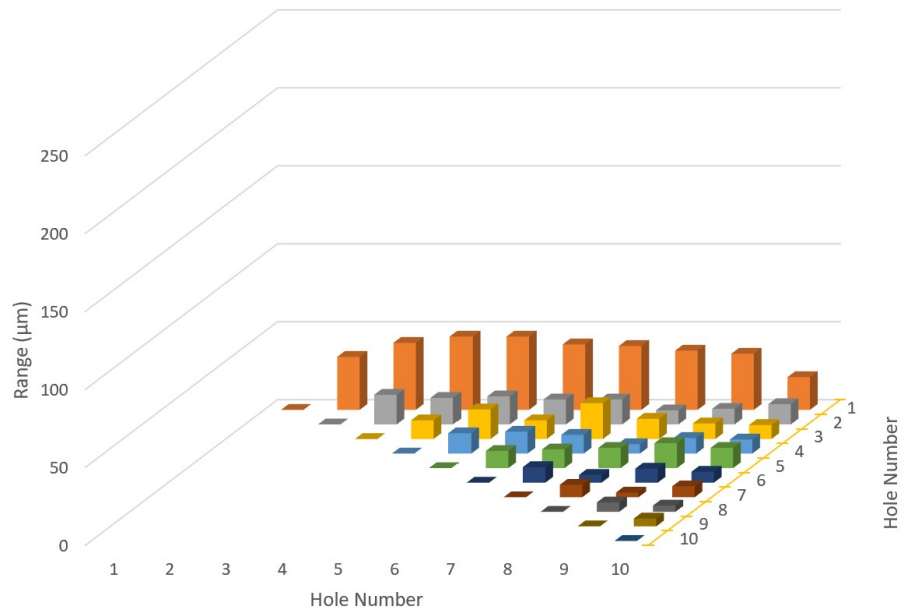


**Figure 5.16:** Range of Distances Between Circle Centers Using 15 Positions

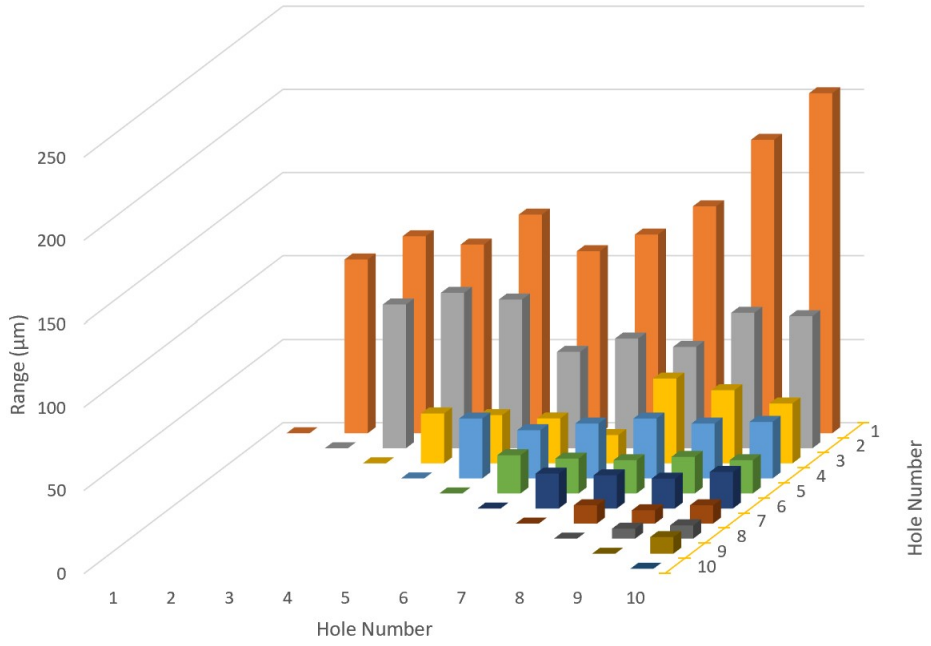


**Figure 5.17:** Range of Distances Between Circle Centers Using 10 Positions

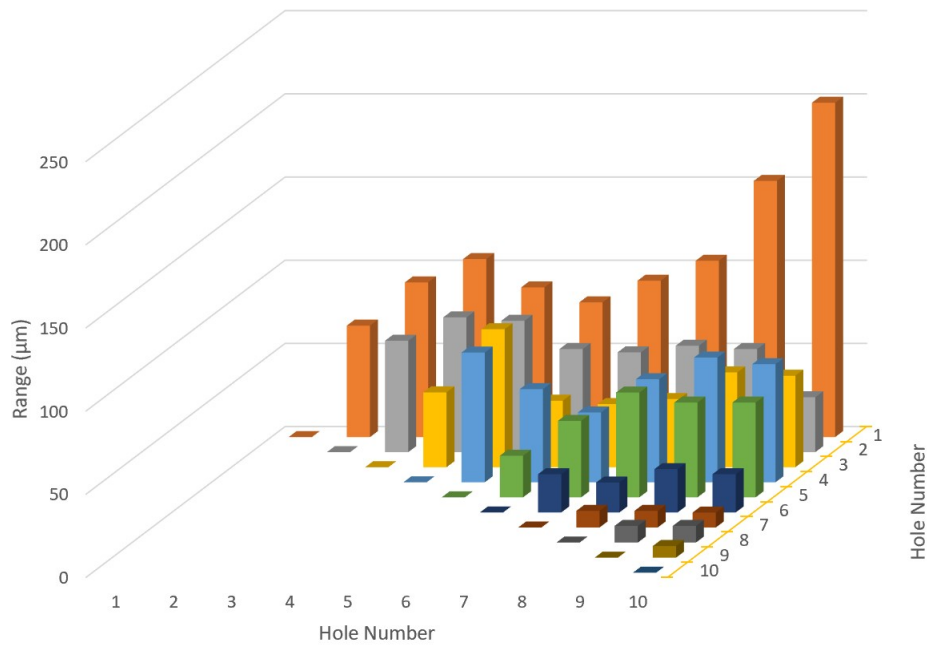


**Figure 5.18:** Range of Distances Between Circle Centers Using 5 Positions



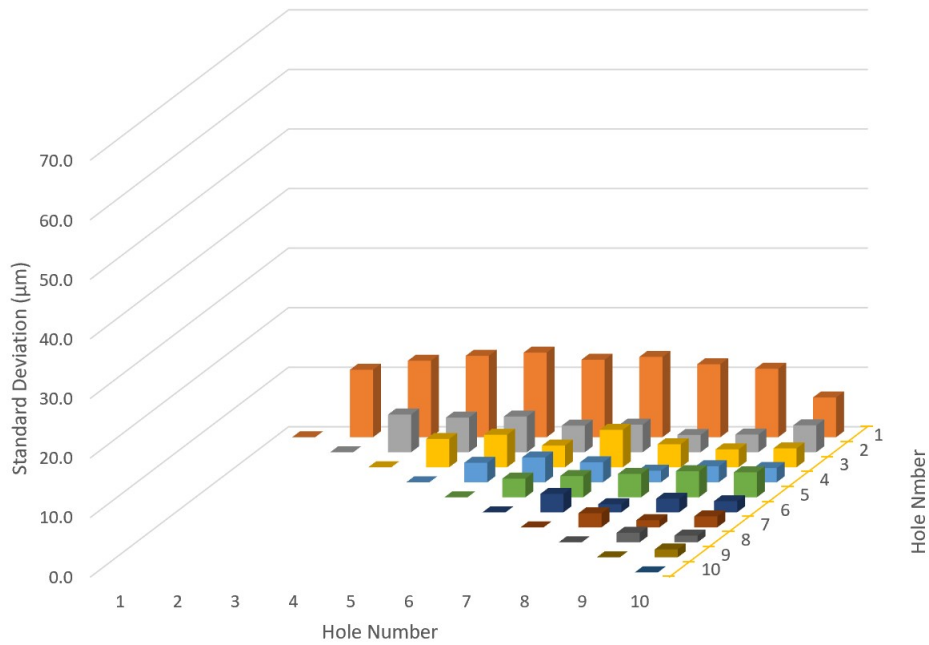


**Figure 5.19:** Standard Deviation of Distances Between Circle Centers Using 15 Positions

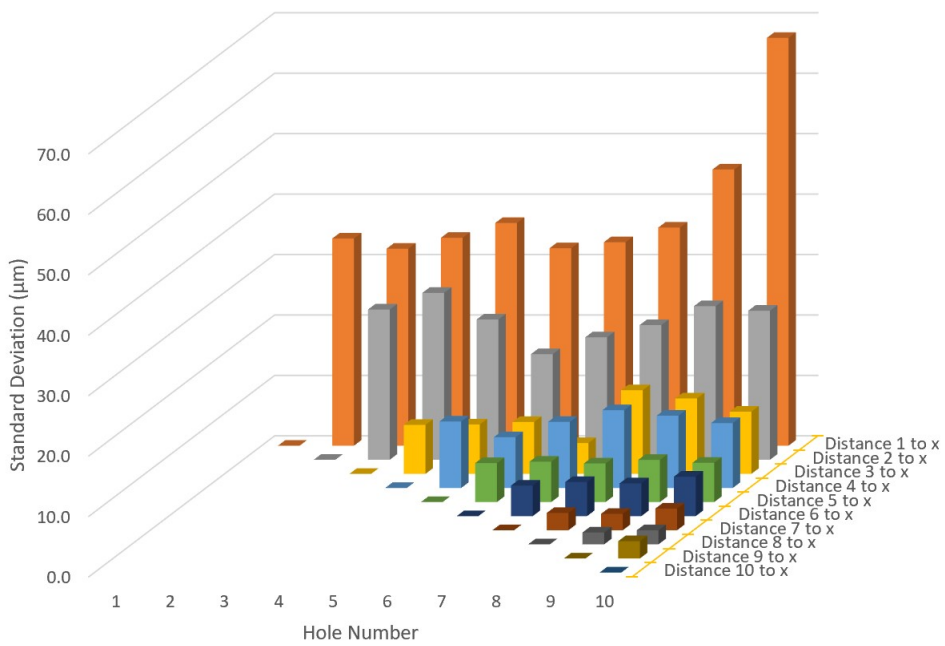


**Figure 5.20:** Standard Deviation of Distances Between Circle Centers Using 10 Positions

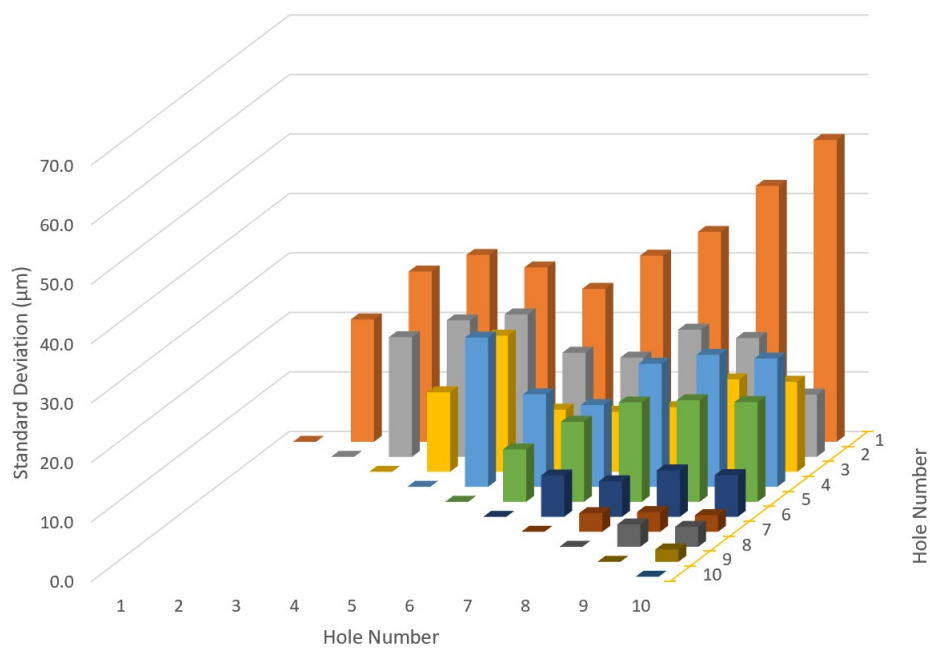
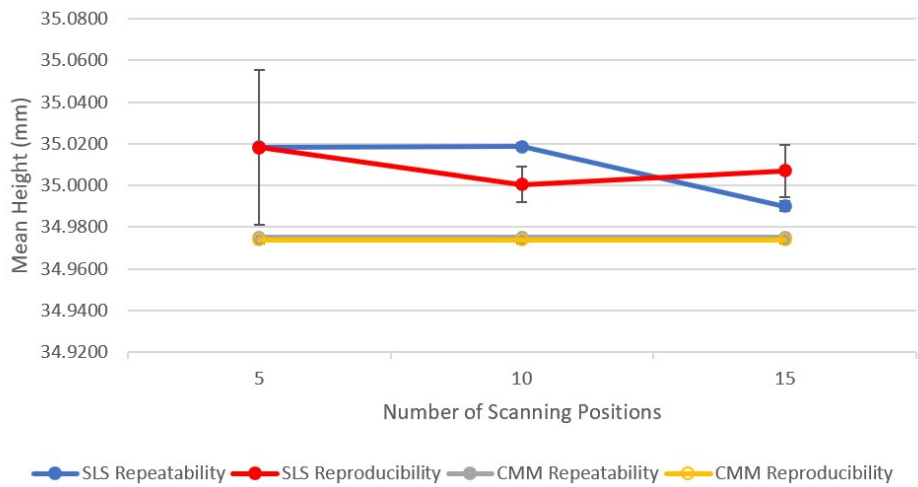


**Figure 5.21:** Standard Deviation of Distances Between Circle Centers Using 5 Positions

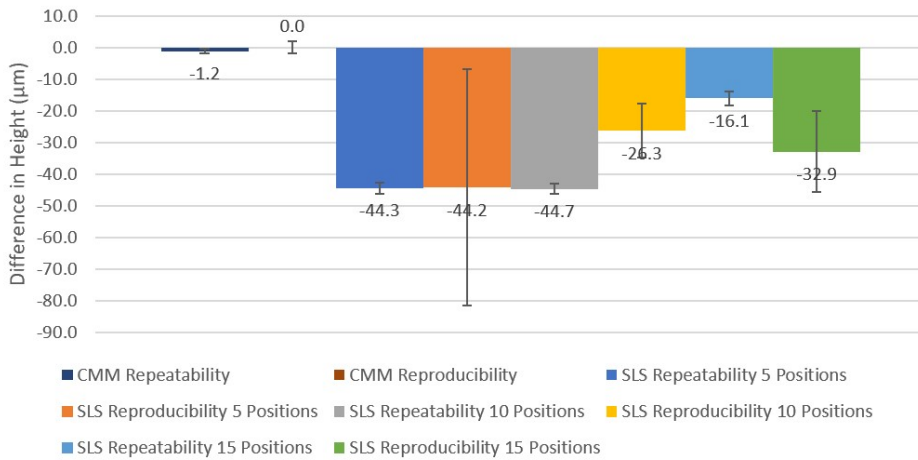
# Chapter 6

## CMM Comparison

The CMM was used to take multiple measurements of the part dimensions to determine the mean and standard deviation, focusing on the four heights and the diameters and center locations of circles 2 through 10. The repeatability of the CMM measurements was determined by taking 20 sets of measurements at the same location on the CMM table and reproducibility was determined by taking 10 sets of measurements at different locations on the CMM table. These measurements were compared to the repeatability and reproducibility results found using the GOM ATOS Q structured light scanner (SLS) using: 1) line graphs plotting the mean measurement over the number of positions; and 2) bar graphs showing the difference between the CMM mean value (from the reproducibility study) for the selected feature and the mean value of the SLS result. Error bars are included to show potential overlap. To give an example, the Height 1 graphs are shown in Fig. 6.1. The graphs for the all the elements are included in Appendix F. These graphs demonstrate the trends found in the data by comparing the different measuring methods. One such trend is that the SLS repeatability data means do not change much with the number of positions, which was expected since all the data came from a single measurement set. The SLS reproducibility data mean values do change showing that the camera and part orientation and position affects the final measurement result.



(a) Line Graph



(b) Difference Graph

**Figure 6.1:** Comparing Structured Light Scanning and CMM Measurements for Height 1

# Chapter 7

## Discussion

A discussion of the study outcomes is provided in this chapter.

### 7.1 Results

The graphs from chapters 4 and 5 show that a larger number of measurement positions reduces the range and the standard deviation of an element. A larger number of positions therefore increases the repeatability and reproducibility of the measurements. For the diameters, it is also noted that the larger diameters have smaller ranges and smaller standard deviations. This relationship remains consistent when applied to the distances between circle centers, and X and Y locations. For the heights, on the other hand, the repeatability of the measurements did not exhibit a clear trend with height. This is due to the difference in the measurements. The smaller holes had a smaller number of points so the measurement performance was degraded. The number of points for the height measurements, however, was not related to the step height value. It depended only on the top and bottom surfaces, which had similar areas for all four heights.

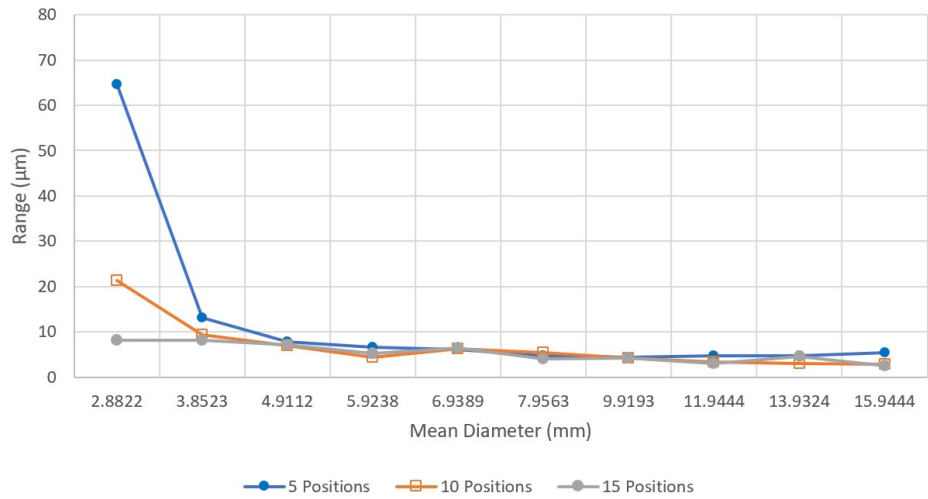
Direct comparison of the repeatability and reproducibility data shows how the diameters and heights measured are significantly smaller in the repeatability data in which the positions remain consistent and has five times the number of meshes on which to perform the measurements. Comparing the repeatability and reproducibility of the range and standard deviation of the mean diameter of the circles (Figs. 7.1 and 7.2) shows that

the reproducibility is larger than the repeatability. Directly comparing the repeatability and reproducibility at the same number of positions shows that differing the location of the positions used to generate the mesh increases the range and standard deviation of the circle diameters (Figs. 7.3 and 7.4). Comparing the repeatability and reproducibility of the range and standard deviation of the mean heights (Figs. 7.5 and 7.6) shows that the reproducibility is again larger than the repeatability. Directly comparing the repeatability and reproducibility at the same number of positions shows that differing the location of the positions used to generate increases the range and standard deviation of the heights (Figs. 7.7 and 7.8).

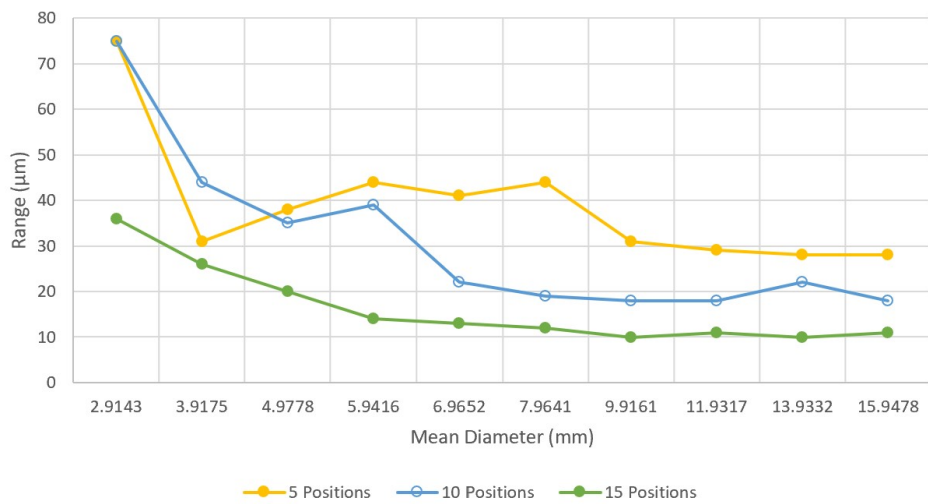
The CMM results in Appendix F provide a comparison between the SLS mean values, as well as their distribution, and the industry standard for dimensional metrology. For the height values (Figs. F.1-F.4), the SLS heights are consistently smaller than the CMM heights. The error is generally 20 micrometers to 40 micrometers. Since the error bars do not overlap, there is an unexplained bias between the two instruments. For the circle diameters (Figs. F.5-F.13), the smaller circles exhibit larger errors. The error decreases with increasing circle diameter and the reproducibility error bars generally overlap for circles 3 to 10. For circles 8 to 10, the errors are only a few micrometers for both the 10 and 15 position results. Both positive and negative errors are seen, which suggests that a consistent bias is not present. The repeatability results, on the other hand, do not appreciably change with an increasing number of measurement positions (less than 5 micrometer difference between the results). This is because the same data set was used for the entire repeatability study. The results for the circle center position comparisons (Figs. F.14-F.31) are good. The errors for the 10 and 15 measurement position reproducibility results are generally just a few micrometers with both positive and negative errors.

## 7.2 Difficulties Encountered During the Study

At several points during the study, issues arose that had the understandable effect of skewing the histogram results significantly. The first of these issues was the fact that some of the meshes did not properly align to each other. For example, this issue caused the circles used

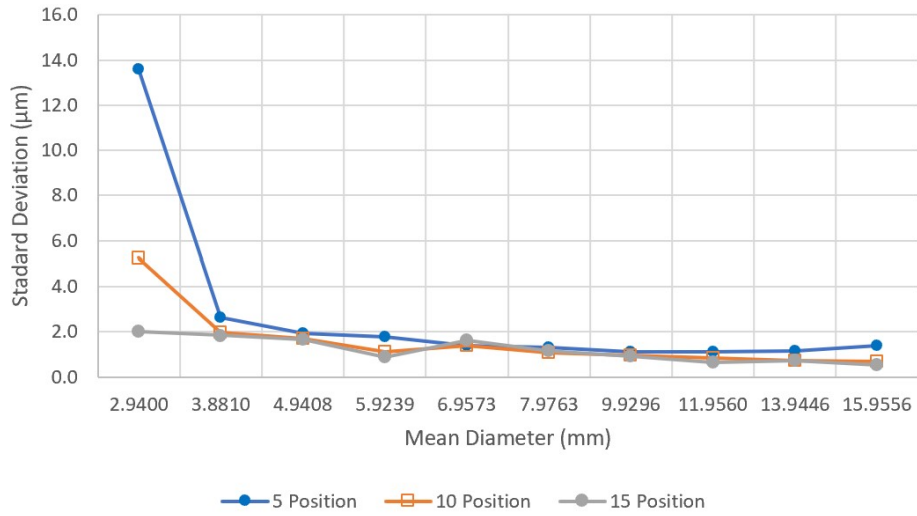


(a) Repeatability

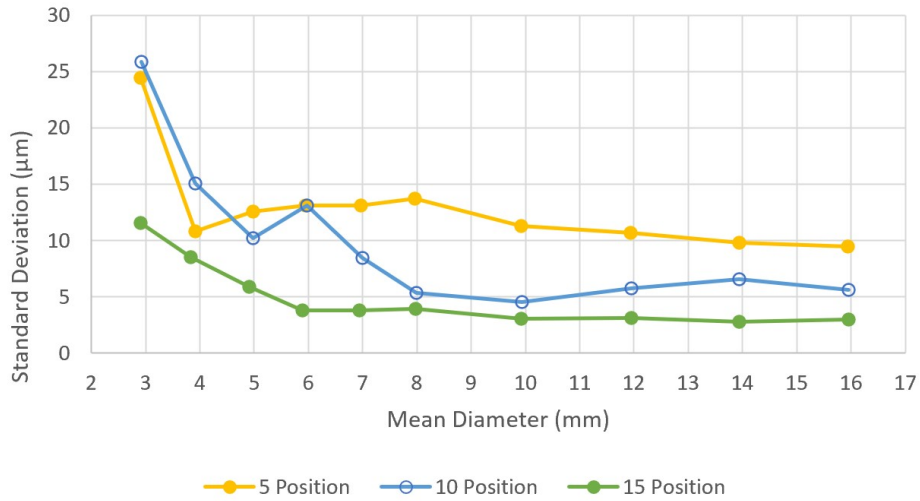


(b) Reproducibility

**Figure 7.1:** Comparing the Repeatability and Reproducibility Range Versus Mean Diameter Summary Graphs



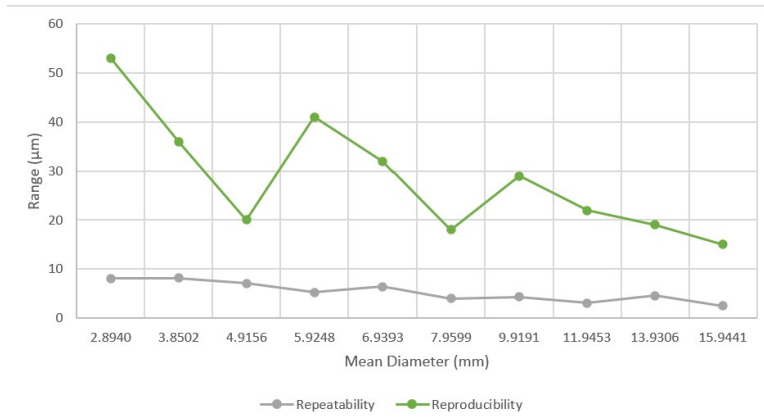
(a) Repeatability



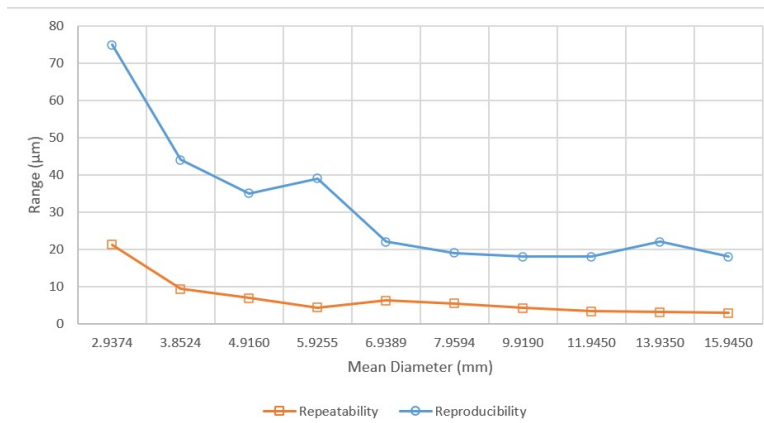
(b) Reproducibility

**Figure 7.2:** Comparing the Repeatability and Reproducibility Standard Deviation Versus Mean Diameter Summary Graphs

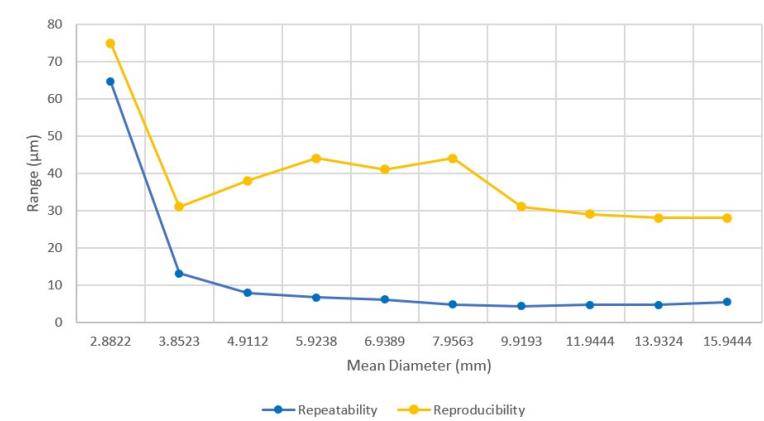




(a) 15 Positions

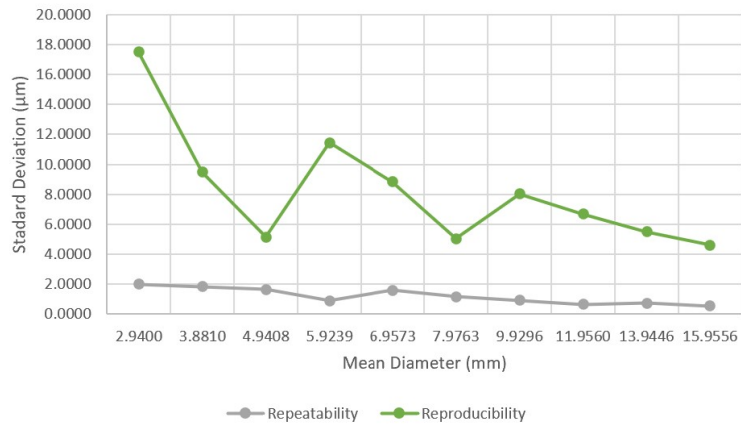


(b) 10 Positions

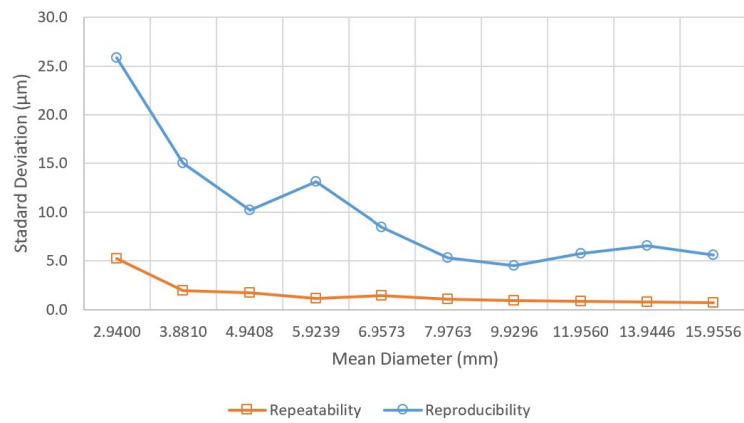


(c) 5 Positions

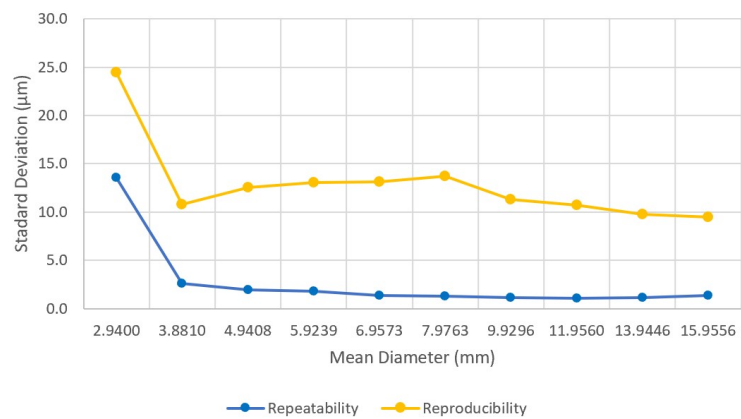
**Figure 7.3:** Directly Comparing the Repeatability and Reproducibility of Range Versus Mean Diameter for 5, 10 and 15 Positions



(a) 15 Positions

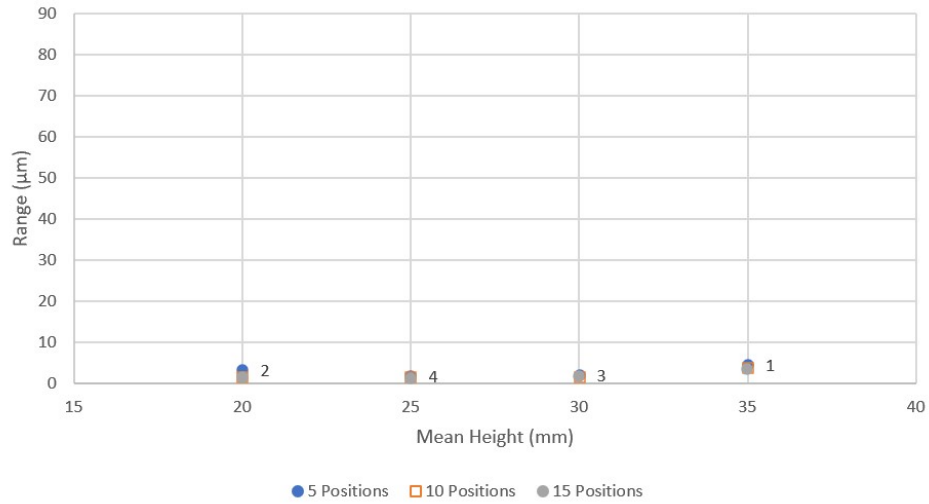


(b) 10 Positions

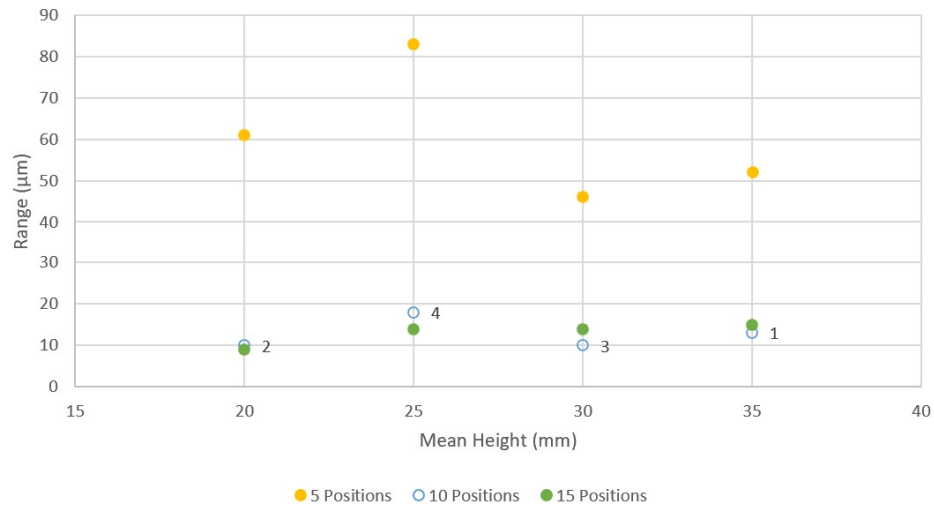


(c) 5 Positions

**Figure 7.4:** Directly Comparing the Repeatability and Reproducibility of Standard Deviation Versus Mean Diameter for 5, 10 and 15 Positions

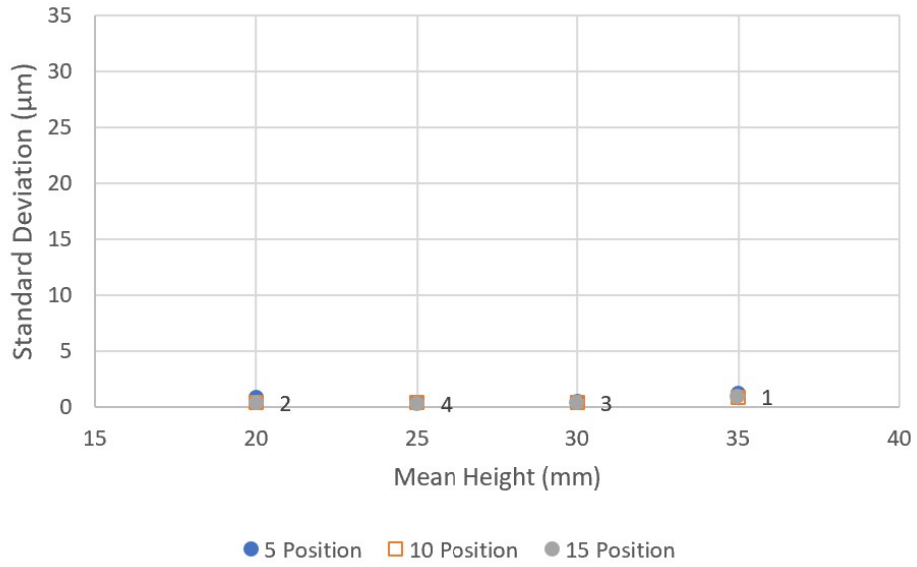


(a) Repeatability

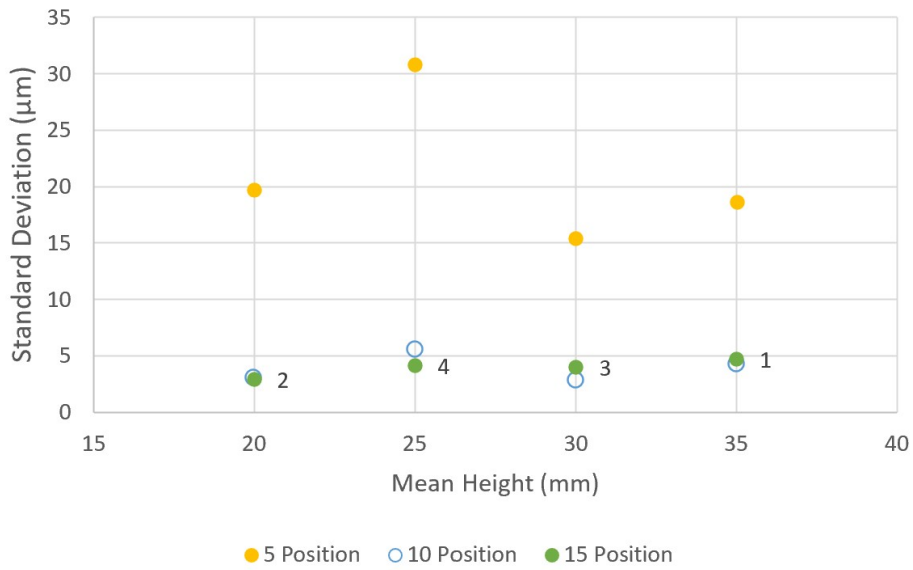


(b) Reproducibility

**Figure 7.5:** Comparing the Repeatability and Reproducibility Range Versus Mean Height Summary Graphs

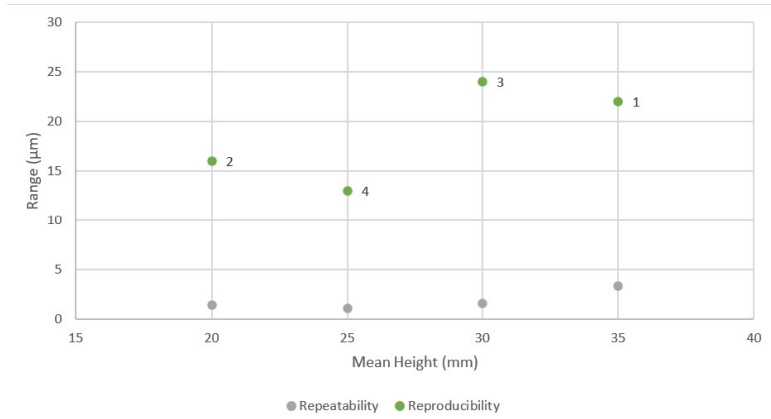


(a) Repeatability

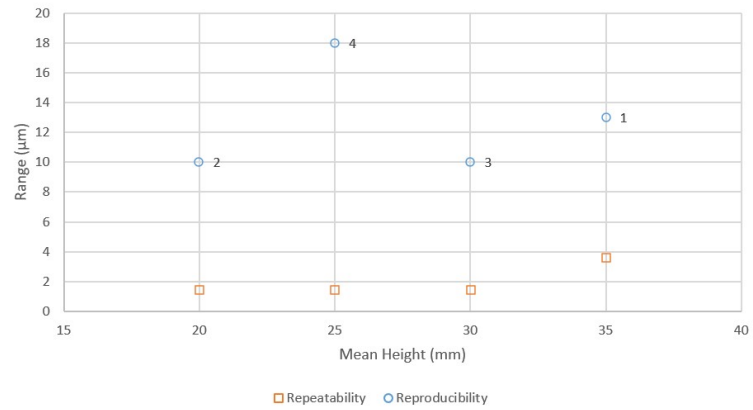


(b) Reproducibility

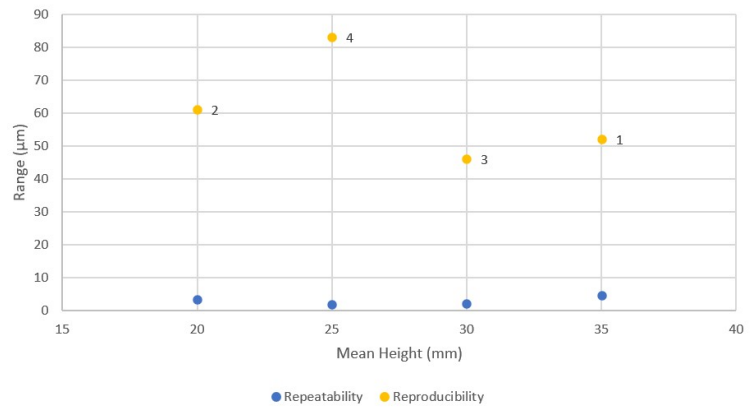
**Figure 7.6:** Comparing the Repeatability and Reproducibility Standard Deviation Versus Mean Height Summary Graphs



(a) 15 Positions

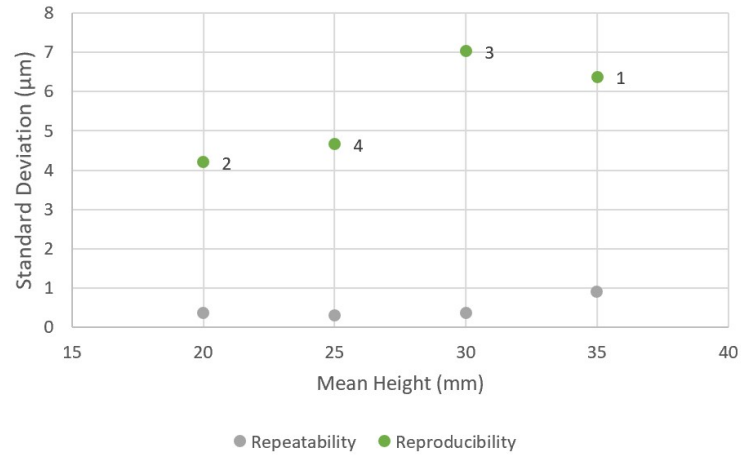


(b) 10 Positions

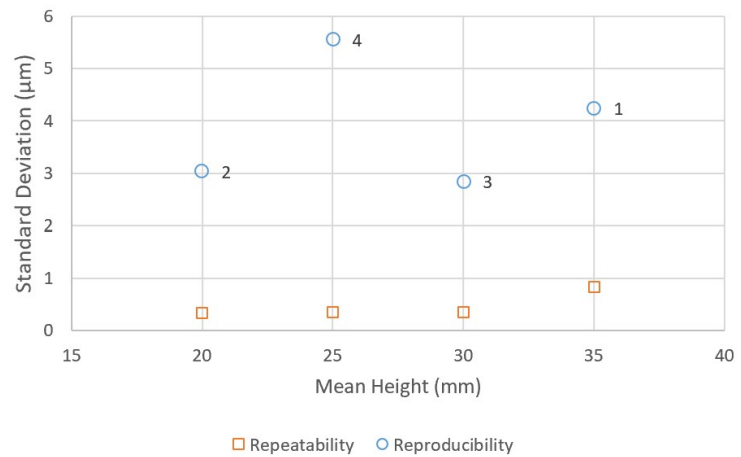


(c) 5 Positions

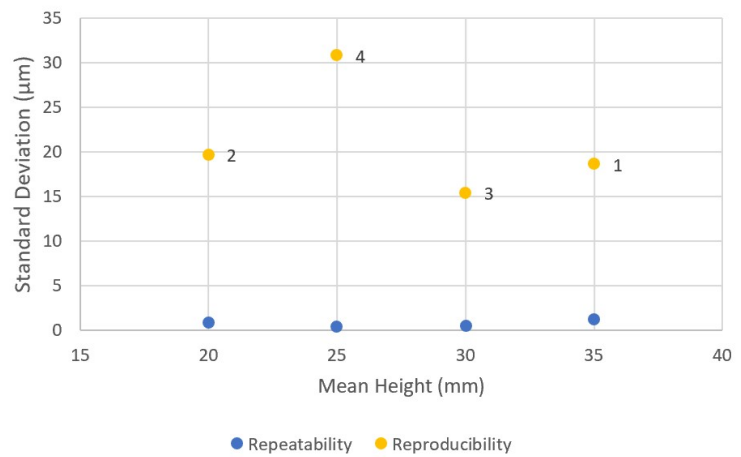
**Figure 7.7:** Directly Comparing the Repeatability and Reproducibility of Range Versus Mean Height for 5, 10 and 15 Positions



(a) 15 Positions



(b) 10 Positions



(c) 5 Positions

**Figure 7.8:** Directly Comparing the Repeatability and Reproducibility of Standard Deviation Over Mean Height for 5, 10 and 15 Positions

to find the diameter of the holes to not compute correctly causing significant outliers in the histograms. In order to fix this issue, the alignment had to be manually adjusted for each mesh. The second issue was the fact that the position of the points used to create the center distances deviated significantly when they were first created causing the distance histograms to have a several millimeter measurement spread. This was corrected by changing the creation parameters of the points so that it used the actual data of the top plane created on the mesh. The third issue comes from GOM Inspect pre- set project default unit preferences. The pre-set default unit preferences are set so that only two decimal places are visible for a measurement. This was not sufficient for the study, so the setting had to be adjusted so that the measurement showed four decimal places each time; the table of measurements was exported as a CSV file. This allowed the variation in the measurements to be determined instead of truncating the values. This adjustment was made by going to the edit menu, selecting preferences, selecting default units, and changing the number of decimal places to four.

In the reproducibility phase of the study, issues with scan alignment arose. This occurred after the GOM ATOS Q scanner was moved into the Machine Tool Research Center (MTRC, 101 Dougherty Engineering Building). During this time in the month of June, the weather in Knoxville was fluctuating upwards of 7 deg C over a 24-hour period. The MTRC has glass windows and a large garage door which makes keeping a constant room temperature difficult. Even a 5 deg change in ambient room temperature can result in scanner errors. To combat this issue, the scanner was calibrated before the measurements were performed. Additionally, adhesive was applied to the bottom of the part to prevent the part from moving during the scanning process. Note that the scans that were done in the MTRC before the HVAC system was put into the room so that the only temperature control the room had was from insulation in the walls of the lab, the windows, and the garage door. While processing the meshes, it was revealed that the circles made using cross-sections of the mesh tended to not line up correctly in the position they were created, and were even bigger than the part completely when the new group of meshes were imported into the project. To fix this issue, the circles created using the Create fitting circle tool were deleted and re-created, allowing the cross-section circles to form correctly in position and relative size. The circles were used

to determine the number of points needed to measure the diameters. It was found that the meshes that used more positions had more points around the circles while the five position meshes had fewer points. This was especially clear for circle one in the five position meshes due to the fact that three of the circles made from the cross-section were much smaller than the actual hole they were based on. This is likely because the circles had less available points in comparison to the 15 position meshes.



# Chapter 8

## Conclusions

Structured light scanning (SLS) repeatability and reproducibility studies were completed using measurements of a manufactured artifact. The repeatability study considered variation due to scanning alone. The sensitivity to number of scan positions was also evaluated. It was shown that repeatability tends to increase with the number of scan positions, which was demonstrated by the decreased range and standard deviation found with the larger number of scan positions. It was also shown that the repeatability increased with a larger number of points available on the measurements feature. Specifically, it was seen that larger circles, with more points around the circle periphery, provided increased repeatability. Reproducibility was assessed by scanning the same part using different positions for each mesh. Reproducibility also increased with the number of scan positions and points on the feature. This was confirmed by the decreased range and standard deviation found with the larger number of scan positions and larger circles. Tables [8.1](#), [8.2](#), and [8.3](#) show the repeatability and reproducibility for each number of positions.

A coordinate measuring machine (CMM) was used to measure the same part and features. The CMM results provide a comparison between the SLS mean values, as well as their distribution, and the industry standard for dimensional metrology. Good agreement was observed for the larger features and larger number of scan positions from the reproducibility data. Poor agreement was seen for the smaller features from the repeatability data. Less effect was observed for the number of positions, since a single dataset was used (five scans at 15 positions) for the repeatability study.

Feature	Repeatability			Reproducibility		
	Mean (mm)	Range ( $\mu\text{m}$ )	Std. Dev. ( $\mu\text{m}$ )	Mean (mm)	Range ( $\mu\text{m}$ )	Std. Dev. ( $\mu\text{m}$ )
Circle 1	2.8940	8.1	2.0	2.9400	36	11.6
Circle 2	3.8502	8.2	1.8	3.8810	26	8.5
Circle 3	4.9156	7.1	1.6	4.9408	20	5.9
Circle 4	5.9248	5.3	0.9	5.9239	14	3.8
Circle 5	6.9393	6.4	1.6	6.9573	13	3.8
Circle 6	7.9599	4	1.2	7.9763	12	4.0
Circle 7	9.9191	4.3	0.9	9.9296	10	3.0
Circle 8	11.9453	3.1	0.7	11.9560	11	3.1
Circle 9	13.9306	4.6	0.7	13.9446	10	2.8
Circle 10	15.9441	2.5	0.5	15.9556	11	3.0
Height 1	34.9901	4.5	1.1	35.0034	15	4.7
Height 2	20.0047	3.2	0.8	19.9944	9	2.9
Height 3	30.0017	1.9	0.4	30.0057	14	4.0
Height 4	25.0097	1.7	0.4	25.0039	14	4.1

**Table 8.1:** Summary of the Repeatability and Reproducibility of the Circle Diameters and Heights for the 15 Position Meshes

Feature	Repeatability			Reproducibility		
	Mean (mm)	Range ( $\mu\text{m}$ )	Std. Dev. ( $\mu\text{m}$ )	Mean (mm)	Range ( $\mu\text{m}$ )	Std. Dev. ( $\mu\text{m}$ )
Circle 1	2.9374	21.3	5.3	2.9235	75	25.9
Circle 2	3.8524	9.4	2.0	3.9162	44	15.0
Circle 3	4.9160	6.9	1.7	4.9797	35	10.2
Circle 4	5.9255	4.4	1.1	5.9756	39	13.1
Circle 5	6.9389	6.3	1.4	6.9976	22	8.5
Circle 6	7.9594	5.5	1.1	7.9908	19	5.3
Circle 7	9.9190	4.3	0.9	9.9389	18	4.5
Circle 8	11.9450	3.4	0.8	11.9471	18	5.7
Circle 9	13.9350	3.1	0.7	13.9401	22	6.6
Circle 10	15.9450	2.9	0.7	15.9564	18	5.6
Height 1	35.0186	3.6	0.8	35.0003	13	4.2
Height 2	20.0187	1.4	0.3	19.9887	10	3.0
Height 3	30.0078	1.4	0.3	30.0035	10	2.8
Height 4	25.0124	1.4	0.3	25.0002	18	5.6

**Table 8.2:** Summary of the Repeatability and Reproducibility of the Circle Diameters and Heights for the 10 Position Meshes

To summarize the study results, two plots are provided: one for the 10 circles (Fig. 8.1) and one for the four step heights (Fig. 8.2). The vertical axis in each plot gives the number of measurement positions and the horizontal axis gives the feature size. The height map shows the reproducibility (one standard deviation) from 10 separate tests for each of the feature size-number of position combinations. The units are micrometers. For the circles this shows that low standard deviations (5  $\mu\text{m}$  or less) is dependent on number of measurement positions and the feature size since more surface area was available for the larger circle diameters.

For the step heights, on the other hand, there is no strong dependence on the feature size (i.e., the contours are approximately flat). This is because the artifact geometry provided approximately the same surface area for measurements regardless of the step height. Low standard deviations (5  $\mu\text{m}$  or less) are only available for a large number of measurement positions (10 to 15).

Using the methodology discussed in this thesis the repeatability and reproducibility of other scanners can be evaluated and compared to the industry standard as determined by a CMM. This allows the scanner to be appraised for usage in various applications. These applications include reverse engineering, height control for additive manufacturing, nondestructive quality control, reconstruction of an object or room, volume measurements, non-contact measurements, precision shape measurements, and more.

Feature	Repeatability			Reproducibility		
	Mean	Range	Std. Dev.	Mean	Range	Std. Dev.
	(mm)	( $\mu\text{m}$ )	( $\mu\text{m}$ )	(mm)	( $\mu\text{m}$ )	( $\mu\text{m}$ )
Circle 1	2.8822	64.6	13.6	2.9143	75	24.4
Circle 2	3.8523	13.1	2.6	3.9175	31	10.8
Circle 3	4.9112	7.9	1.9	4.9778	38	12.6
Circle 4	5.9238	6.7	1.8	5.9416	44	13.1
Circle 5	6.9389	6.1	1.4	6.9652	41	13.1
Circle 6	7.9563	4.8	1.3	7.9641	44	13.7
Circle 7	9.9193	4.4	1.1	9.9161	31	11.3
Circle 8	11.9444	4.7	1.1	11.9317	29	10.7
Circle 9	13.9324	4.7	1.1	13.9332	28	9.8
Circle 10	15.9444	5.5	1.4	15.9478	28	9.5
Height 1	35.0183	3.3	0.9	35.0182	52	18.6
Height 2	20.0190	1.4	0.3	20.0012	61	19.7
Height 3	30.0080	1.6	0.3	30.0003	46	15.4
Height 4	25.0131	1.1	0.3	25.0059	83	30.8

**Table 8.3:** Summary of the Repeatability and Reproducibility of the Circle Diameters and Heights for the 5 Position Meshes

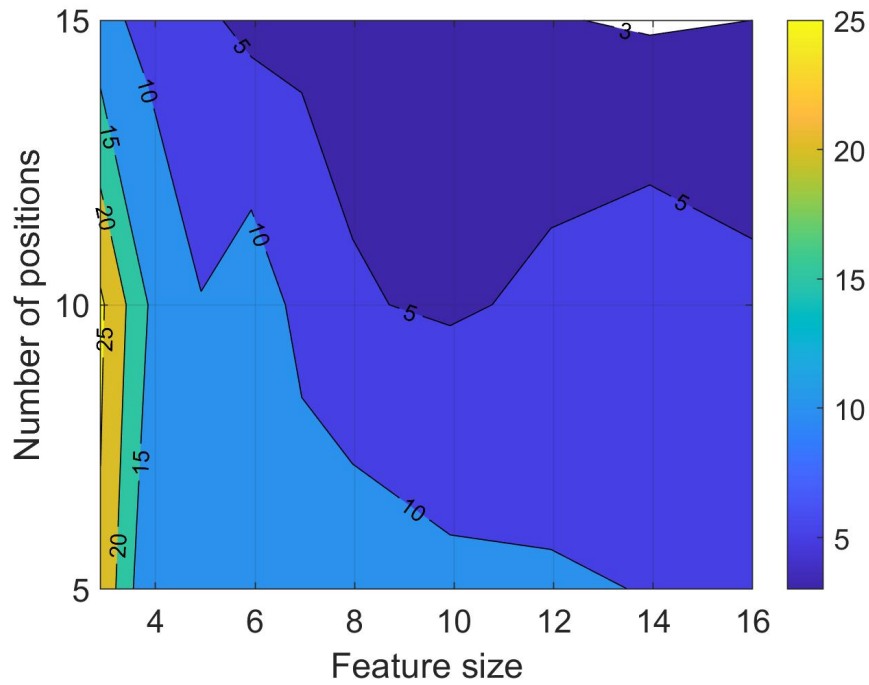


**Figure 8.1:** Summary of the Reproducibility Standard Deviations Based on Circle Diameter and Number of Positions in Micrometers

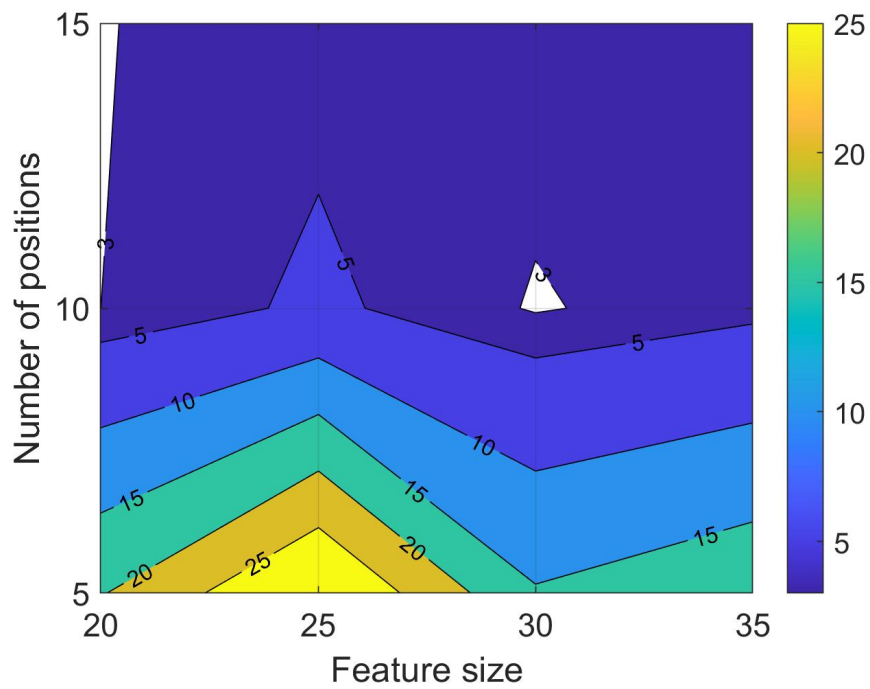


**Figure 8.2:** Summary of the Reproducibility Standard Deviations Based on Step Height and Number of Positions in Micrometers

# Bibliography

- [1] Bernal, C., de Agustina, B., Marín, M. M., and Camacho, A. M. (2013). Performance evaluation of optical scanner based on blue led structured light. *Procedia Engineering*, 63:591–598. [2](#)
- [2] Eiriksson, E. R., Wilm, J., Pedersen, D. B., and Aanaes, H. (2016). Precision and accuracy parameters in structured light 3-d scanning. *International Archives of the Photogrammetry, Remote Sensing and Spatial Info Sciences*, XL-5/W8:7–15. [2](#)
- [3] Elsmar (2021). Repeatability & reproducibility studies. [3](#)
- [4] Freeman Gebler, O., Goudswaard, M., Hicks, B., Jones, D., Nassehi, A., Snider, C., and Yon, J. (2021). A comparison of structured light scanning and photogrammetry for the digitisation of physical prototypes. *INTERNATIONAL CONFERENCE ON ENGINEERING DESIGN*, pages 11–20. [2](#)
- [5] Ghandali, P., Khameneifar, F., and JRR., M. (2019). A pseudo-3d ball lattice artifact and method for evaluating the metrological performance of structured-light 3d scanners. *Optics and Lasers in Engineering*, 121:87—95. [2](#)
- [6] GOM (2020). Atos q. [13](#)
- [7] Guerraa, M., Lavecchiaa, F., Maggipintob, G., Galantuccia, L., and Longoc, G. (2019). Measuring techniques suitable for verification and repairing of industrial components: A comparison among optical systems. *CIRP Journal of Manufacturing Science and Technology*, 27:114–123. [2](#)
- [8] ISIXSIGMA (2019). Reproducibility. [3](#)

- [9] Li, S., Wang, Z., Guan, J., and Wang, J. (2021). Uncertainty evaluation in surface structured light measurement. *IEEE 15th International Conference on Electronic Measurement & Instruments*, pages 395–400. [2](#)
- [10] Martínez-Pellitero, S., Cuesta, E., Giganto, S., and J., B. (2018). New procedure for qualification of structured light 3d scanners using an optical feature-based gauge. *Optics and Lasers in Engineering*, 110:193—206. [2](#)
- [11] McCarthy, M., Brown, S., Evenden, A., and Robinson, A. (2011). Npl freeform artefact for verification of non-contact measuring systems. *Three-dimensional imaging, interaction, and measurement*, 7864. [2](#)
- [12] Mendricky, R. (2016). Determination of measurement accuracy of optical 3d scanners. *MM Science Journal*, 2016:1565—1572. [2](#)
- [13] Microsoft (2020). How can i import multiple csv files into one workbook as separate tabs. [27](#)
- [14] NIST (2022). Nist tn 1297: Appendix d1. terminology. [3](#)
- [15] Polo, M. E., Cuartero, A., and Felicísimo, A. M. (2019). Study of uncertainty and repeatability in structured light 3d scanners. pages 1–9. [2](#), [3](#)
- [16] Zeiss (2021). Versatile, precise, compact – atos q. [ix](#), [14](#)

# Appendices

## Appendix A

### Tips and Tricks

#### A.1 GOM Inspect Software

1. GOM Inspect Professional is fully compatible with python.
2. Make sure the first scan has as many reference points as possible.
3. At least three reference points need to be visible between scans (more makes the registration better).
4. In the display section of the properties window it is possible to show the mesh structure.
5. The automatic hole filling tool requires at least part of the mesh to be selected.
6. The interactive hole filling tool requires a hole being selected; this can be done by clicking on the mesh near the hole to be selected.



7. When a hole is ready to be filled using the interactive hole filling tool, pressing the green triangle moves the tool to the next detected hole after filling the current one.
8. The data table can be exported as a CSV file and then imported into excel.

## **A.2 Other**

1. Goldbond Foot spray is effective at dulling shiny surfaces for improved scanning.
2. Pressing the forward button on the connected presentation remote allows a scan to be started without having to return to the computer every time.
3. Pressing the spacebar also starts a scan.

# Appendix B

## Suggested or Useful GOM Tutorials

### B.1 Found on the GOM Training Website

- Starter Training GOM Inspect (GOM Software 2021)  
<https://training.gom.com/home/LearningPath/7265?r=False&ts=637993268278207895>
- (eLearning) 022 How To Take Your Workflow and Results to the Next Level with GOM Inspect Professional (GOM Software 2019)  
<https://training.gom.com/course/40007?r=False&ts=637993271240202608>
- Mesh Editing with GOM Software  
<https://training.gom.com/home/LearningPath/8374?r=False&ts=637993270092780651>
- It's A Hack  
<https://training.gom.com/course/278511?r=False&ts=637993270092780651>

# Appendix C

## Other Useful Information

### C.1 Term and Acronym Definitions

- GDT - Geometric Dimensioning and Tolerancing is used to determine the dimensions of an element on the mesh.
- CMM - Coordinate Measuring Machine is used to measure the physical geometry of an object.
- SLS - Structured Light Scanner is used to measure the physical geometry of an object without touching the object.

### C.2 The Website Links from the Bibliography

- <https://www.gom.com/en/products/3d-scanning/atos-q>
- <https://answers.microsoft.com/en-us/msoffice/forum/all/how-can-i-import-multiple-csv-files-into-one/c43f011d-62cb-4b8d-b5be-2f3c587ed71d>
- <https://www.zeiss.com/metrology/innovation-magazine/2021/atos-q.html>
- <https://www.isixsigma.com/dictionary/repeatability/>
- <https://www.isixsigma.com/dictionary/reproducibility/>

- <https://www.nist.gov/pml/nist-technical-note-1297/nist-tn-1297-appendix-d1-terminology>

# Appendix D

## The text of the program to combine individual CSV files into a single Excel workbook as separate sheets

```
Sub CombineCsvFiles()  
'updateby Extendoffice  
    Dim xFilesToOpen As Variant  
    Dim I As Integer  
    Dim xWb As Workbook  
    Dim xTempWb As Workbook  
    Dim xDelimiter As String  
    Dim xScreen As Boolean  
    On Error GoTo ErrHandler  
    xScreen = Application.ScreenUpdating  
    Application.ScreenUpdating = False  
    xDelimiter = "—"   
    xFilesToOpen = Application.GetOpenFilename("Text Files (*.csv), *.csv", , "Kutools  
for Excel", , True)  
    If TypeName(xFilesToOpen) = "Boolean" Then  
        MsgBox "No files were selected", , "Kutools for Excel"
```

```

        GoTo ExitHandler
    End If
    I = 1
Set xTempWb = Workbooks.Open(xFilesToOpen(I))
    xTempWb.Sheets(1).Copy
    Set xWb = Application.ActiveWorkbook
    xTempWb.Close False
    Do While I <= UBound(xFilesToOpen)
        I = I + 1
        Set xTempWb = Workbooks.Open(xFilesToOpen(I))
        xTempWb.Sheets(1).Move , xWb.Sheets(xWb.Sheets.Count)
    Loop
ExitHandler:
    Application.ScreenUpdating = xScreen
    Set xWb = Nothing
    Set xTempWb = Nothing
    Exit Sub
ErrorHandler:
    MsgBox Err.Description, , "Kutools for Excel"
    Resume ExitHandler
End Sub

```

# Appendix E

## Report developed using the CMM

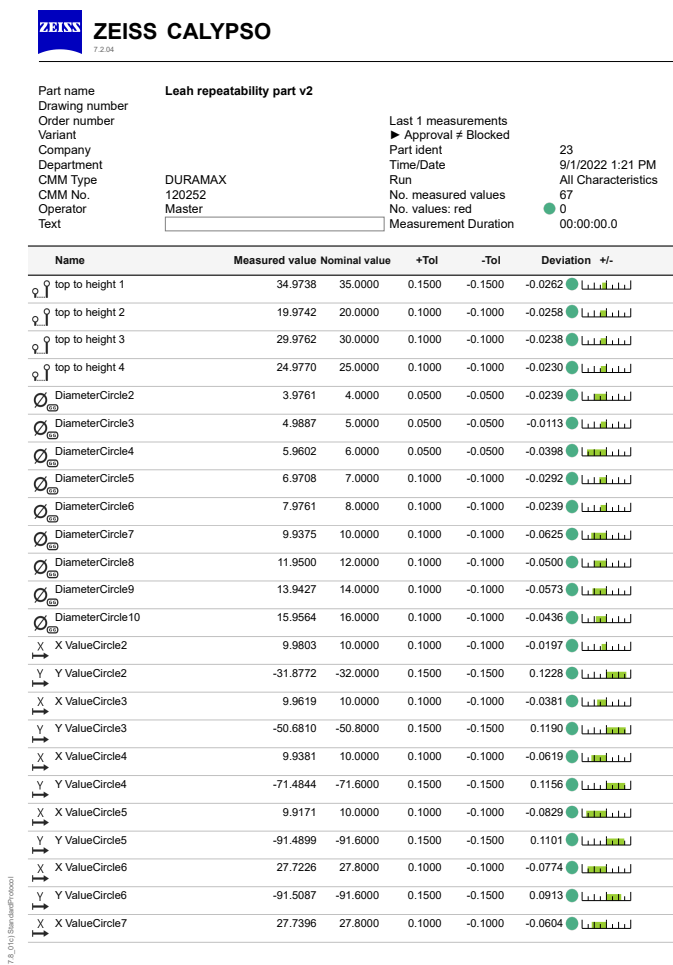


Figure E.1: First page of measurements from the report made using the CMM

Name	Measured value	Nominal value	+Tol	-Tol	Deviation +/-
Y Y ValueCircle7	-71.5110	-71.6000	0.1500	-0.1500	0.0890
X X ValueCircle8	27.7599	27.8000	0.1000	-0.1000	-0.0401
Y Y ValueCircle8	-50.7122	-50.8000	0.1500	-0.1500	0.0878
X X ValueCircle9	27.7788	27.8000	0.1000	-0.1000	-0.0212
Y Y ValueCircle9	-31.9108	-32.0000	0.1500	-0.1500	0.0892
X X ValueCircle10	27.7994	27.8000	0.1000	-0.1000	-0.0006
Y Y ValueCircle10	-11.9052	-12.0000	0.1000	-0.1000	0.0948
C2 to C3	18.8015	18.8000	0.1000	-0.1000	0.0015
C2 to C4	39.6046	39.6000	0.1500	-0.1500	0.0046
C2 to C5	59.6084	59.6000	0.1500	-0.1500	0.0084
C2 to C6	62.2106	62.2013	0.1500	-0.1500	0.0093
C2 to C7	43.4230	43.4166	0.1500	-0.1500	0.0064
C2 to C8	25.8914	25.8898	0.1000	-0.1000	0.0017
C2 to C9	17.7985	17.8000	0.1000	-0.1000	-0.0015
C2 to C10	26.7738	26.7739	0.1000	-0.1000	-0.0001
C3 to C4	20.8031	20.8000	0.1000	-0.1000	0.0031
C3 to C5	40.8069	40.8000	0.1500	-0.1500	0.0069
C3 to C6	44.5214	44.5138	0.1500	-0.1500	0.0076
C3 to C7	27.3802	27.3766	0.1000	-0.1000	0.0036
C3 to C8	17.7980	17.8000	0.1000	-0.1000	-0.0020
C3 to C9	25.8888	25.8898	0.1000	-0.1000	-0.0010
C3 to C10	42.6896	42.6882	0.1500	-0.1500	0.0014
C4 to C5	20.0038	20.0000	0.1000	-0.1000	0.0038
C4 to C6	26.7803	26.7739	0.1000	-0.1000	0.0064
C4 to C7	17.8015	17.8000	0.1000	-0.1000	0.0015
C4 to C8	27.3779	27.3766	0.1000	-0.1000	0.0013
C4 to C9	43.4203	43.4166	0.1500	-0.1500	0.0037
C4 to C10	62.2069	62.2013	0.1500	-0.1500	0.0056
C5 to C6	17.8055	17.8000	0.1000	-0.1000	0.0055
C5 to C7	26.7762	26.7739	0.1000	-0.1000	0.0023

Figure E.2: Second page of measurements from the report made using the CMM



Name	Measured value	Nominal value	+Tol	-Tol	Deviation +/-
C5 to C8	44.5188	44.5138	0.1500	-0.1500	0.0050
C5 to C9	62.2089	62.2013	0.1500	-0.1500	0.0076
C5 to C10	81.5754	81.5659	0.1500	-0.1500	0.0095
C6 to C7	20.0016	20.0000	0.1000	-0.1000	0.0016
C6 to C8	40.8054	40.8000	0.1500	-0.1500	0.0054
C6 to C9	59.6081	59.6000	0.1500	-0.1500	0.0081
C6 to C10	79.6098	79.6000	0.1500	-0.1500	0.0098
C7 to C8	20.8037	20.8000	0.1000	-0.1000	0.0037
C7 to C9	39.6064	39.6000	0.1500	-0.1500	0.0064
C7 to C10	59.6082	59.6000	0.1500	-0.1500	0.0082
C8 to C9	18.8027	18.8000	0.1000	-0.1000	0.0027
C8 to C10	38.8045	38.8000	0.1500	-0.1500	0.0045
C9 to C10	20.0018	20.0000	0.1000	-0.1000	0.0018

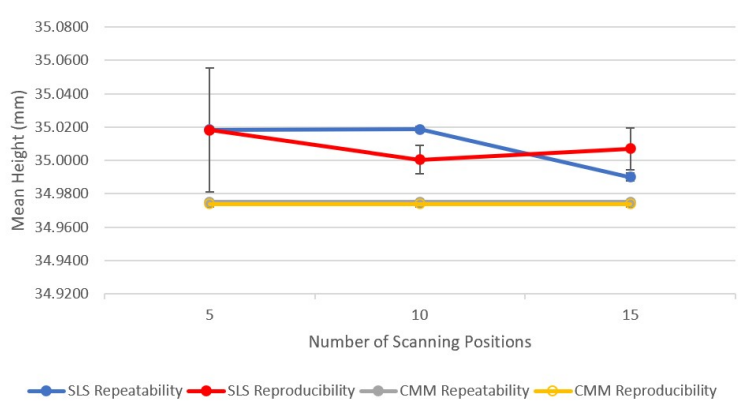
  

Text	Event
	-
	n.def.

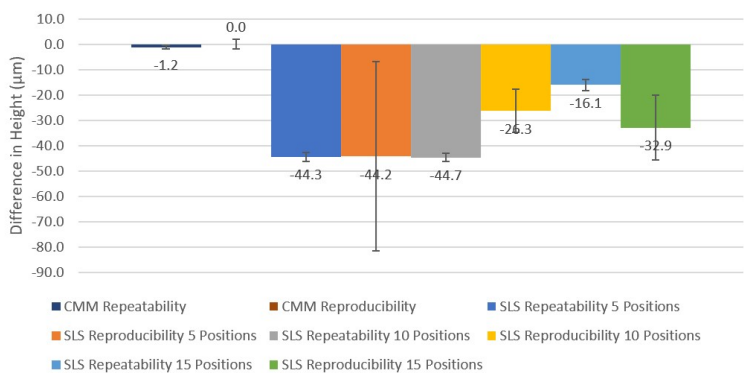
**Figure E.3:** Last page of measurements from the report made using the CMM

# Appendix F

## Structured Light Scanner to CMM Comparison Graphs

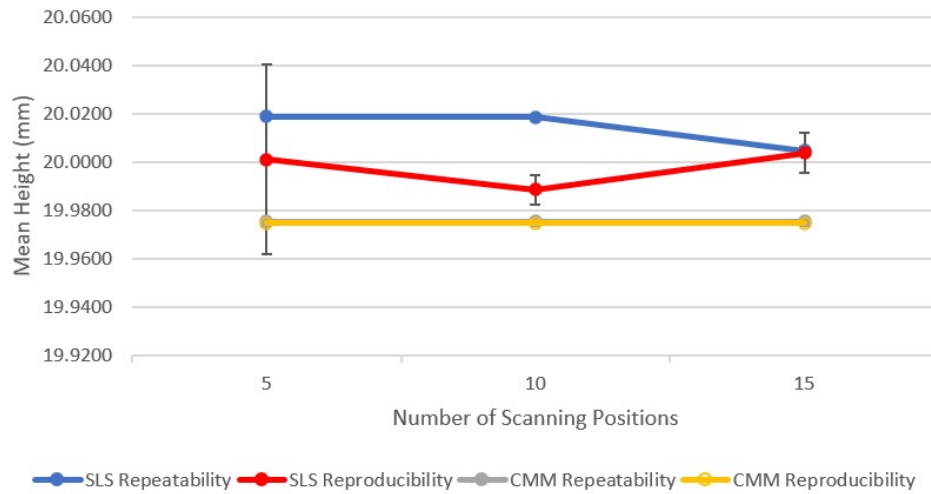


(a) Line Graph

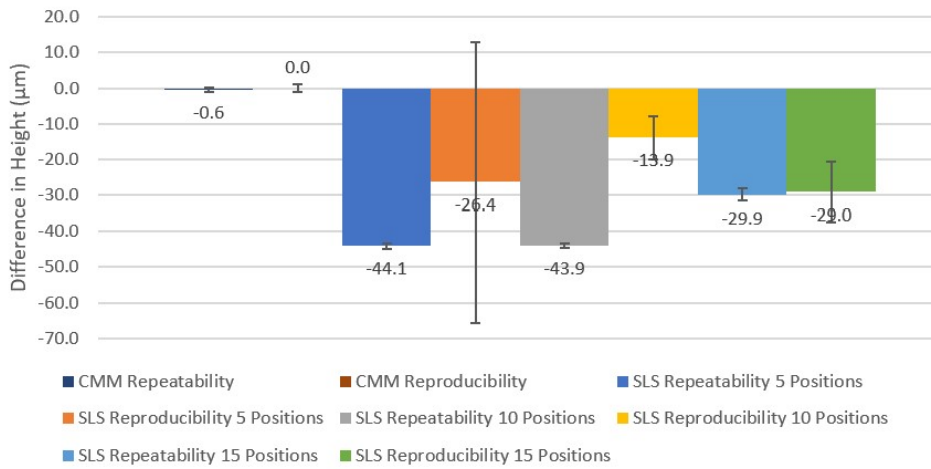


(b) Difference Graph

Figure F.1: Comparing Structured Light Scanning and CMM Measurements for Height 1

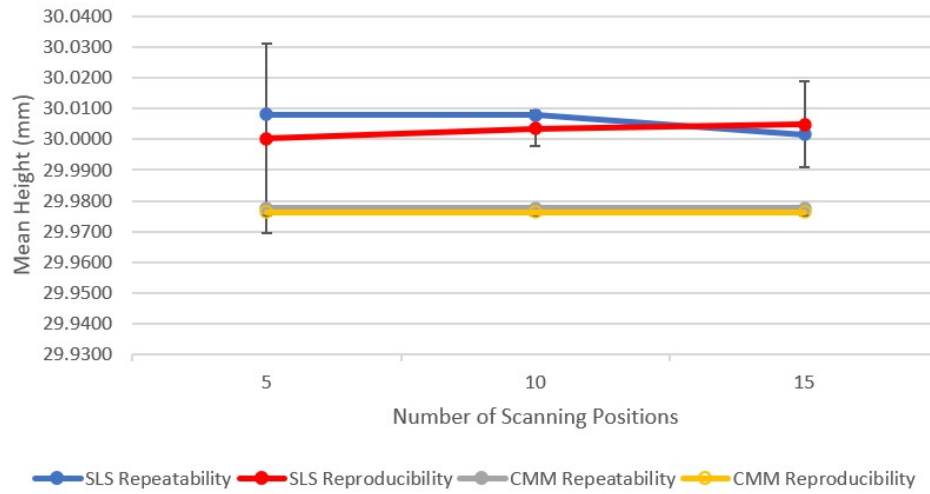


(a) Line Graph

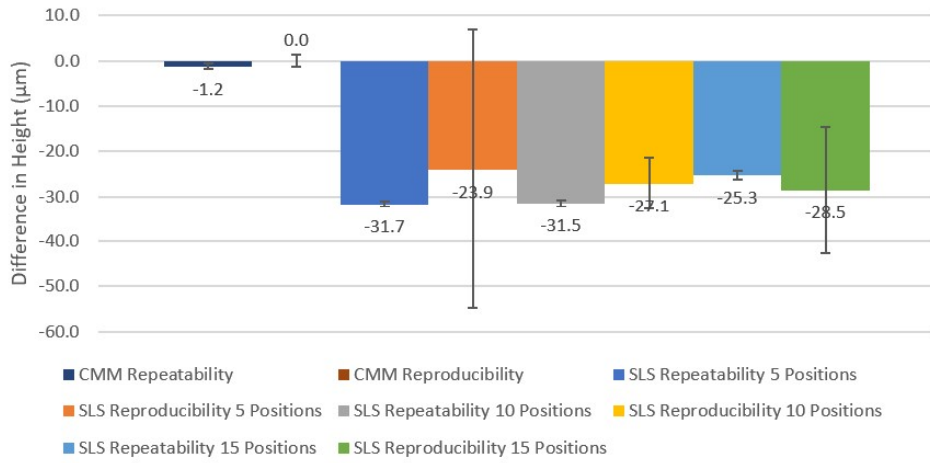


(b) Difference Graph

Figure F.2: Comparing Structured Light Scanning and CMM Measurements for Height 2

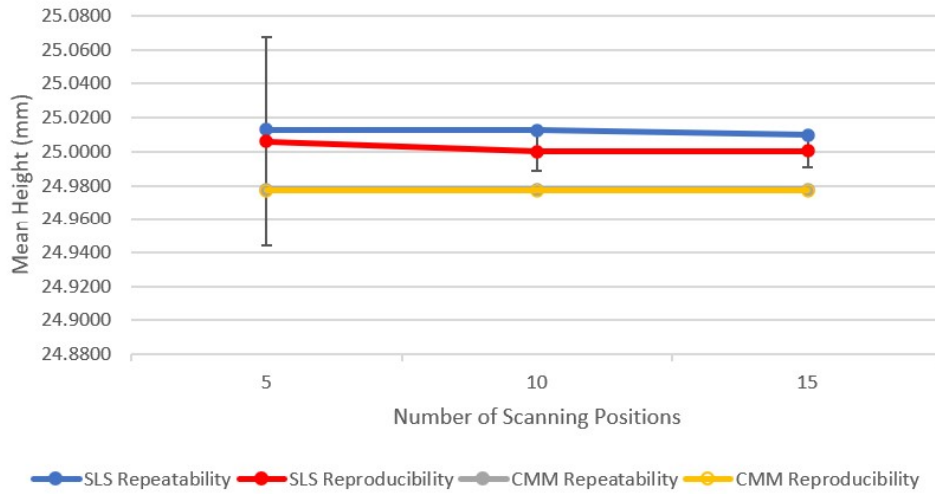


(a) Line Graph

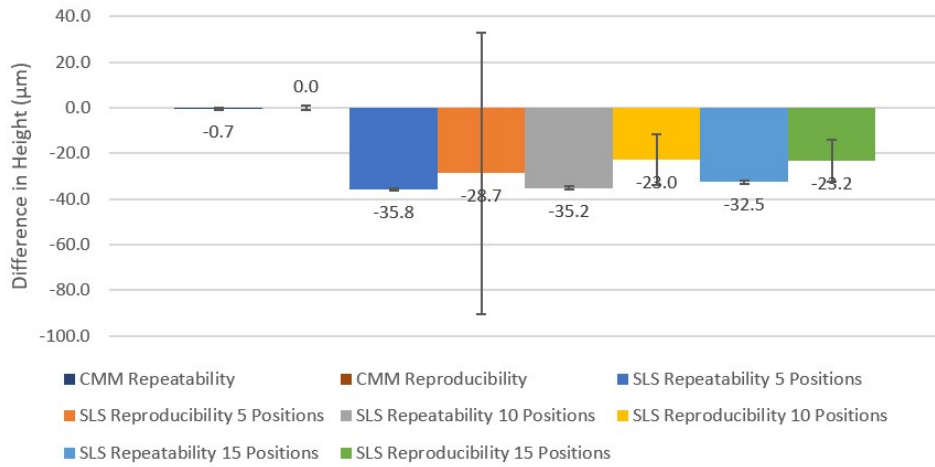


(b) Difference Graph

**Figure F.3:** Comparing Structured Light Scanning and CMM Measurements for Height 3

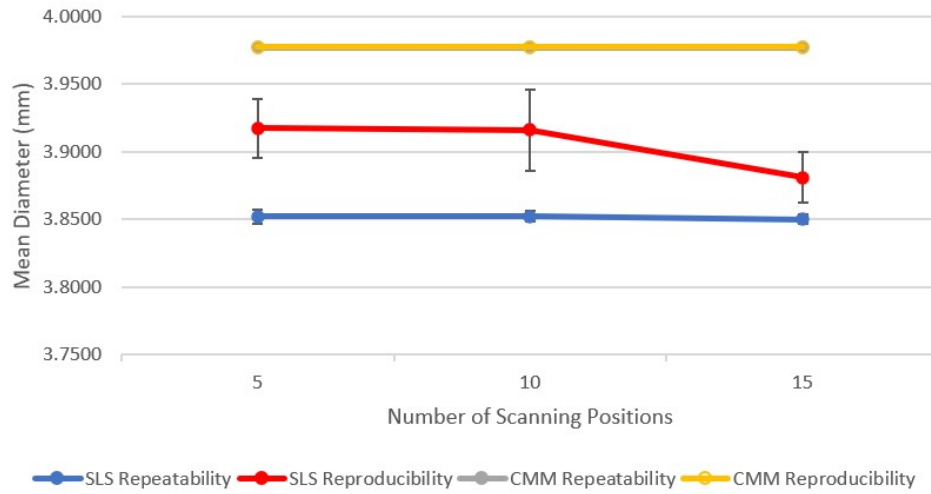


(a) Line Graph

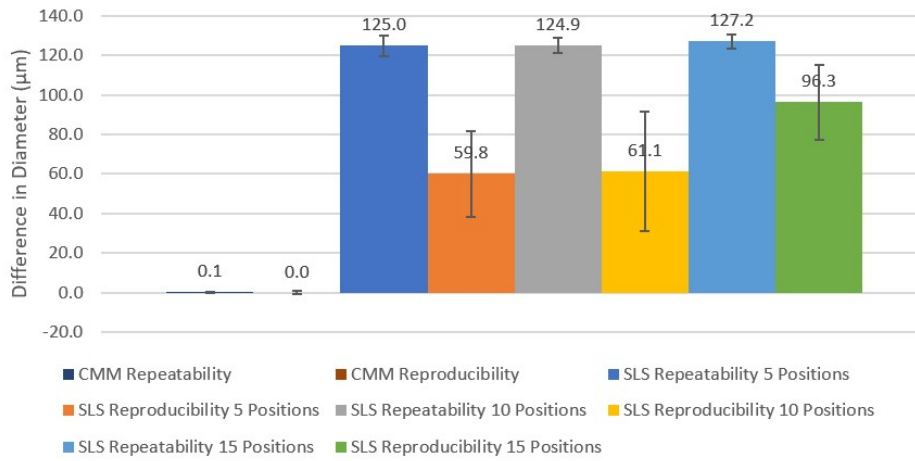


(b) Difference Graph

Figure F.4: Comparing Structured Light Scanning and CMM Measurements for Height 4

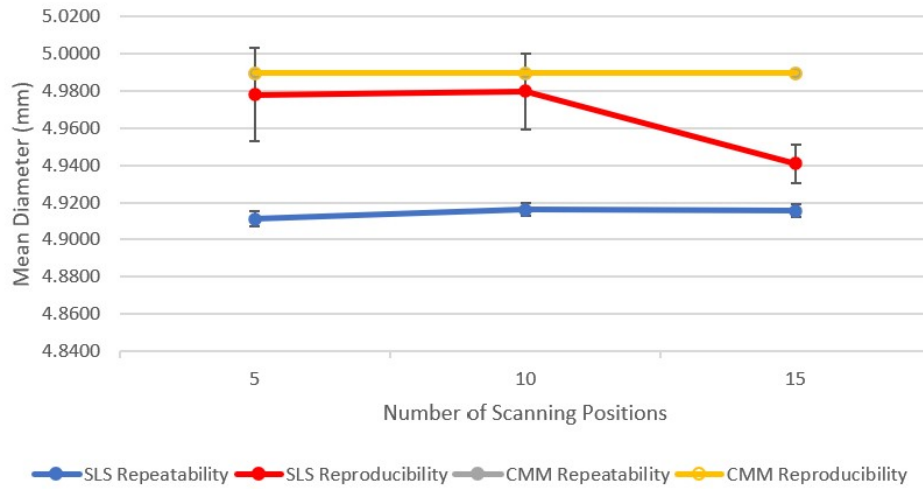


(a) Line Graph

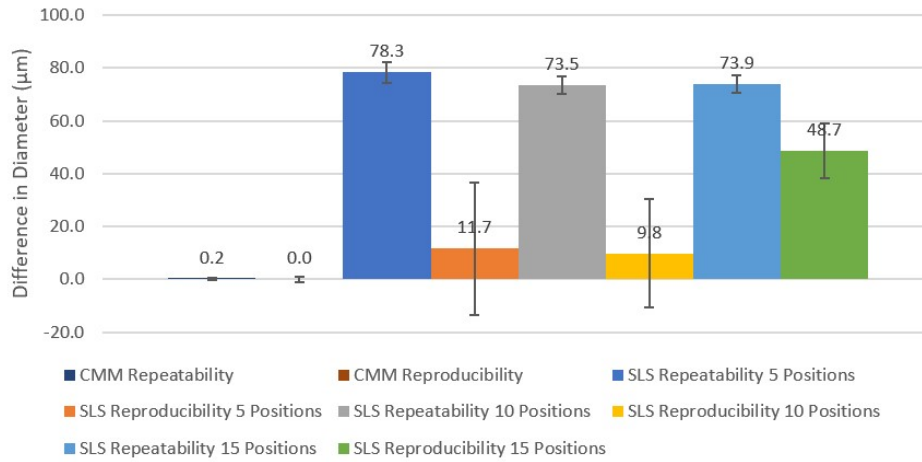


(b) Difference Graph

Figure F.5: Comparing Structured Light Scanning and CMM Measurements for Circle 2

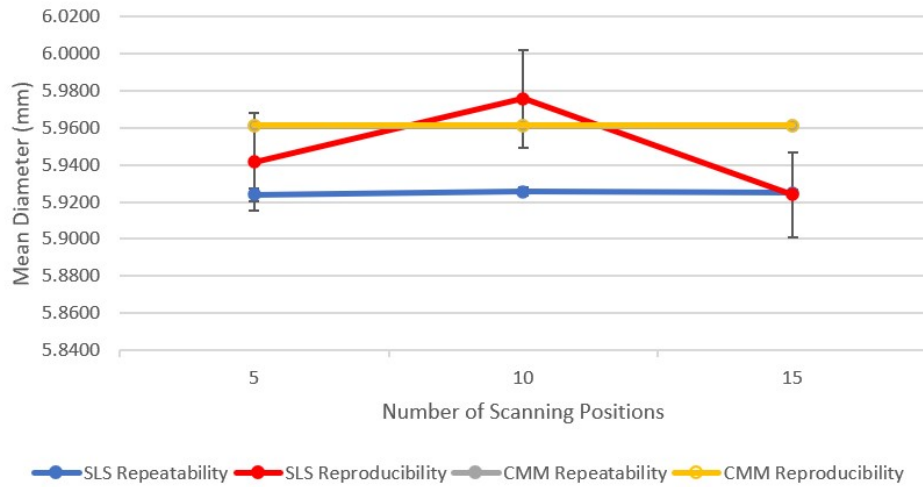


(a) Line Graph

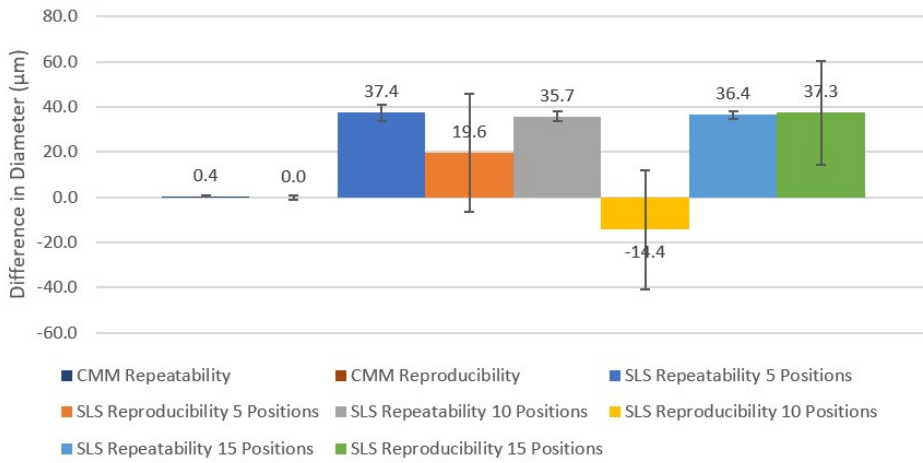


(b) Difference Graph

**Figure F.6:** Comparing Structured Light Scanning and CMM Measurements for Circle 3



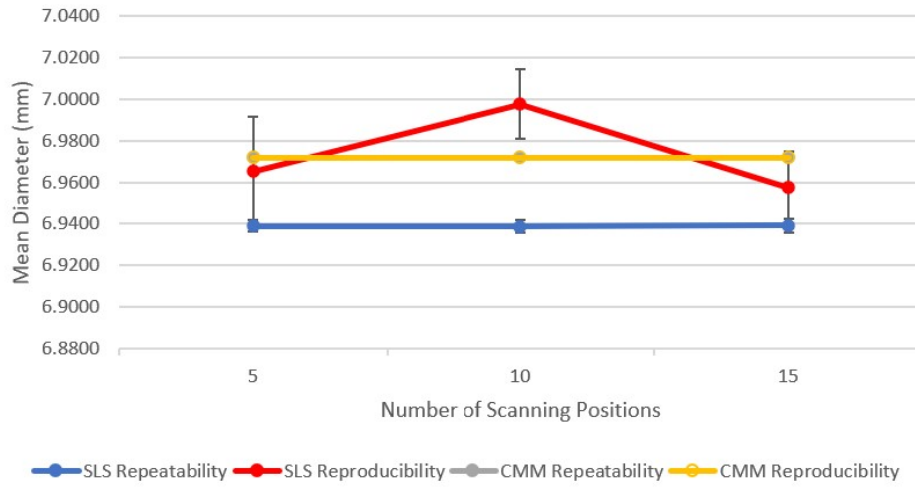
(a) Line Graph



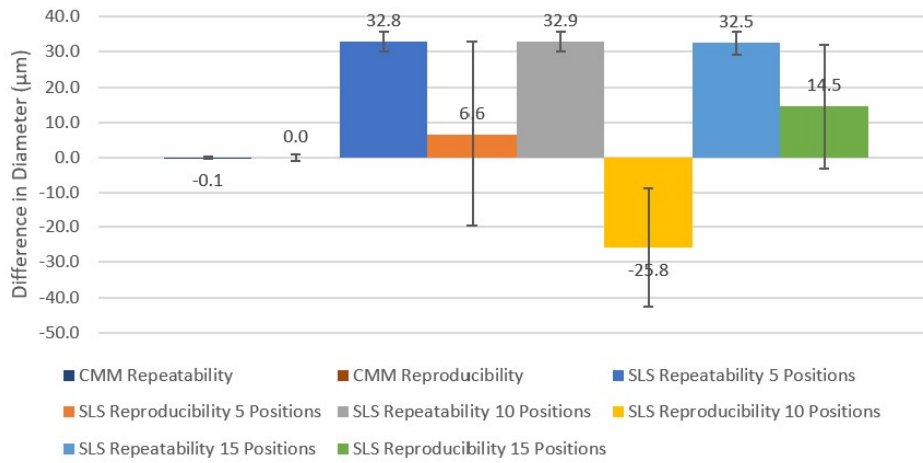
(b) Difference Graph

**Figure F.7:** Comparing Structured Light Scanning and CMM Measurements for Circle 4



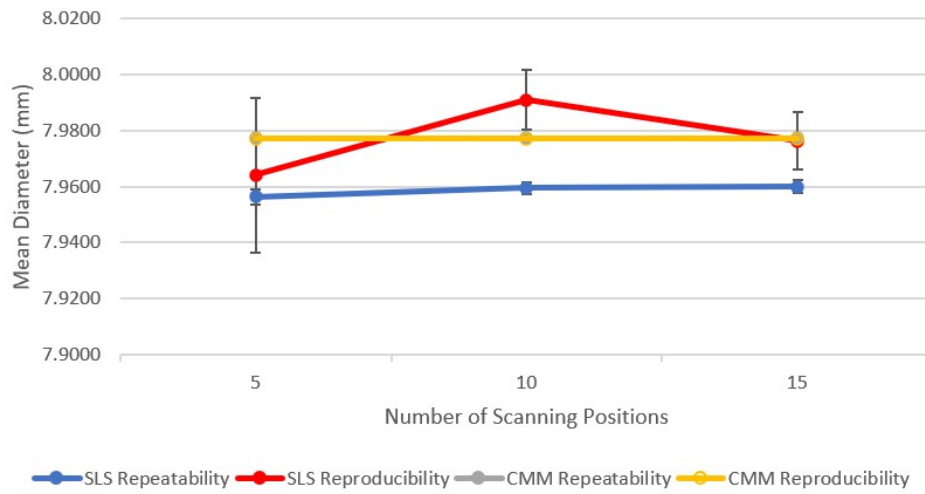


(a) Line Graph

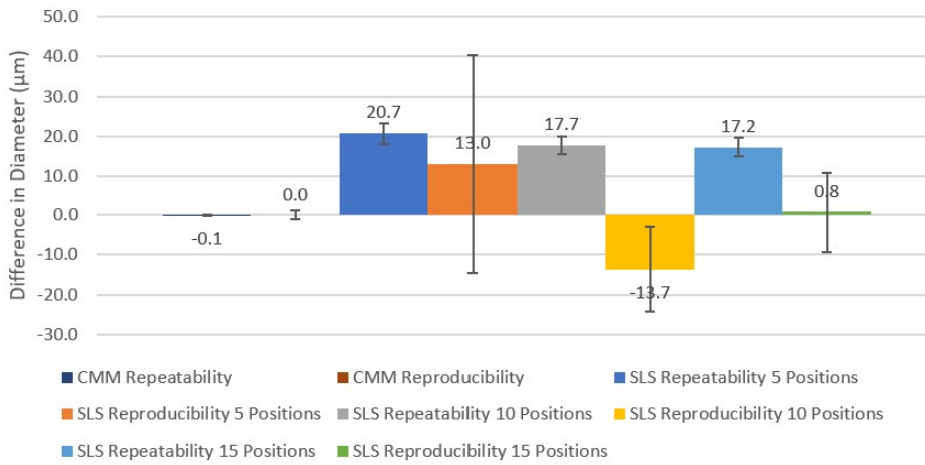


(b) Difference Graph

**Figure F.8:** Comparing Structured Light Scanning and CMM Measurements for Circle 5

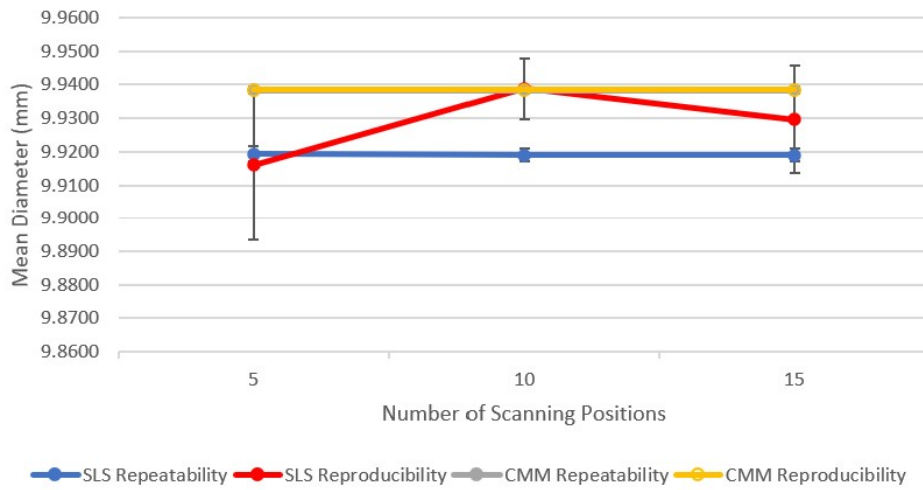


(a) Line Graph

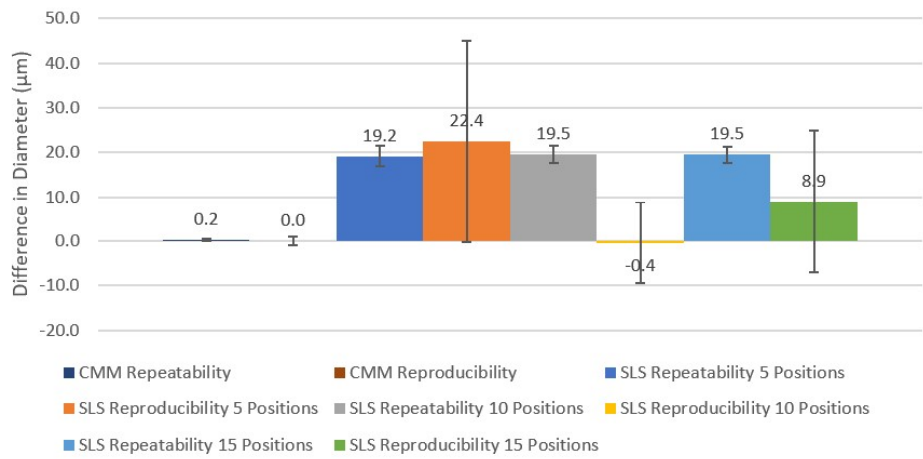


(b) Difference Graph

**Figure F.9:** Comparing Structured Light Scanning and CMM Measurements for Circle 6

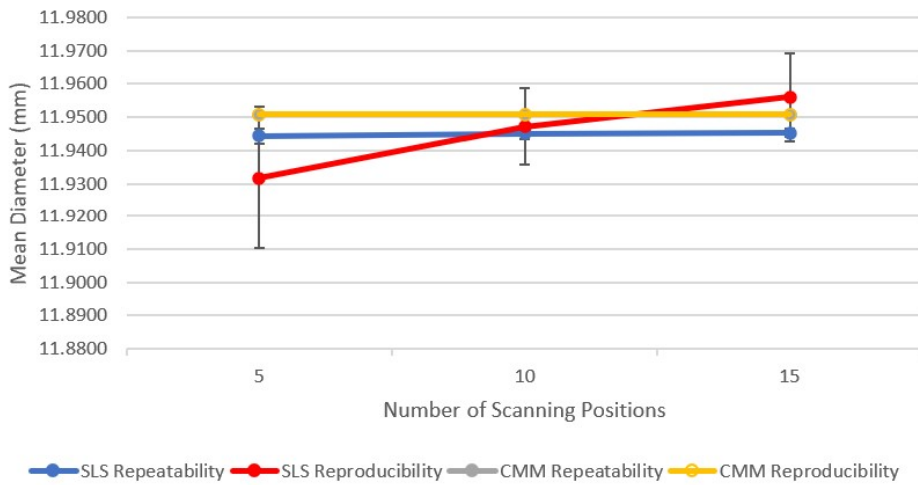


(a) Line Graph

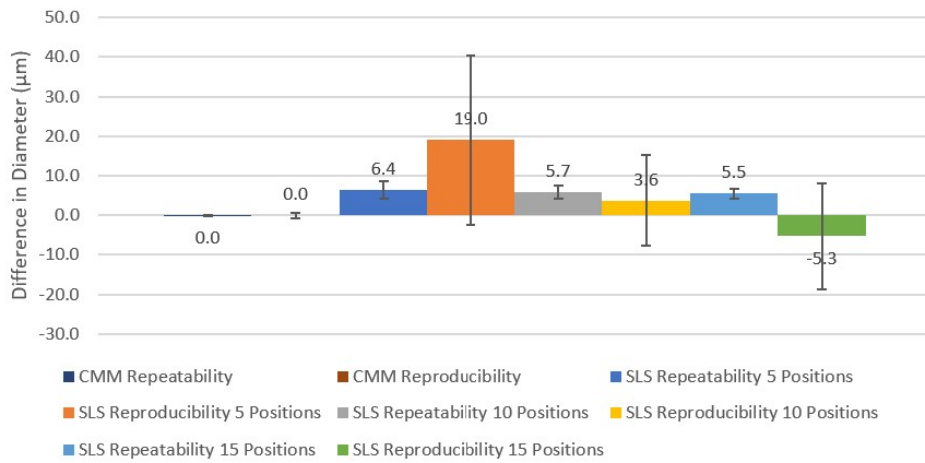


(b) Difference Graph

**Figure F.10:** Comparing Structured Light Scanning and CMM Measurements for Circle 7

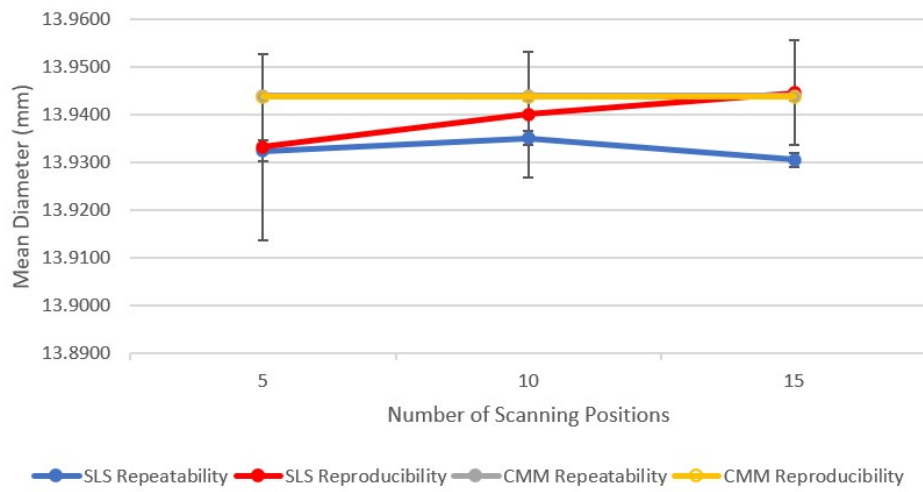


(a) Line Graph

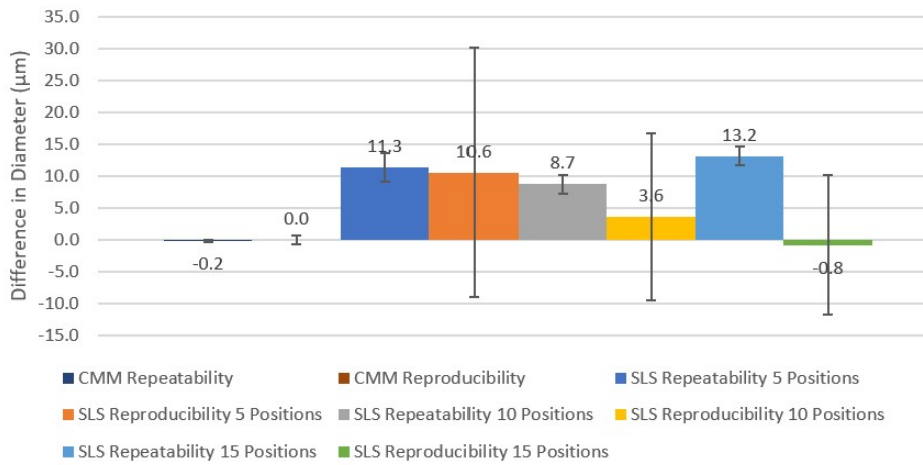


(b) Difference Graph

**Figure F.11:** Comparing Structured Light Scanning and CMM Measurements for Circle 8

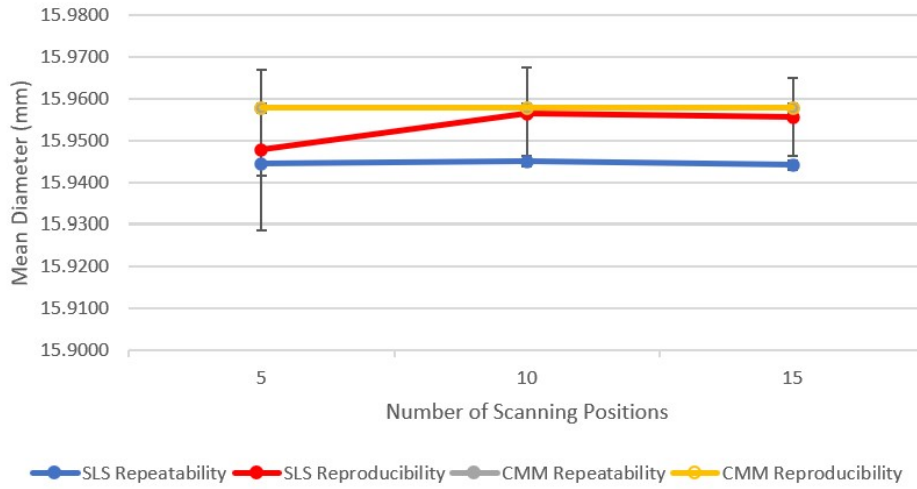


(a) Line Graph

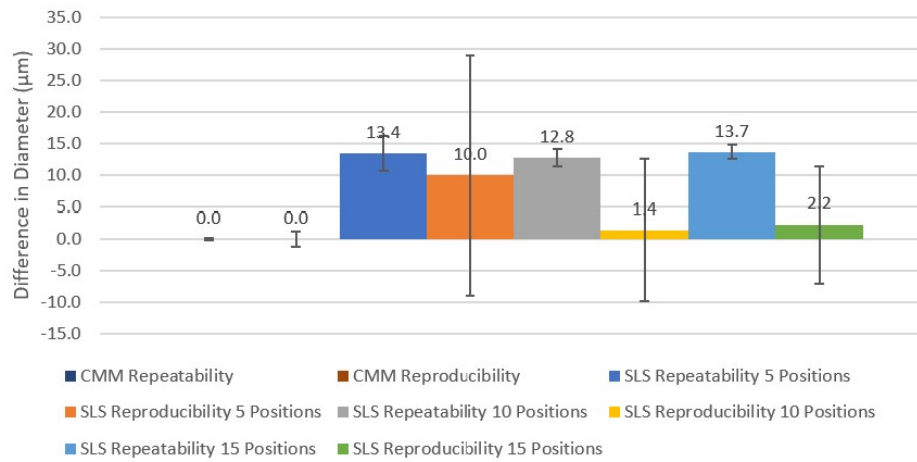


(b) Difference Graph

**Figure F.12:** Comparing Structured Light Scanning and CMM Measurements for Circle 9

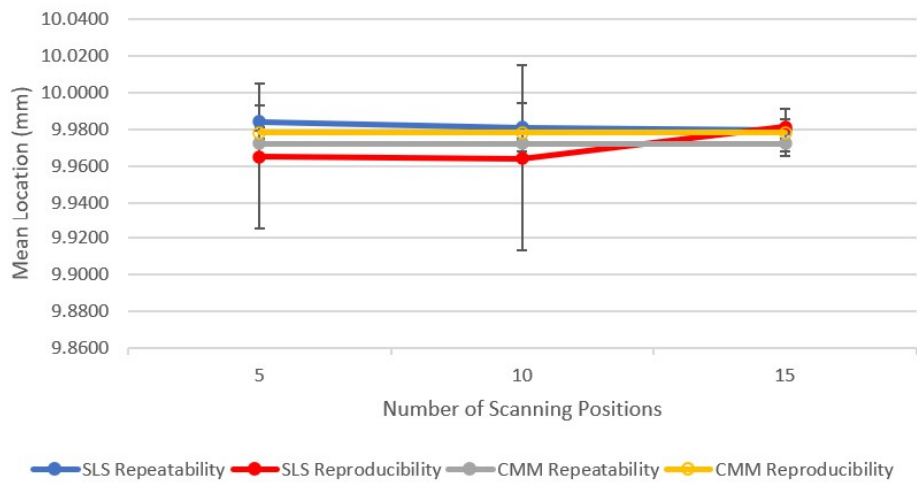


(a) Line Graph

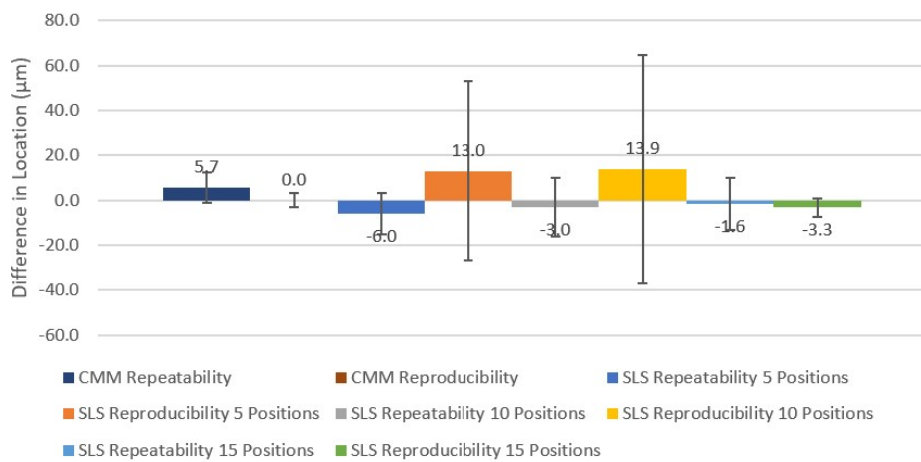


(b) Difference Graph

**Figure F.13:** Comparing Structured Light Scanning and CMM Measurements for Circle 10

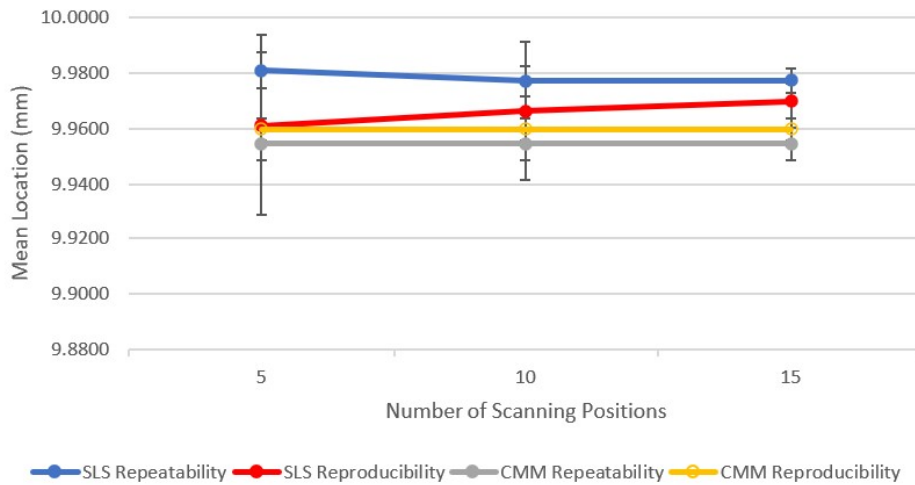


(a) Line Graph

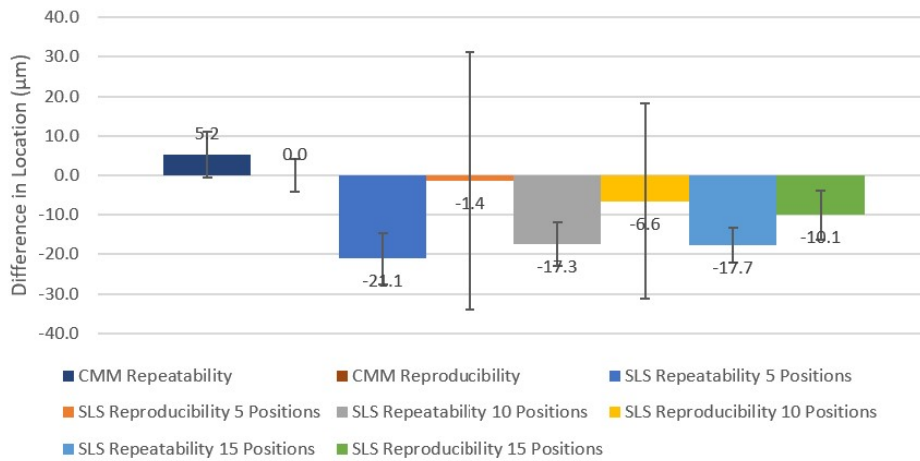


(b) Difference Graph

**Figure F.14:** Comparing Structured Light Scanning and CMM Measurements for X Location of Circle 2



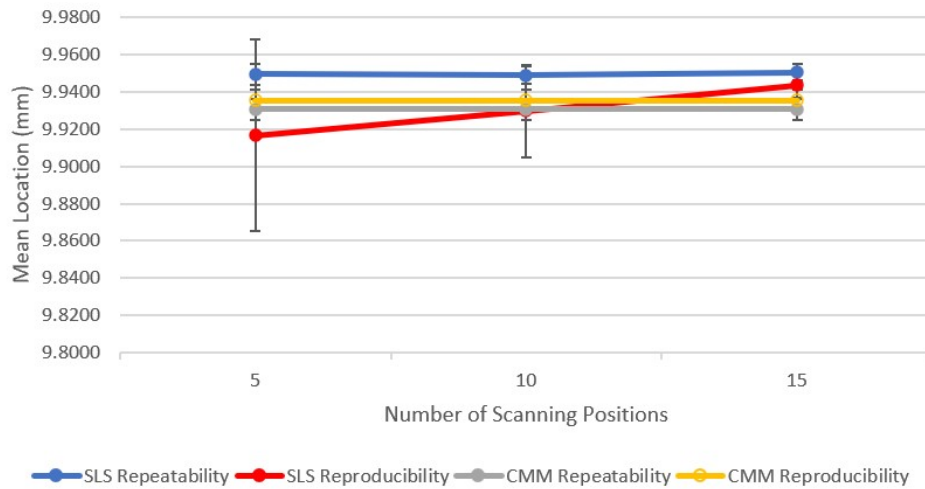
(a) Line Graph



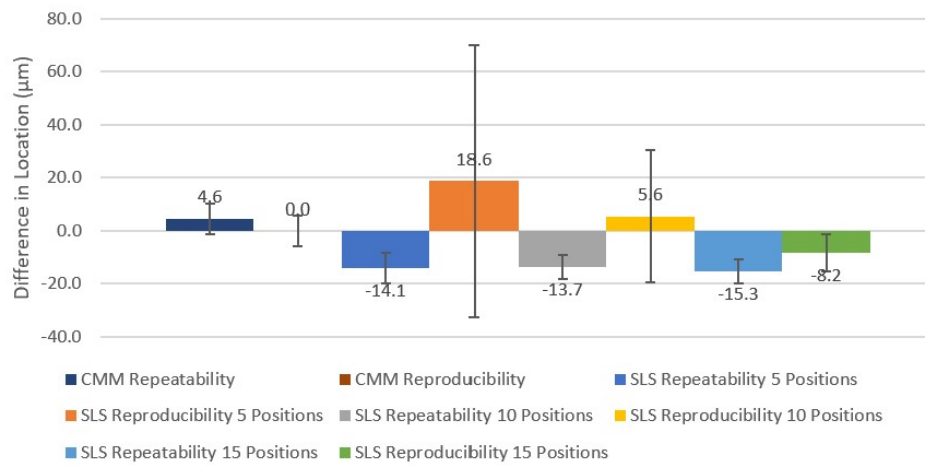
(b) Difference Graph

**Figure F.15:** Comparing Structured Light Scanning and CMM Measurements for X Location of Circle 3



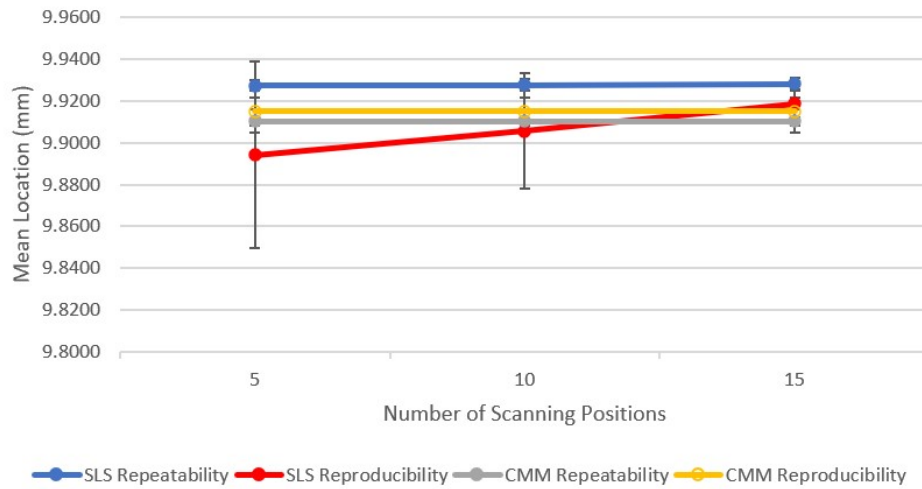


(a) Line Graph

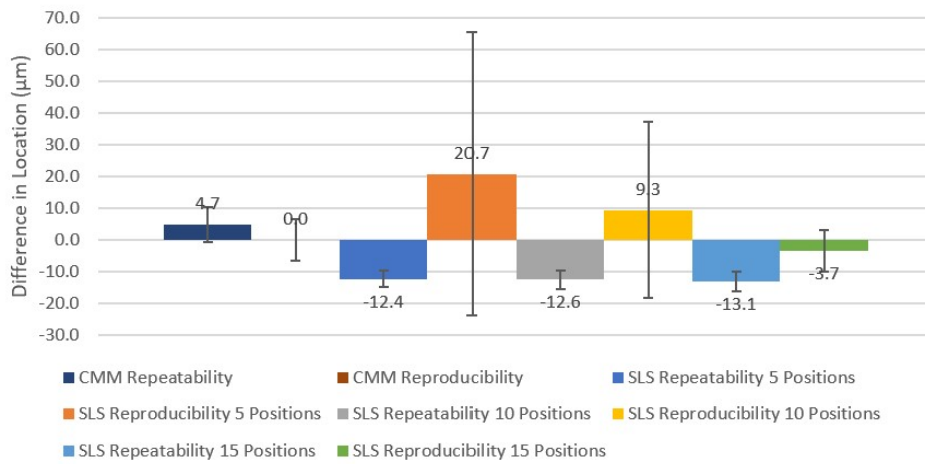


(b) Difference Graph

**Figure F.16:** Comparing Structured Light Scanning and CMM Measurements for X Location of Circle 4

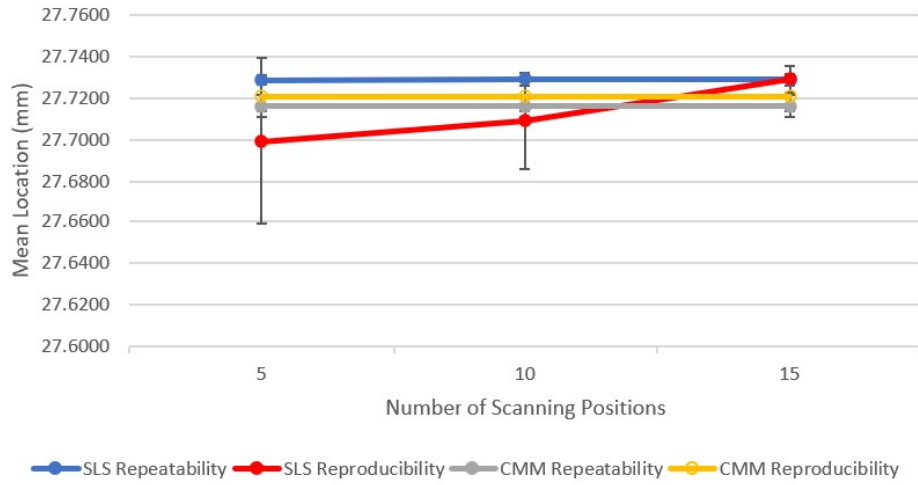


(a) Line Graph

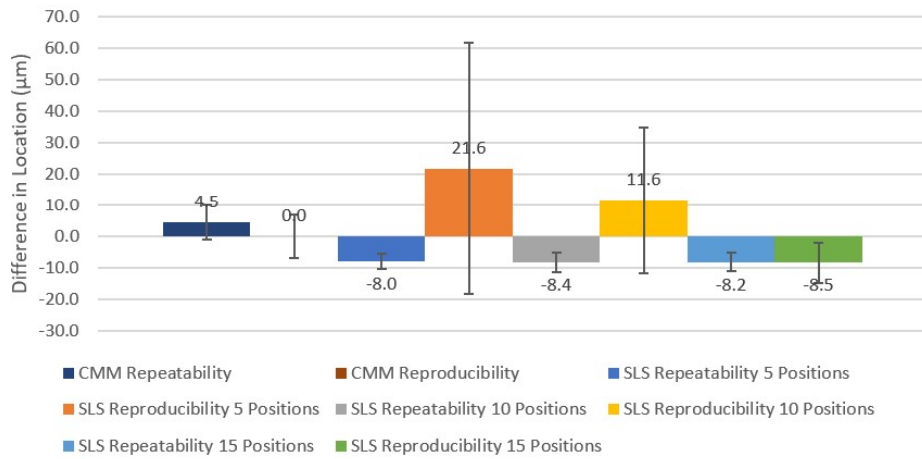


(b) Difference Graph

**Figure F.17:** Comparing Structured Light Scanning and CMM Measurements for X Location of Circle 5

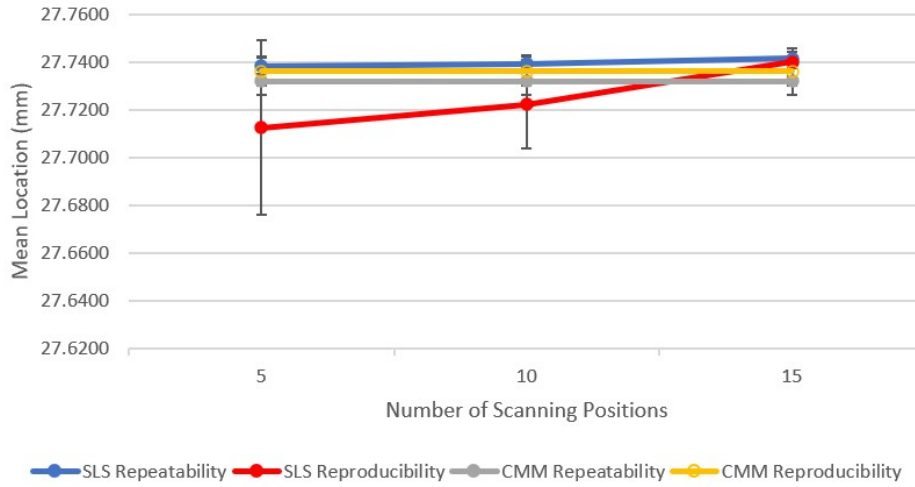


(a) Line Graph

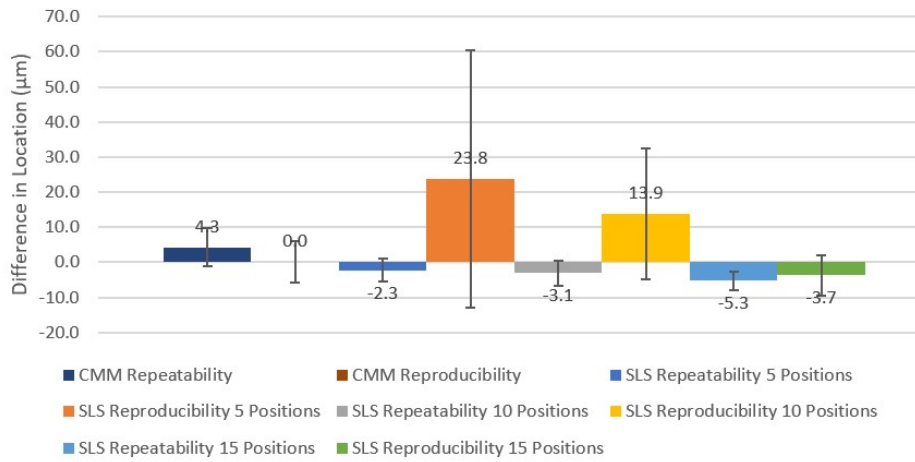


(b) Difference Graph

**Figure F.18:** Comparing Structured Light Scanning and CMM Measurements for X Location of Circle 6

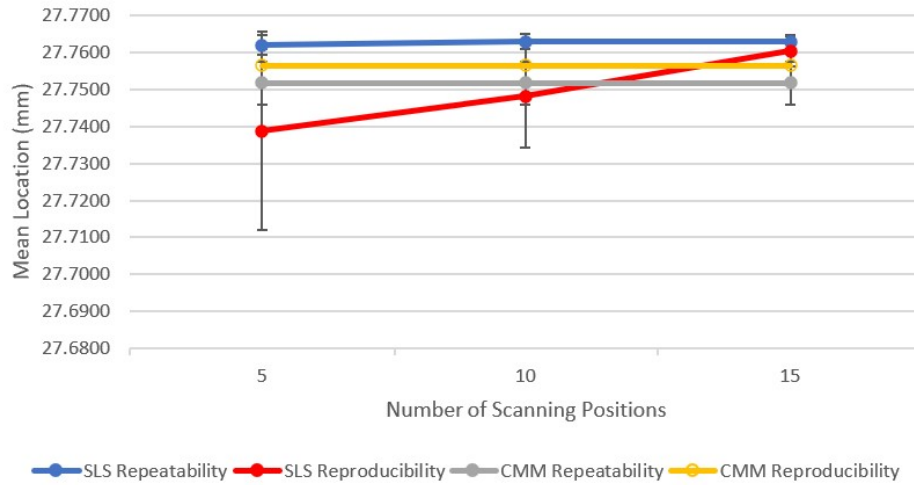


(a) Line Graph

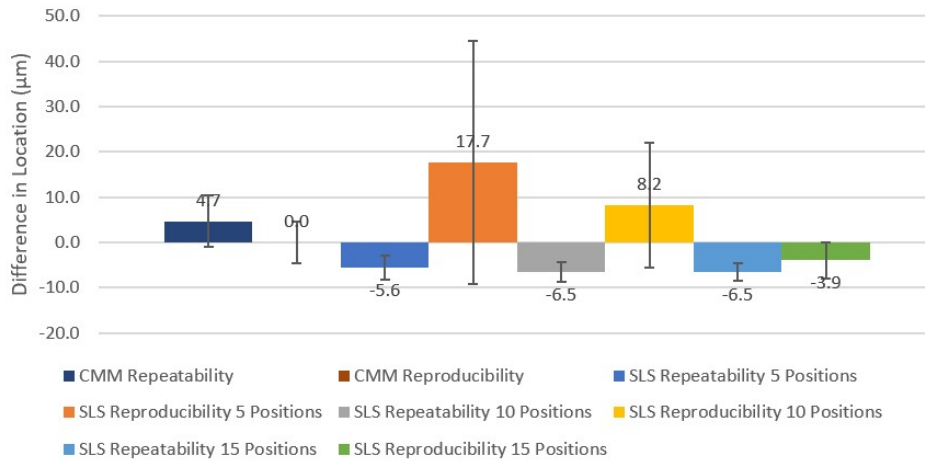


(b) Difference Graph

**Figure F.19:** Comparing Structured Light Scanning and CMM Measurements for X Location of Circle 7

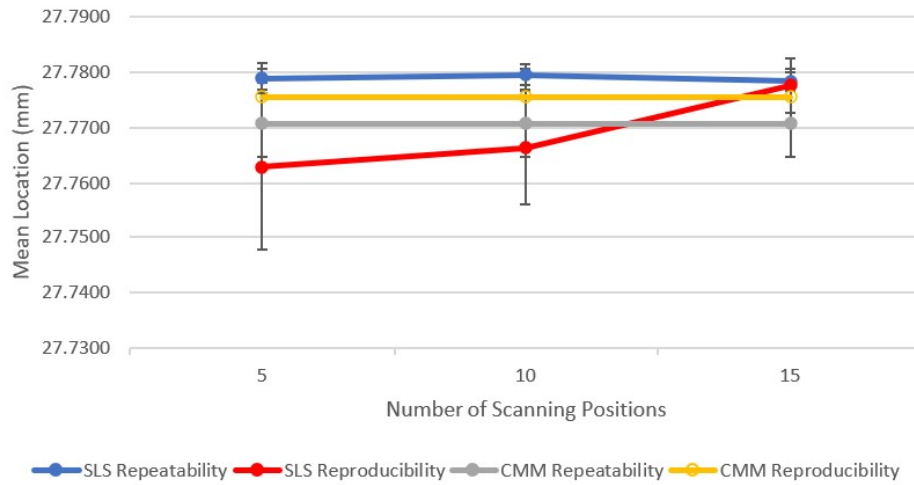


(a) Line Graph

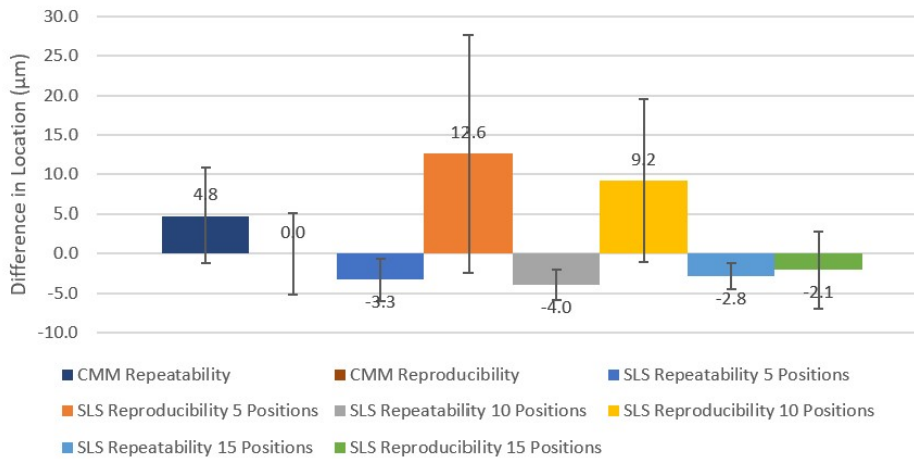


(b) Difference Graph

**Figure F.20:** Comparing Structured Light Scanning and CMM Measurements for X Location of Circle 8

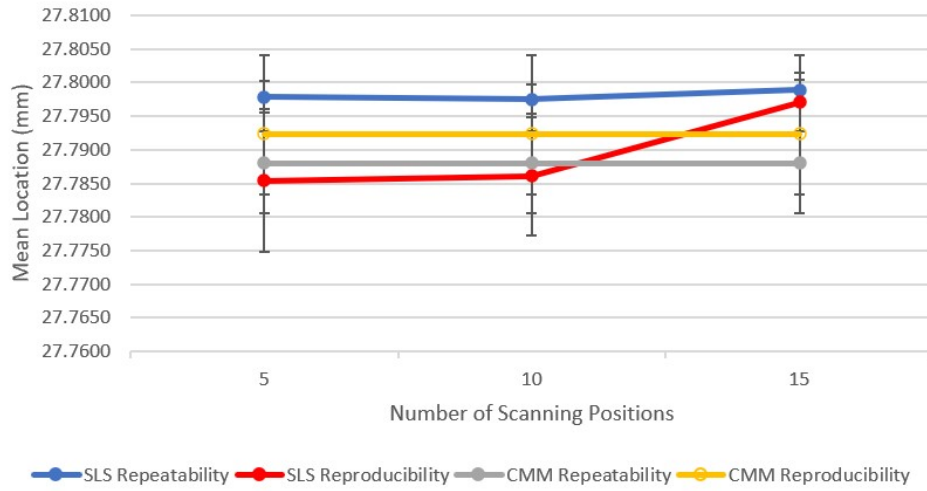


(a) Line Graph

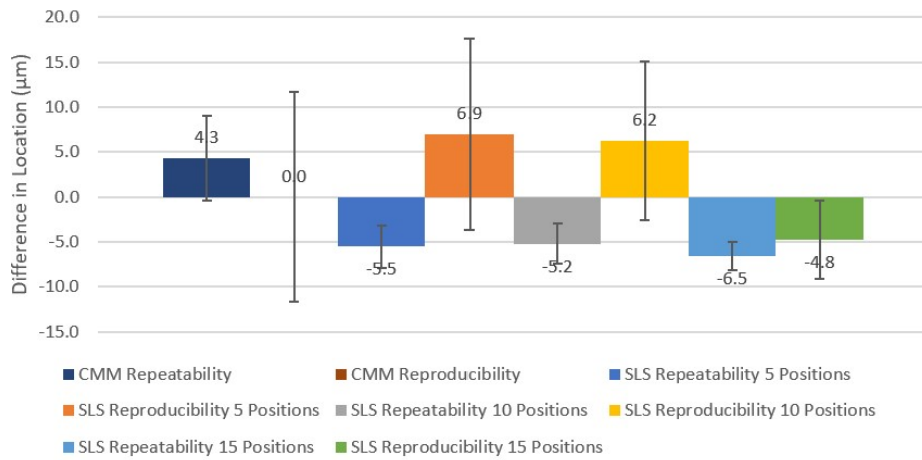


(b) Difference Graph

**Figure F.21:** Comparing Structured Light Scanning and CMM Measurements for X Location of Circle 9

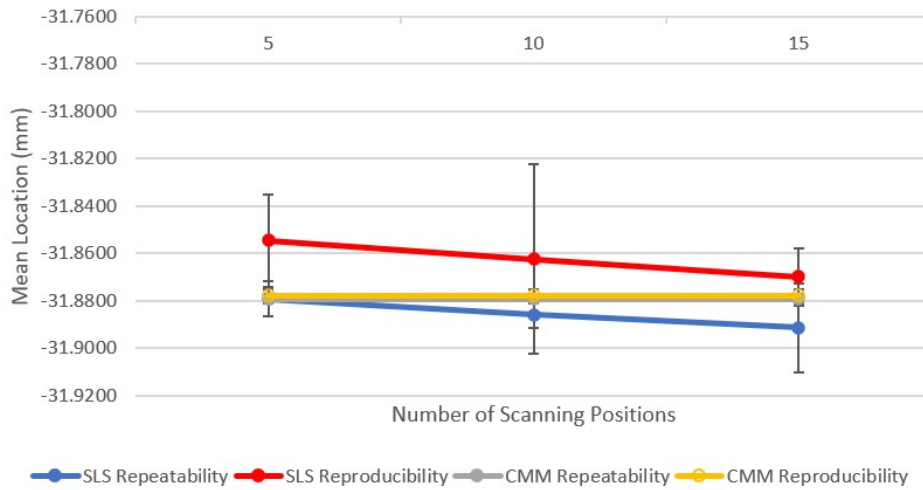


(a) Line Graph

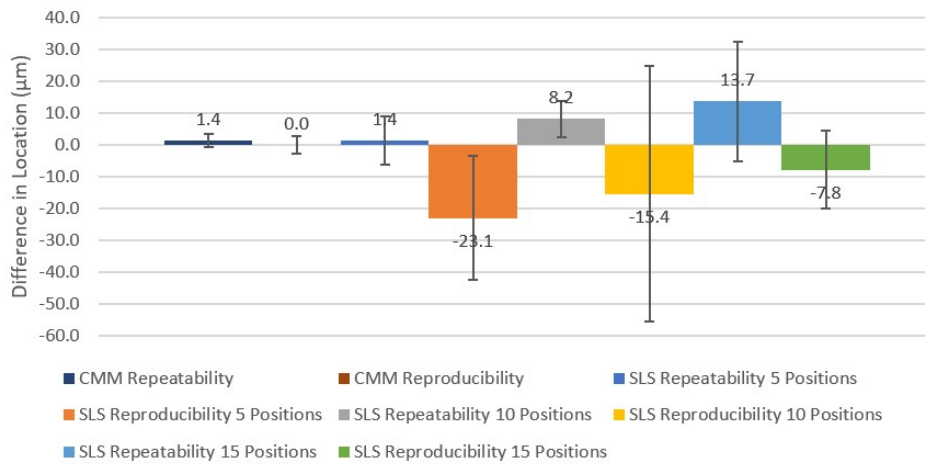


(b) Difference Graph

**Figure F.22:** Comparing Structured Light Scanning and CMM Measurements for X Location of Circle 10



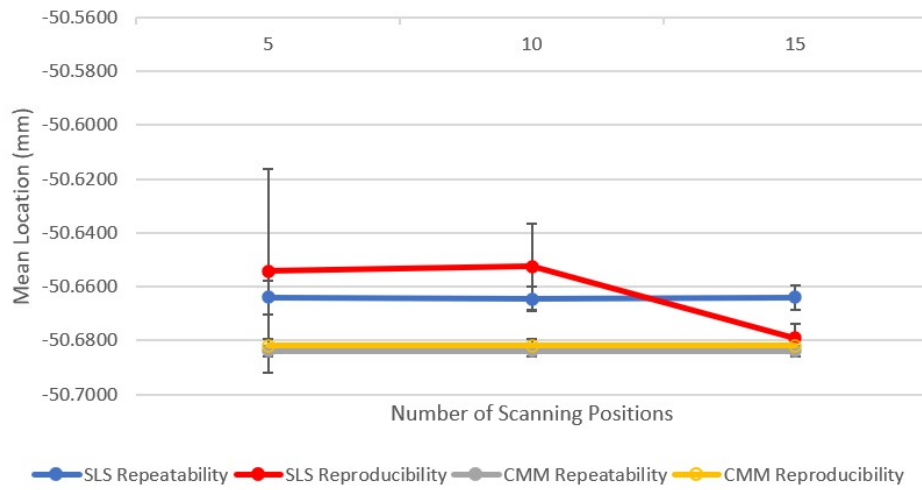
(a) Line Graph



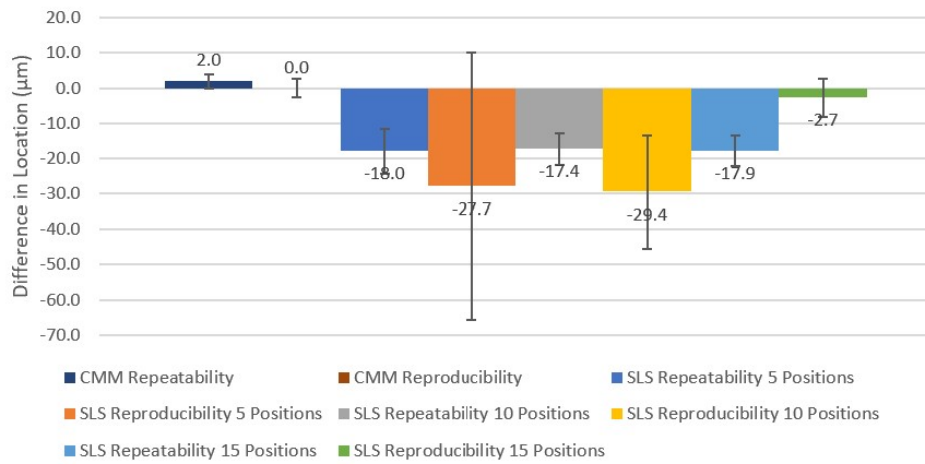
(b) Difference Graph

**Figure F.23:** Comparing Structured Light Scanning and CMM Measurements for Y Location of Circle 2



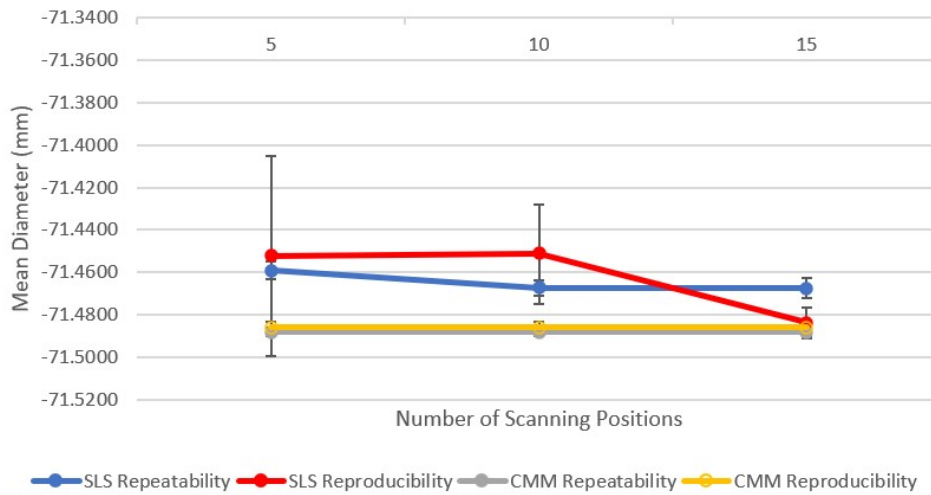


(a) Line Graph

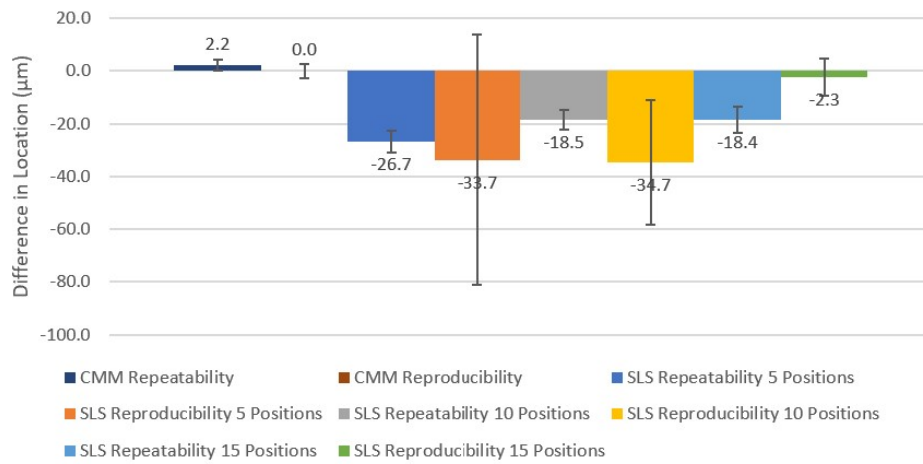


(b) Difference Graph

**Figure F.24:** Comparing Structured Light Scanning and CMM Measurements for Y Location of Circle 3

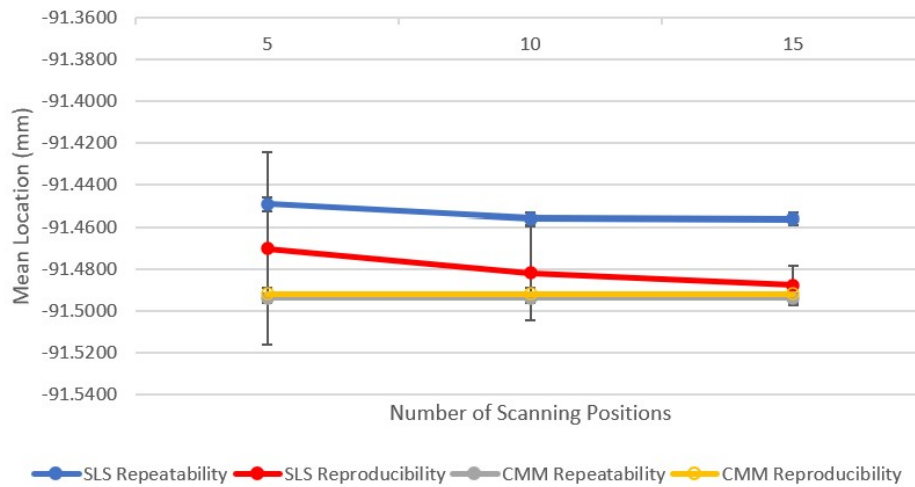


(a) Line Graph

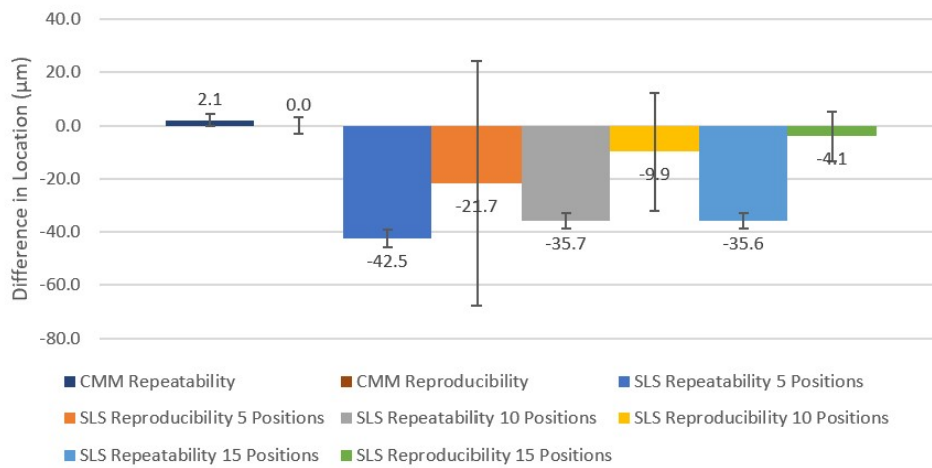


(b) Difference Graph

**Figure F.25:** Comparing Structured Light Scanning and CMM Measurements for Y Location of Circle 4

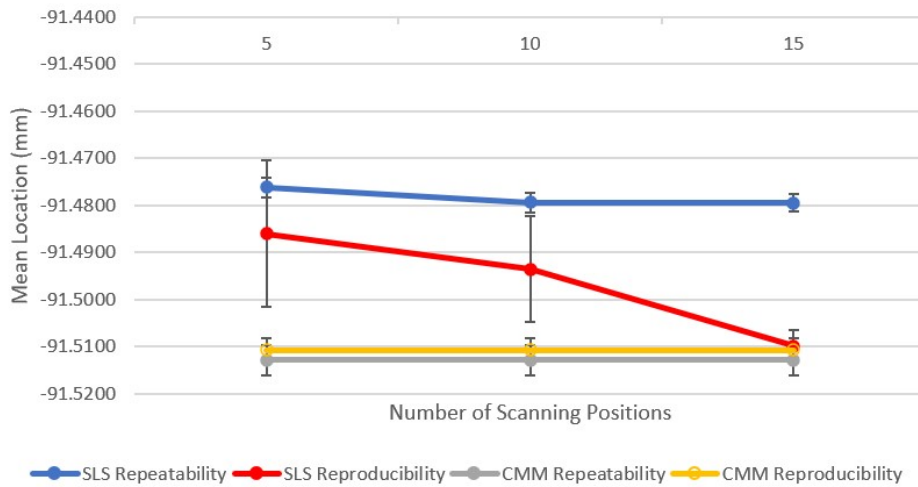


(a) Line Graph

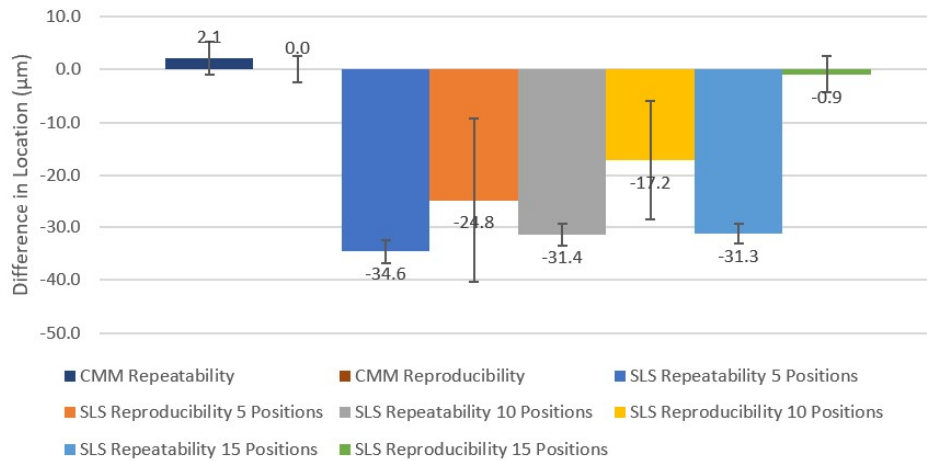


(b) Difference Graph

**Figure F.26:** Comparing Structured Light Scanning and CMM Measurements for Y Location of Circle 5

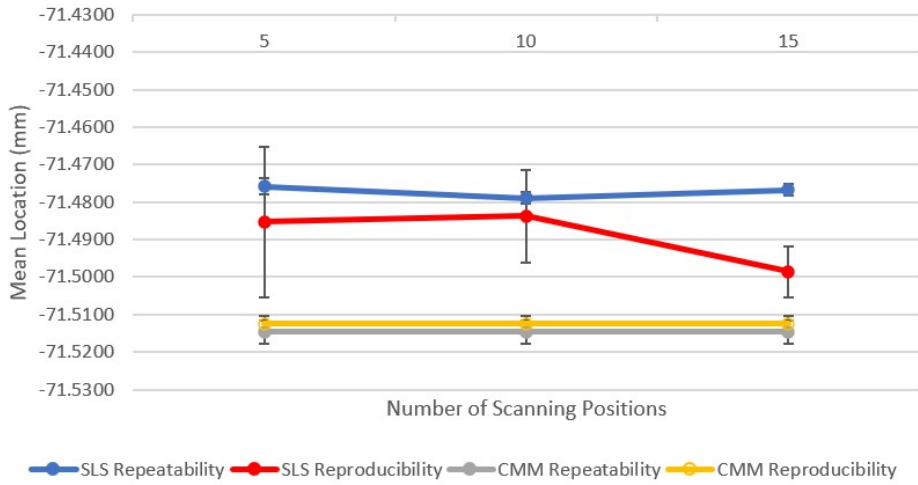


(a) Line Graph

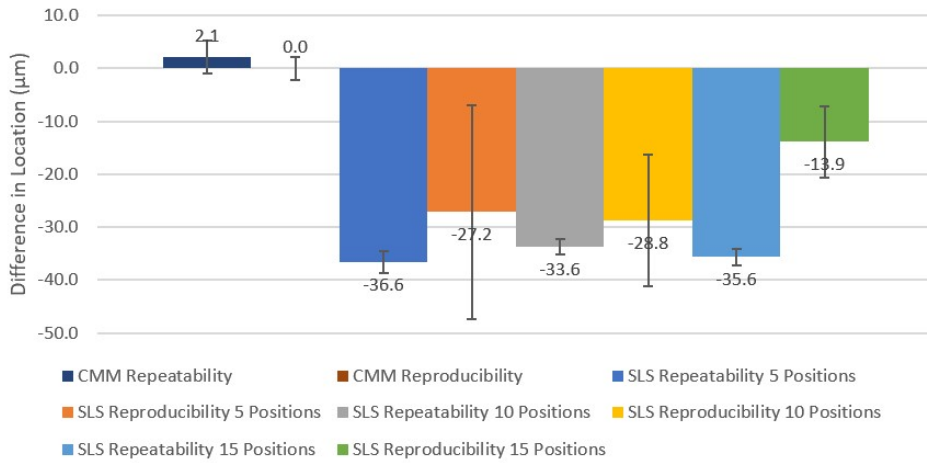


(b) Difference Graph

**Figure F.27:** Comparing Structured Light Scanning and CMM Measurements for Y Location of Circle 6

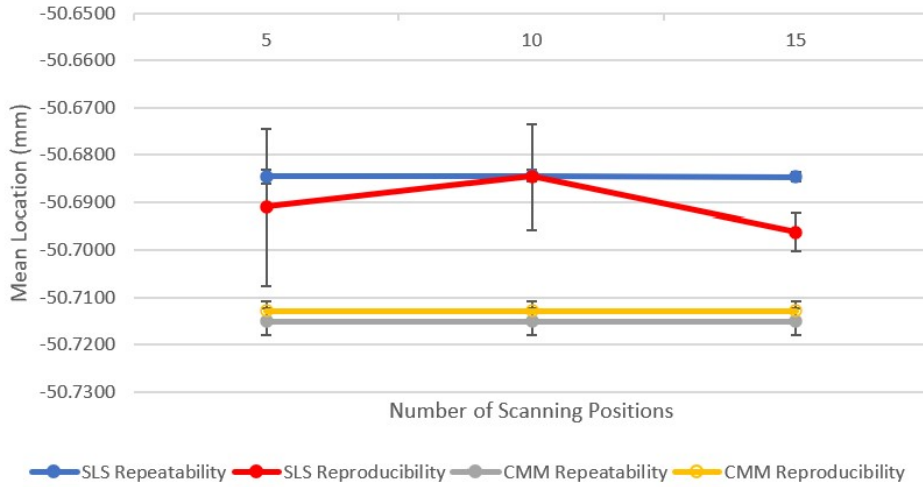


(a) Line Graph

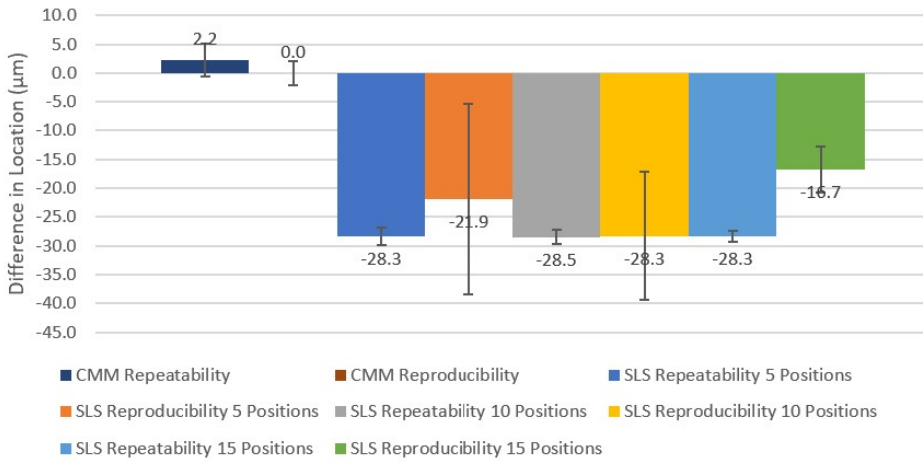


(b) Difference Graph

**Figure F.28:** Comparing Structured Light Scanning and CMM Measurements for Y Location of Circle 7

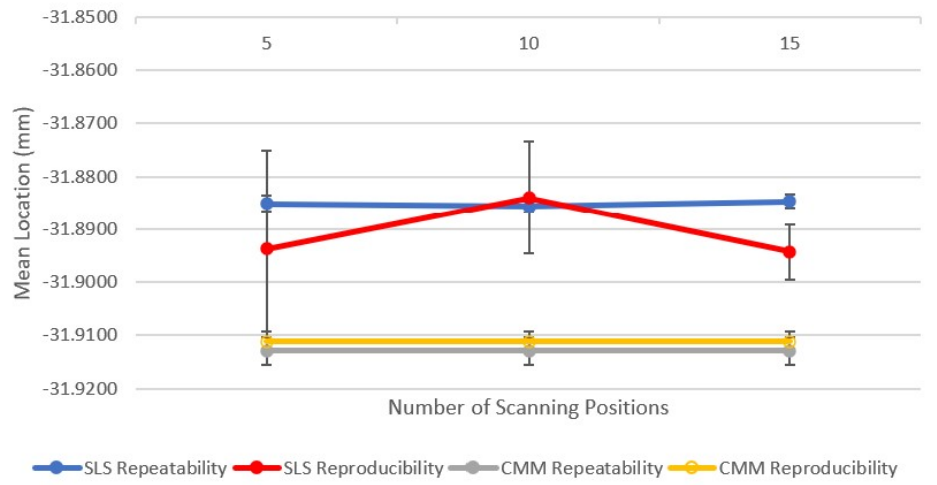


(a) Line Graph

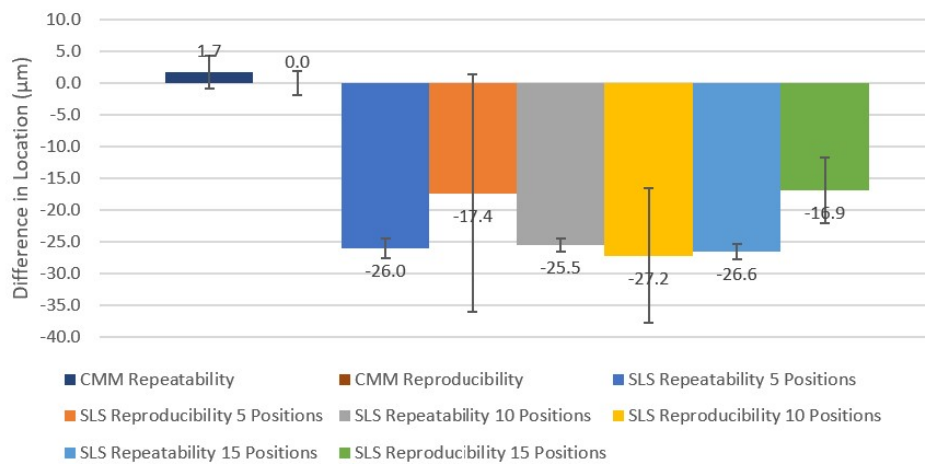


(b) Difference Graph

**Figure F.29:** Comparing Structured Light Scanning and CMM Measurements for Y Location of Circle 8

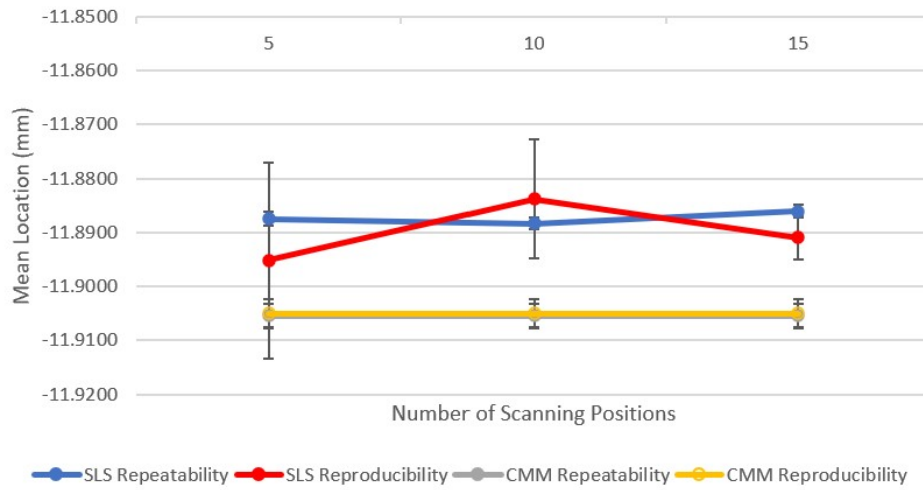


(a) Line Graph

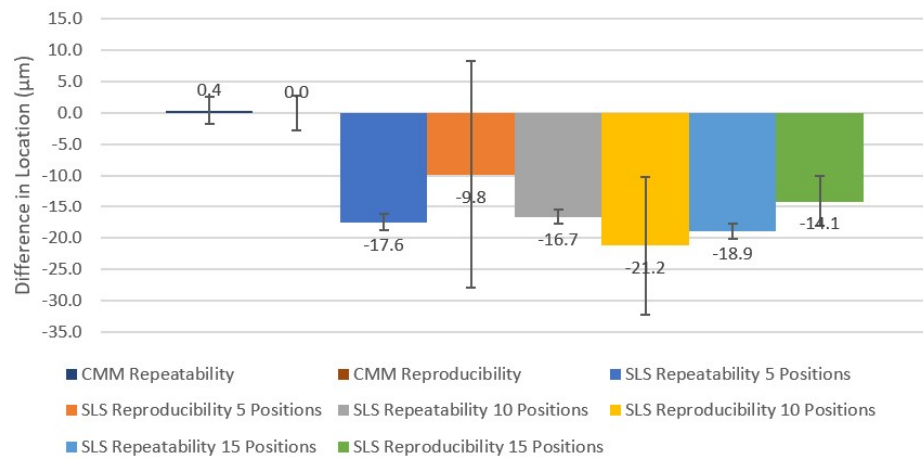


(b) Difference Graph

**Figure F.30:** Comparing Structured Light Scanning and CMM Measurements for Y Location of Circle 9



(a) Line Graph



(b) Difference Graph

**Figure F.31:** Comparing Structured Light Scanning and CMM Measurements for Y Location of Circle 10



# Vita

Leah Jacobs was born in Oklahoma City, Oklahoma, on May 7, 1997. She attended multiple schools in the Dallas-Fort Worth and Houston, Texas areas and graduated from Kinkaid High School in June 2016. The following August she entered Lipscomb University and in May 2020 received the Degree of Bachelors of Science in Mechanical Engineering where she was a honors student and an integral member of the Bison "student rocket launch team". In August 2020, she entered the University of Tennessee Knoxville to study for a Masters of Science Degree in Mechanical Engineering and works as a graduate research assistant under Dr. Tony Schmitz.